

Comprehensive Summaries of Uppsala Dissertations  
from the Faculty of Pharmacy 275



## Pulmonary Drug Absorption

*In vitro and in vivo investigations of drug absorption across the lung barrier and its relation to drug physicochemical properties*

BY

ANN TRONDE



ACTA UNIVERSITATIS UPSALIENSIS  
UPPSALA 2002

Dissertation for the Degree of Doctor of Philosophy (Faculty of Pharmacy) in  
Biopharmaceutics presented at Uppsala University in 2002

## ABSTRACT

Tronde, A., 2002. Pulmonary Drug Absorption: In Vitro and In Vivo Investigations of Drug Absorption Across the Lung Barrier and Its Relation to Drug Physicochemical Properties. Acta Universitatis Upsaliensis. *Comprehensive Summaries of Uppsala Dissertations from the Faculty of Pharmacy* 275. 86 pp. Uppsala. ISBN 91-554-5373-2.

Although, pulmonary drug delivery is a well established means for targeting of drugs to the lungs for the treatment of respiratory diseases as well as for the systemic delivery of volatile anesthetic agents, drug absorption kinetics in the lung have not been subjected to extensive research. The main objective of this thesis was to investigate drug absorption characteristics of the lung barrier, using the isolated and perfused rat lung model and in vivo pharmacokinetic studies in rats. Physicochemically diverse drugs (i.e. atenolol, budesonide, cromolyn, cyanocobalamin, enalapril, enalaprilate, formoterol, imipramine, losartan, metoprolol, propranolol, talinolol, terbutaline, and the tetrapeptide TArPP) were used as model compounds. In connection to these investigations, a nebulization catheter device was successfully adapted and evaluated as a new technique for delivery of defined aerosol doses to the rat lung. In addition, a physicochemical profile of the inhaled drugs on the market worldwide during 2001 was made.

The pulmonary first-order absorption rate constant and bioavailability were found to correlate to the drug lipophilicity, the molecular polar surface area, and the apparent permeability of Caco-2 cell monolayers. In contrast to the intestinal mucosa and the blood-brain barrier, the pulmonary epithelium was highly permeable to drugs with a high molecular polar surface area. Accordingly, a small hydrophilic tetrapeptide (oral bioavailability ~0.5%) showed a complete bioavailability after pulmonary delivery to rats in vivo. Regional differences in bioavailability, absorption rate, and first-pass metabolism of the peptide was demonstrated after targeted delivery to different regions of the respiratory tract in rats in vivo. The high pulmonary bioavailability of the efflux transporter substrates losartan and talinolol provides functional evidence for an insignificant role of efflux transporters such as P-glycoprotein in limiting the absorption of these drugs from the rat lung.

The results of this thesis demonstrate that the lung efficiently absorbs drugs with a wide range of lipophilicity. The pulmonary route should thus be regarded as a potential alternative for administration of drugs with low oral bioavailability. In addition, drug inhalation present an opportunity to attain a more rapid onset of drug action than can be attained by the oral route.

*Ann Tronde, Department of Pharmacy, Uppsala Biomedical Centre, Box 580,  
SE-751 23 Uppsala, Sweden*

© Ann Tronde 2002

ISSN 0282-7484

ISBN 91-554-5373-2

Printed in Sweden by Uppsala University, Tryck & Medier, Uppsala 2002

*Till Ulf*

*“In the middle of the difficulty lies the opportunity”*

*Albert Einstein*

# CONTENTS

1. PAPERS DISCUSSED	7
2. ABBREVIATIONS	8
3. INTRODUCTION	9
3.1 Background	9
3.2 Structure and function of the lung	10
3.2.1 Airways	11
3.2.2 Blood circulation	12
3.3 Major components of the lung – barriers to drug absorption	13
3.3.1 Epithelium	13
3.3.2 Endothelium	14
3.3.3 Alveolar macrophages	14
3.3.4 Interstitium and basement membrane	14
3.3.5 Lymphatic system	14
3.3.6 Epithelial lining fluid	15
3.3.7 Surfactant	15
3.3.8 Mucociliary clearance	16
3.3.9 Pathophysiological changes	17
3.3.10 Species differences	17
3.4 Metabolic activity and pulmonary distribution of drugs	19
3.4.1 Metabolic activity	19
3.4.2 Pulmonary distribution of drugs	20
3.5 Mechanisms of drug transport across the lung barrier	20
3.5.1 Passive diffusion	21
3.5.2 Transporter-mediated absorption and efflux	22
3.5.3 Vesicle-mediated endocytosis and transcytosis	22
3.5.4 Particle transport	23
3.6 Drug delivery to the lung	23
3.6.1 Particle deposition	23
3.6.2 Techniques for pulmonary drug delivery	24
3.7 Biological models for assessment of pulmonary drug absorption	26
3.7.1 In vivo animal models	26
3.7.2 The isolated and perfused lung	27
3.7.3 Cell culture models	27
4. AIMS OF THE THESIS	29
5. MATERIALS AND METHODS	30
5.1 Drugs and marker compounds	30
5.2 Animals	30
5.3 Nebulization catheters and breath synchronized aerosol delivery	32
5.3.1 Nebulization catheters	32
5.3.2 Breath synchronized aerosol delivery in the isolated and perfused rat lung	33
5.3.3 Breath synchronized aerosol delivery to the rat lung in vivo	33

5.4	Aerosol characterization and dosing uniformity ( <i>Paper I</i> )	33
	5.4.1 Delivered dose weight	33
	5.4.2 Aerosol cloud formation	33
	5.4.3 Droplet-size distribution	33
	5.4.4 Lung distribution experiments	35
5.5	The isolated and perfused rat lung ( <i>Paper I, II, IV</i> )	35
	5.5.1 Experimental setup	35
	5.5.2 Lung absorption and metabolism experiments	37
5.6	In vivo pharmacokinetic models in anesthetized rats ( <i>Paper III, V</i> )	37
	5.6.1 Anesthesia and treatment protocols	37
	5.6.2 Pharmacokinetic calculations	39
5.7	Epithelial cell culture experiments ( <i>Paper II, IV, V</i> )	40
	5.7.1 Cell culture	40
	5.7.2 Transport experiments in Caco-2 cell monolayers	40
5.8	Sample analysis	41
5.9	Inhaled drugs dataset ( <i>Paper V</i> )	41
5.10	Calculation of drug parameters ( <i>Paper IV, V</i> ) and physicochemical profiling of the inhaled drugs ( <i>Paper V</i> )	42
5.11	Data analysis ( <i>Paper IV, V</i> )	42
5.12	Statistics	43
6.	RESULTS AND DISCUSSION	43
6.1	Nebulization catheters as a new approach for delivery of defined aerosol doses to the rat lung ( <i>Paper I</i> )	43
6.2	Absorption and metabolism of the $\mu$ -selective opioid tetrapeptide agonist (TArPP) after respiratory delivery to the rat ( <i>Paper II, III</i> )	46
6.3	Physicochemical profile of inhaled drugs ( <i>Paper V</i> )	52
6.4	Drug absorption from the rat lung ( <i>Paper IV, V</i> )	55
6.5	Permeability characteristics of investigated drugs in the epithelial permeability screening model, Caco-2 ( <i>Paper II, IV, V</i> )	60
6.6	Influence of drug physicochemical properties and epithelial permeability on the absorption rate and bioavailability after pulmonary drug administration ( <i>Paper IV, V</i> )	61
6.7	Applicability of the biological models used to investigate the pulmonary drug absorption and distribution ( <i>Paper II-V</i> )	64
6.8	Comparison of the transport of drugs across the pulmonary and intestinal barriers ( <i>Paper V</i> )	66
7.	CONCLUSIONS	68
8.	PERSPECTIVES	70
9.	ACKNOWLEDGMENTS	71
10.	REFERENCES	73

# 1. PAPERS DISCUSSED

This thesis is based on the following papers, which will be referred to by their Roman numerals in the text.

- I Tronde, A., Baran, G., Eirefelt, S., Lennernäs, H., Hultkvist Bengtsson, U. Miniaturized nebulization catheters -A new approach for delivery of defined aerosol doses to the rat lung. *J. Aerosol Med.* 15: 283-296, (2002).
- II Tronde, A., Krondahl, E., von Euler-Chelpin, H., Brunmark, P., Hultkvist Bengtsson, U., Ekström, G., Lennernäs, H. High airway-to-blood transport of an opioid tetrapeptide in the isolated and perfused rat lung after aerosol delivery. *Peptides*, 23: 469-478, (2002).
- III Krondahl, E., Tronde, A., Eirefelt, S., Forsmo-Bruce, H., Ekström, G., Hultkvist Bengtsson, U., Lennernäs, H. Regional differences in bioavailability of an opioid tetrapeptide in vivo in rats after administration to the respiratory tract. *Peptides*, 23:479-488, (2002).
- IV Tronde, A., Nordén, B., Jeppsson, A-B., Brunmark, P., Nilsson, E., Lennernäs, H., Hultkvist Bengtsson, U. Drug absorption from the rat lung -Correlations with drug physicochemical properties and epithelial permeability. *Submitted*.
- V Tronde, A., Nordén, B., Marchner, H., Wendel, A-K., Lennernäs, H., Hultkvist Bengtsson, H. Pulmonary absorption rate and bioavailability of drugs in vivo in rats: Structure-absorption relationships and physicochemical profiling of inhaled drugs. *Submitted*.

Reprints were made with permission from the journals.

## 2. ABBREVIATIONS

A-B	apical-to-basolateral
ADME	absorption, distribution, metabolism, elimination
ANOVA	analysis of variance
AUC	area under the plasma concentration-time curve
AVC	air-valve control unit
B-A	basolateral-to-apical
BAL	bronchoalveolar lavage
BCDU	breath-controlled dosing unit
Caco-2	epithelial cell line derived from human colonic adenocarcinoma
CL	systemic clearance
C <sub>max</sub>	maximum plasma concentration
COPD	chronic obstructive pulmonary disease
F	systemic bioavailability
fa	fraction absorbed
HBA	number of hydrogen bond acceptors
HBD	number of hydrogen bond donors
HB	HBA+HBD
HPLC	high performance liquid chromatography
IPL	isolated and perfused rat lung
i.p.	intraperitoneal
i.v.	intravenous
i.t.	intratracheal
i.n.	intranasal
ka <sub>lung</sub>	apparent first order absorption rate constant for air-to-blood transport in IPL
LC-MS	liquid chromatography- mass spectrometry
LC-MS-MS	liquid chromatography- tandem mass spectrometry
cLogD(7.4)	logarithm of the calculated octanol/water distribution coefficient at pH 7.4
cLog P	logarithm of the calculated octanol/water partitioning coefficient
MMD	mass median diameter of aerosol particle distribution
MW	molecular weight
P <sub>app</sub>	apparent permeability
PDR	Physicians' desk reference
PLS	partial least squares, multivariate regression technique
PSA	molecular polar surface area
s.c.	subcutaneous
SD	standard deviation
TArPP	μ-selective opioid tetrapeptide agonist, Tyr-D-Arg-Phe-Phe
t <sub>max</sub>	time to reach maximum plasma concentration
t <sub>1/2</sub>	elimination half-life
t <sub>1/2</sub> abs	time for 50% absorption of the transferred dose in IPL
T <sub>50%</sub>	time to absorb 50% of the bioavailable dose
T <sub>90%</sub>	time to absorb 90% of the bioavailable dose
V <sub>ss</sub>	volume of distribution at steady state

## 3. INTRODUCTION

### 3.1 Background

The therapeutic benefits of drug inhalation have been appreciated for several decades for the treatment of respiratory diseases, such as asthma, chronic obstructive pulmonary disease (COPD), cystic fibrosis, and pulmonary infections, as well as for the systemic delivery of anesthetic agents (Anonymous, 1946; Brewis et al., 1995; Camps, 1929; Dale et al., 1987; Graeser et al., 1935). By direct targeting of locally acting drugs to the lungs, a high local concentration of the drugs at the target site, rapid onset of drug action, lower systemic exposure, and consequently reduced side-effects can be achieved (Lipworth, 1996; van den Bosch et al., 1993).

The use of the inhaled route outside the respiratory therapeutic area is today uncommon. However, the advantageous drug absorption characteristics of the lung, e.g. the highly vascularized respiratory mucosa, large absorptive surface area, thin air-blood barrier, and the relatively low enzymatic activity in the lung, have attracted attention to pulmonary delivery as a potential alternative for systemic administration of drugs with poor oral absorption (Anttila et al., 1997; Patton, 1996; Wall et al., 1993). For instance, several investigations regarding inhalation of therapeutic peptides, proteins, oligonucleotides, and vaccines, which are subjected to poor enzymatic stability and low permeation across biological membranes, have been reported (LiCalsi et al., 1999; Niven, 1995; Russell et al., 2001; Skyler et al., 2001). In addition, pulmonary drug delivery is currently evaluated for the delivery of analgetic drugs, such as morphine, for which a rapid onset of drug action is of significant therapeutic importance (Dershwitz et al., 2000).

The efficacy of an inhaled drug is determined by its absorption across the lung barrier and on the location of the pharmacological site of action. For locally acting drugs, the absorption into the systemic circulation may imply the removal and consequently the termination of action of the drug in the lung. On the other hand, for systemically acting drugs, the absorption profile of the drug from the lung may determine the onset, intensity, and duration of action of the drug (Taylor G., 1990). Although inhalation is a well established means for drug administration, drug absorption kinetics in the lung has not been subjected to extensive research. Yet, investigations of the absorption rate and bioavailability of pulmonary delivered drugs in relation to the drugs' molecular properties are important to aid the design of new inhaled drugs for local and systemic action.

The development of combinatorial chemistry and high throughput screening programs has stimulated drug discovery research to find experimental and computational models to estimate and predict drug absorption, distribution, metabolism, and elimination (ADME) based on drug physicochemical properties. However, so far the main focus of the research has been to predict the drug transport across the intestinal- and blood-brain barriers, and relatively few investigators have used *in vivo* models in animals and humans (Egan et al., 2002; Norinder et al., 2002; Winiwarter et al., 1998). In the absence of a significant amount of human lung absorption data, there is an obvious need

for accurate pharmacokinetic in vivo investigations in animals to establish reliable in vitro-in vivo correlations and drug structure-permeability relationships to guide drug discovery programs.

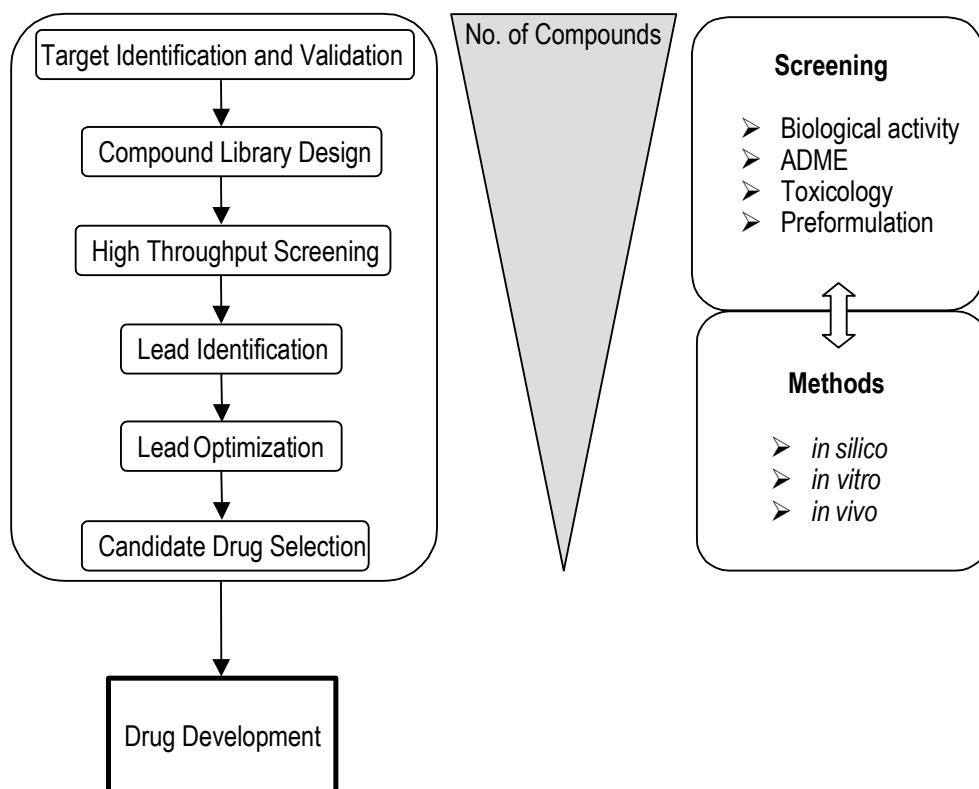


**Figure 1.** Flow chart schematically illustrating the phases of a generic drug discovery process. In the early drug discovery phase, top of figure, there is a large number of compounds, which are sieved through a number of screening models to enable the selection of one potential candidate drug for transfer into drug development phase. Establishment of structure-activity relationships based on in vivo experimental data is crucial to improve the reliability of in silico predictions of ADME profile, and pharmacological and toxicological activity.

### 3.2 Structure and function of the lung

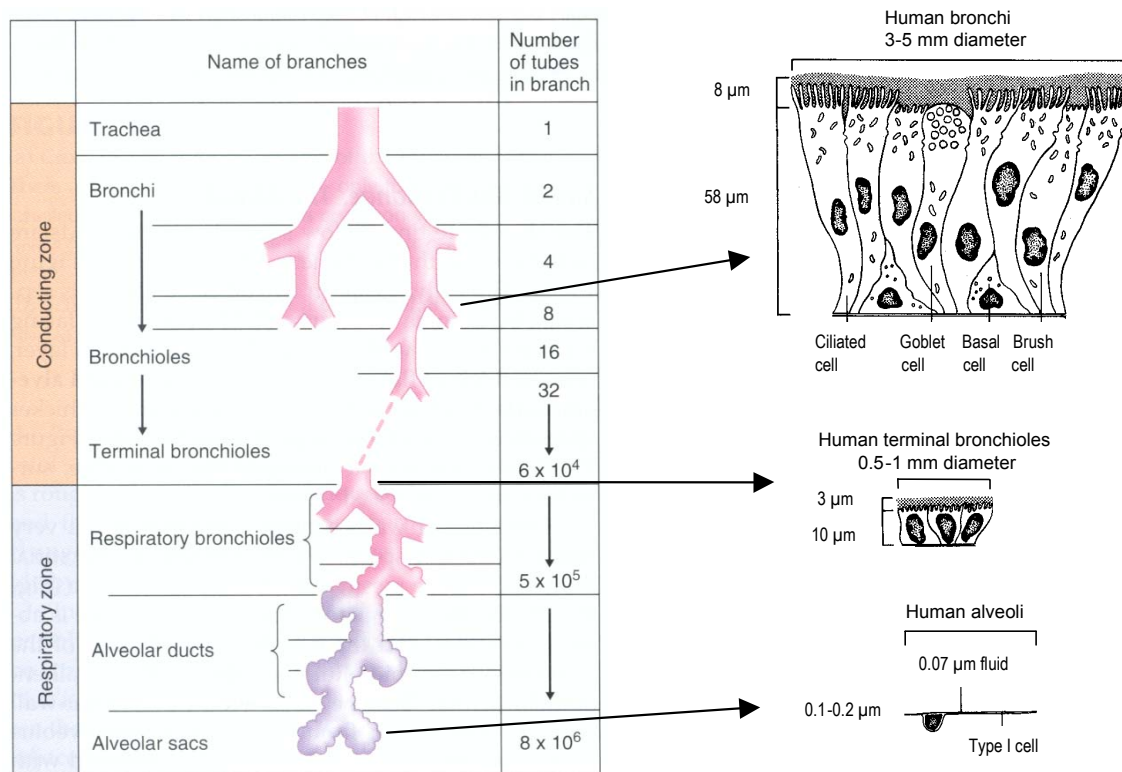
The principal function of the lung is to distribute the inspired air and pulmonary blood to assure efficient gas exchange, i.e. oxygenation of the blood and removal of carbon dioxide from the body. Optimal matching of the ventilation to the blood perfusion is required to accomplish the gas exchange at a minimal energy cost.

About 85% of the total lung volume consist of gas exchange parenchyma (alveolar sacs, alveoli, and alveolar capillary network), and about 6-10% of conducting airways

(bronchi and bronchioles). The remaining part of the lung consists of nervous and vascular tissue (Gehr P., 1984; Plopper, 1996).

### 3.2.1 Airways

The human respiratory system can be divided in two functional regions: the conducting airways and the respiratory region. The conducting airways, which are composed of the nasal cavity and associated sinuses, the pharynx, larynx, trachea, bronchi, and bronchioles, filter and condition the inspired air. From trachea to the periphery of the airway tree, the airways repeatedly branch dichotomously into two daughter branches with smaller diameters and shorter length than the parent branch (Weibel, 1991). For each new generation of airways, the number of branches is doubled and the cross-sectional area is exponentially increased. The conducting region of the airways generally constitutes generation 0 (trachea) to 16 (terminal bronchioles). The respiratory region, where gas exchange takes place, generally constitutes generation 17-23 and is composed of respiratory bronchioles, the alveolar ducts, and the alveolar sacs (Figure 2). The number of times the bronchial tree branches before the gas exchange area is reached can vary from as few as 6 to as many as 28-30 (Plopper, 1996).



A.

B.

**Figure 2.** (A) Structure of the airways (Reprinted from *Human Physiology*, 8<sup>th</sup> Ed, 2001, McGraw Hill©, with permission from the publisher). (B) Regional differences in relative epithelial cell sizes and thickness of epithelial lining fluid (Modified from Patton, 1996).

The air-blood barrier of the gas exchange area is composed of the alveolar epithelial cells (surface area  $140 \text{ m}^2$ ) on one side and the capillary bed (surface area  $130 \text{ m}^2$ ) on the other side of a thin basement membrane (Simionescu, 1991; Stone et al., 1992). The extensive surface area of the air-blood barrier in combination with its extreme thinness ( $0.1\text{-}0.5 \text{ }\mu\text{m}$ ) permit rapid gas exchange by passive diffusion (Plopper, 1996).

### 3.2.2 Blood circulation

Two different circulatory systems, the bronchial and the pulmonary, supply the lungs with blood (Staub, 1991). The bronchial circulation is a part of the systemic circulation and is under high pressure. It receives about 1% of the cardiac output and supplies the airways (from the trachea to the terminal bronchioles), pulmonary blood vessels and lymph nodes with oxygenated blood and nutrients and conditions the inspired air (Staub, 1991). In addition, it may be important to the distribution of systemically administered drugs to the airways and to the absorption of inhaled drugs from the airways (Chediak et al., 1990). The pulmonary circulation comprise an extensive low-pressure vascular bed, which receives the entire cardiac output. It perfuses the alveolar capillaries to secure efficient gas exchange and supplies nutrients to the alveolar walls. Anastomoses between bronchial and pulmonary arterial circulations have been found in the walls of medium-sized bronchi and bronchioles (Chediak et al., 1990; Kröll et al., 1987).

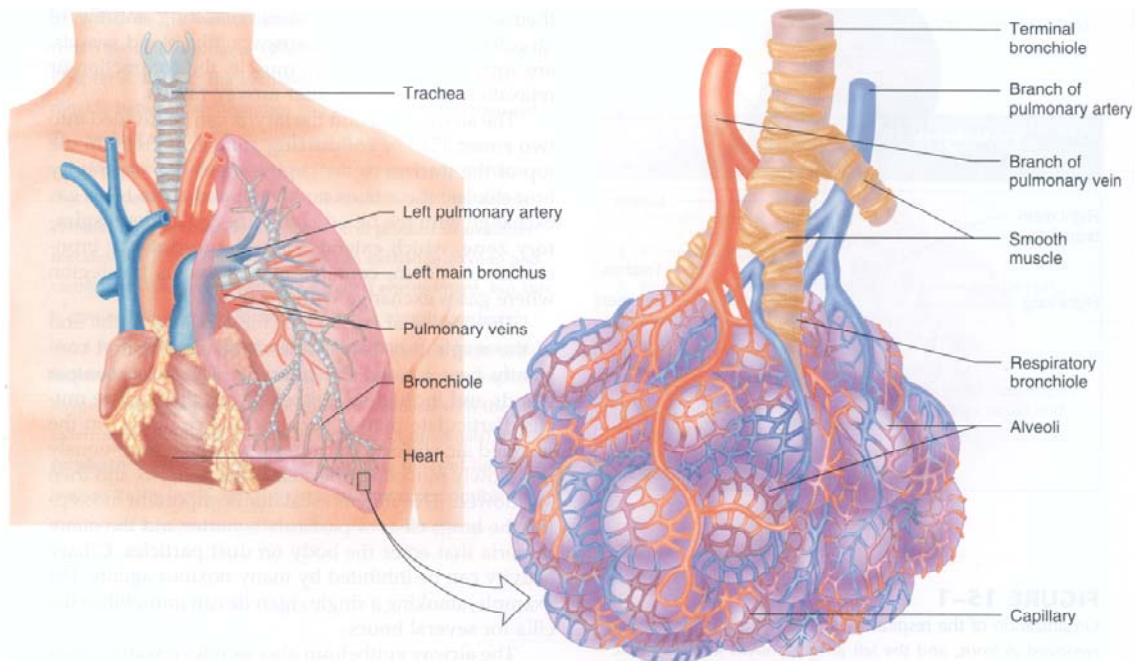


**Figure 3.** Anatomy of the human lung. (Reprinted from *Human Physiology*, 8<sup>th</sup> Ed, 2001, McGraw Hill©, with permission from the publisher).

### **3.3 Major components of the lung – barriers to drug absorption**

As one of the primary interfaces between the organism and the environment, the respiratory system is constantly exposed to airborne particles, potential pathogens, and toxic gases in the inspired air (Plopper, 1996). As a result a sophisticated respiratory host defense system, present from the nostrils to the alveoli, has evolved to clear offending agents (Twigg, 1998). The system comprises mechanical (i.e. air filtration, cough, sneezing, and mucociliary clearance), chemical (antioxidants, antiproteases and surfactant lipids), and immunological defense mechanisms and is tightly regulated to minimize inflammatory reactions that could impair the vital gas-exchange (Nicod, 1999; Twigg, 1998).

From a drug delivery perspective, the components of the host defense system comprise barriers that must be overcome to ensure efficient drug deposition and absorption from the respiratory tract.

#### *3.3.1 Epithelium*

The airway epithelial cells provides a tight ciliated barrier that clears the airways from debris trapped in the airway mucus, prevents indiscriminant leakage of water and solutes into the airways, secretes components for the airway lining fluid and mucus layer, repairs injuries to the epithelium, and modulates the response of inflammatory cells, vessels, and smooth muscle (Rennard et al., 1991). The epithelium lining the tracheobronchial airways is composed of seven different cell types, i.e. basal cells, goblet cells, ciliated cells, brush cells, serous cells, Clara cells, and neuroendocrine cells (Plopper, 1996). A variety of migratory cells such as lymphocytes, leukocytes, and mast cells are also present in the epithelium (Plopper, 1996). The epithelium lining the terminal bronchioles is columnar or cuboidal and is composed of ciliated cells and Clara cells (Plopper, 1996). In the alveolar region, four cell types are present: the epithelial type I and II cells, alveolar brush cells (type III) and alveolar macrophages (Ma et al., 1996; Plopper, 1996). The squamous type I cell covers approximately 96% of the alveolar surface area and has an average cell thickness of 0.26  $\mu\text{m}$ . Characteristically the alveolar type I cell has a large cytoplasmic volume and displays only sparse cellular organells most of which are located in the perinuclear region of the cells (Crapo et al., 1982). These morphometric features are favorable for drug transport. About 3% of the alveolar surface is covered by the much smaller cuboidal type II cells, which synthesize and secrete surface active materials (Mason R. J. et al., 1998).

The apical membranes of the epithelial cells are joined by tight junctions that divide the cell membranes into the functionally distinct apical and basolateral domains (Summers, 1991). The tight junctions are highly dynamic structures that act as barriers to fluid flow and control the transport of ions and solutes through the intercellular space (Summers, 1991). The heterogenous composition of the lung epithelium results in a large variation of tight junctional forms with variable tightness (Godfrey, 1997; Schneeberger, 1980).

### *3.3.2 Endothelium*

The lung is unique among tissues in that about 40% of its total cellular composition is capillary endothelium, which is the largest capillary endothelial surface in the body (Simionescu, 1991). The alveolar-capillary endothelium has specialized organell-free domains to provide a particularly thin (from 200 nm down to 30-35 nm) barrier for gas exchange (Simionescu, 1991). Furthermore, the endothelial cells have a relatively large number of endocytotic vesicles (Schnitzer, 2001). The endothelial cells are joined by tight junction with few parallel arrays of contacts, which renders them leaky when the hydrostatic pressure increase (Plopper, 1996; Simionescu, 1991).

### *3.3.3 Alveolar macrophages*

The alveolar macrophages are found on the alveolar surface. These phagocytic cells play important roles in the defense mechanisms against inhaled bacteria and particles that have reached the alveoli (Haley et al., 1991). Particles deposited in the lung parenchyma of rabbits and rats have been demonstrated to be phagocytized by alveolar macrophages within a few hours (Brain et al., 1984; Takenaka et al., 2001). The macrophages are cleared from the alveoli to the bronchioles by the lining fluid, and then from the airways by the mucociliary escalator (Jeffery, 1995).

### *3.3.4 Interstitium and basement membrane*

The interstitium of the lung, the extracellular and extravascular space between cells in the tissue, contains a variety of cells (fibroblasts, myofibroblasts, pericytes, monocytes, lymphocytes, plasma cells), collagen, elastic fibers, and interstitial fluid (Plopper, 1996). Its main role is to separate and bind together the specific cell layers in the tissue. The main drainage pathway for the interstitial fluid is the lymphatic vessels. The outer border of the interstitium is defined by the epithelial and endothelial basement membranes (Weibel et al., 1991). The basement membrane modulates the movement of fluid, molecules, particles, and cells from the air space and blood into the interstitium (Weibel et al., 1991). However, plasma proteins and most solutes are thought to diffuse relatively unhindered through it (Patton, 1996).

### *3.3.5 Lymphatic system*

The pulmonary lymphatic system contributes to the clearance of fluid and protein which has filtered from the vascular compartment into the lung tissue interstitium and helps to prevent fluid accumulation in the lungs (Puchelle et al., 1995). The lymphatic vessels are present in the interstitium near the small airways and blood vessels, but not in the alveolar walls (Leak et al., 1983). The leaky lymphatic endothelia allow micron-sized particles (e.g. lipoproteins, plasma proteins, bacteria, and immune cells) to pass freely into the lymph fluid (Patton, 1996). The flow rate of the lymphatic fluid is normally very slow (1/500 relative the blood flow), but is increased at high pulmonary venous

pressure (Patton, 1996). The lymph is filtered through regional lymph nodes and returned to the venous blood circulation at the right jugular and subclavian veins.

### *3.3.6 Epithelial lining fluid*

Solid drug particles delivered to the respiratory tract need to be wetted and dissolved before they can exert their therapeutic activity. Although the humidity in the lung is near 100%, the volume of the epithelial lining fluid is small (Wiedmann et al., 2000). The thickness of the lining fluid in the airways is estimated to 5-10  $\mu\text{m}$  and is gradually decreased along the airway tree until the alveoli, where the thickness is estimated to be about 0.05-0.08  $\mu\text{m}$  (Patton, 1996). The volume and composition of the epithelial lining fluid is determined by active ion transport and passive water permeability of the respiratory epithelium (Puchelle et al., 1995). However, due to the inaccessibility and small volume available, the composition of the epithelial lining fluid is not fully known. Like the gastric mucosa, the airway mucosa is coated with a layer of phospholipids, which in association with mucins lubricate and protect the epithelium from offending agents (Girod et al., 1992; Puchelle et al., 1995). Phospholipids and proteins in bronchial secretions inhibit the adhesion of cilia to the mucus gel and accelerate ciliary beat frequency (Morgenroth et al., 1985). Bacteriostatic and bactericidal proteins present in the lining fluid, e.g. IgA, lactoferrin, and lysozyme, are synthesized and secreted by submucosal gland cells and participate in the airway antibacterial defense (Puchelle et al., 1995). In the alveolar region, the surface fluid consists of a thin biphasic layer of plasma filtrates overlaid by a monolayer of pulmonary surfactant (Patton, 1996).

### *3.3.7 Surfactant*

The lung surfactant is synthesized and secreted by the alveolar type II cells and comprises a unique mixture of phospholipids and surfactant-specific proteins (Staub, 1991). It forms an insoluble film at the surface of the alveolar lining fluid and decreases the surface tension in the alveoli. Thereby the extensive alveolar air-liquid interface is stabilized, which promotes lung expansion on inspiration and prevents lung collapse on expiration (Staub, 1991). The lung surfactant has also been found to enhance local pulmonary host defense mechanisms by serving as a barrier against adhesion of microorganisms and to enhance phagocytosis by alveolar macrophages (Hamm et al., 1992). The lung surfactant undergoes a constant dynamic process of turnover and metabolism, including removal by the mucociliary escalator, phagocytosis, and recycling. The turnover half-life of secreted phospholipids has been demonstrated to be 15-30 h (Hamm et al., 1992). Stimuli such as increased ventilation rate and high volume of lung inflation stimulate the secretion of surfactant from the lamellar bodies of the alveolar type II cells (Hamm et al., 1992).

#### *Implications for drug delivery*

The airway and alveolar lining fluids are thus covered by at least a monolayer of lung surfactant projecting the fatty acid tails into the air space (Patton, 1996). Consequently,

interactions between the phospholipids in the lung surfactant and inhaled drugs have been reported. For instance, lung surfactant was shown to enhance the solubility of glucocorticosteroids, which may affect the residence time of the steroid in the lung (Wiedmann et al., 2000). Furthermore, strong interactions of the polypeptides ditirelix and cyclosporin A with phospholipids have been demonstrated and has been suggested to limit the absorption from the lung, thus leading to a prolonged retention of the drugs in the lungs (McAllister et al., 1996). The use of exogenous surfactant as a vehicle for pulmonary drug delivery has been suggested as a means to enhance the spreading of the drug within the lungs (Van' t Veen et al., 1999). However, in a study with intratracheally instilled Tc-99m-tobramycin in rats it was concluded that the exogenous surfactant increased the lung clearance rate of Tc-99m-tobramycin (Van' t Veen et al., 1999). In another study, a decrease in bactericidal activity of tobramycin and gentamicin through binding to lung surfactant was demonstrated in vitro (Van' t Veen et al., 1995). These results reflect a complex interaction between drugs and lung surfactant, which should be considered in drug development.

### *3.3.8 Mucociliary clearance*

The mucociliary clearance is probably the most important mechanical host defense in the lung. By the coordinated movements of cilia, the mucus is swept out of the nasal cavity and lungs, respectively, towards the pharynx where it is swallowed. In the nose, clearance rates of 3-25 mm/min have been shown in normal subjects (Mygind et al., 1998). The reported tracheal mucociliary clearance rate in young healthy subjects range from 4 to 20 mm/min (Salathé et al., 1997). There is an inverse relationship between mucus velocity and airway generation, which relates to the lower percentage of ciliated cells, shorter cilia, lower ciliary beat frequency, and lower number of secretory cells in the peripheral airways (Salathé et al., 1997). The thickness of the mucus layer varies along the conducting airways, being about 8  $\mu\text{m}$  in the trachea and about 2  $\mu\text{m}$  in the bronchioles (Mercer et al., 1992). The mucus layer is continuous in the larger human bronchial airways, but consists of discontinuous rafts in the smaller bronchi and bronchioles (Mercer et al., 1992). The surface liquids of the ciliated airways are composed of two phases: one aqueous periciliary phase of epithelial lining fluid close to the cell surface, in which the cilia beat, and one gel phase of mucus on top of the aqueous phase. A phospholipid layer between the phases lowers the surface tension between them (Samet et al., 1994). Mucus is secreted primarily from the serous cells of submucosal glands and from goblet cells, and is composed of water (95%), glycoproteins (mucins) (2%), proteins (1%), inorganic salts (1%), and lipids (1%) (Samet et al., 1994). Regulation of the water content is of significant importance to maintain the optimal viscoelastic properties of the mucus.

#### *Implications for drug delivery*

The residence time of an inhaled drug in the lungs depends on the site of deposition. A significant proportion of the drug reaching the lungs from an inhaled aerosol is entrapped in the mucus in the conducting airways. The ability of the drug to penetrate the mucus barrier depend on particle charge, solubility, lipophilicity, and size (Bhat et al., 1995; Rubin, 1996). For instance, a reduced transport across respiratory mucus

layers have been demonstrated *in vitro* for corticosteroids (Hashmi et al., 1999) and antibiotics (Lethem, 1993).

### *3.3.9 Pathophysiological changes*

Pathological conditions affecting the airway and lung tissue, such as pulmonary edema, inflammatory conditions, and damage caused by chemical toxicants or insoluble particles, may severely affect the permeability properties of the epithelial and endothelial barriers and the disposition of drugs in the tissue. Inflammatory lung diseases or repeated mucosal injury, by for instance allergens, viruses, and pollutants, may result in chronic structural changes to the airways such as subepithelial fibrosis, hyperplasia of smooth muscle and goblet cells, epithelial disruption, and plasma exudation (Redington, 2001), collectively referred to as airway remodeling. The structural tissue-changes are related to the severity and duration of the disease and are consistently associated with a decline in lung function. The sequestration of drugs (e.g. amines) in the lung tissue has been reported to be altered with lung injury and disease, such as inflammation, due to the changes in lung tissue composition (Audi et al., 1999; Pang et al., 1982).

Inflammatory lung diseases, such as asthma and chronic bronchitis, are associated with an impaired mucociliary clearance and hyperplasia of submucosal glands and goblet cells leading to a hypersecretion of mucus and obstruction of the airways (Lethem, 1993; Samet et al., 1994). Similar pathophysiological changes to the airways may be induced by respiratory tract infections, allergen challenge, and cigarette smoke (Salathé et al., 1997). As a consequence of the airway obstruction, a proximal shift in the airway deposition pattern of inhaled therapeutic aerosols is observed (Rubin, 1996).

There are conflicting results in the literature on the effect of inflammation and allergic reactions on the airway permeability. Some investigations state that the permeability from the air space into the systemic circulation is increased during lung inflammation (Folkesson et al., 1991; Hogg, 1981; Ilowite et al., 1989), whereas other investigators have demonstrated an unchanged or even decreased airway absorption explained by an instantaneous epithelial restitution in response to epithelial injury (Greiff et al., 2002; O'Byrne et al., 1984; Persson et al., 1997). An increased epithelial permeability of hydrophilic compounds i.e. terbutaline (Mw 225 Da),  $^{99m}\text{Tc}$ -labeled diethylene triamine penta-acetate ( $^{99m}\text{Tc}$ -DTPA; Mw 492 Da), and  $^{113m}\text{In}$ -labeled biotinylated DTPA (Mw 1215 Da) has been demonstrated in smokers as compared to non-smokers (Jones et al., 1980; Mason G.R. et al., 2001; Schmekel et al., 1991).

### *3.3.10 Species differences*

In contrast to the human airways, the airways of dogs and common laboratory rodents (e.g. rat, guinea pig, and rabbit) exhibit a predominantly monopodial branching system (Miller et al., 1993). The major daughter branches have significantly larger diameters and branch with a smaller angle than the minor daughter branches (Sweeney et al.,

1991). Consequently, the monopodial airways have direct pathways to the lung parenchyma (Sweeney et al., 1991), which may have implications for the deposition of pulmonary delivered drugs. In the peripheral airways of all species, the branching of the airways becomes more regular and dichotomous (Sweeney et al., 1991).

In contrast to humans, where the pulmonary circulation only supplies the alveolar region, the pulmonary circulation in rats also supplies blood to the bronchioles and terminal bronchioles (Chediak et al., 1990).

**Table 1.** Comparison of the airways and gas-exchange barrier of human and rat lung

	<b>Human</b>	<b>Rat</b>
Lung lobes	Left lung: 2 Right lung: 3	Left lung: 1 Right lung: 4
Branching	dichotomous, symmetrical, sharp bifurcations for first ten generations	strongly monopodial, very sharp
Respiratory bronchioles	several generations	absent
<i>Structure of gas exchange barrier</i>		
Average body weight (kg)	74	0.140
<i>n</i>	8	8
Thickness of gas diffusion barrier ( $\mu\text{m}$ )	0.62	0.38
Gas exchange surface area/unit lung volume ( $\text{cm}^2/\text{cm}^3$ )	371	750
Capillary volume/ unit lung volume ( $\text{ml}/\text{cm}^3$ )	0.057	0.092
<i>Cellular composition in alveoli (%)</i>		
Average body weight (kg)	74	0.360
<i>n</i>	8	8
Type I	8	9
Type II	16	14
Endothelial	30	46
Interstitial	36	28
Macrophage	9	3
<i>Alveolar surface covering (%)</i>		
Type I	93	96
Type II	7	4

Compiled from (Berg et al., 1989; Crapo et al., 1982; Gehr P., 1984)

The size and function of the pulmonary gas-exchange apparatus in mammals have been found to depend on body size and physical activity (Gehr Peter et al., 1981). Compared

to animal species often used in drug research (such as the rat, mouse, rabbit, and dog), the human lung has the thickest air-blood barrier, the smallest gas-exchange surface area per unit lung volume, and the smallest capillary volume per unit lung volume, Table 1 (Gehr P., 1984).

### **3.4 Metabolic activity and pulmonary distribution of drugs**

#### *3.4.1 Metabolic activity*

The metabolism of many endogenous compounds (e.g. serotonin, norepinephrine, bradykinin, and enkephalin) occur in the endothelial cells of the lung, whereas most xenobiotic metabolizing enzymes (i.e. phase I and II enzymes) are located within the epithelial cells (mainly the Clara cells and alveolar type II cells) (de Wet et al., 1998). The metabolism of xenobiotic compounds in the lung tissue is only partially characterized (Yost, 1999). As the lung is composed of over 60 different cell types (Stone et al., 1992), the characterization of drug metabolizing functions of the different cell types is a complex task. Generally, all metabolizing enzymes found in the liver are also present in the lung, although in lesser amounts (Ma et al., 1996). However, the lung does not express the full range of isoenzymes present in the liver (Upton et al., 1999). For instance, whereas CYP3A4 is the main CYP form in human liver, expression of the isozyme was only found in 20% of the investigated subjects (Anttila et al., 1997). The level of cytochrome P-450 (CYP) in the lung shows approximately 10 fold species variation and is 5-20 times lower than that of the liver (Ma et al., 1996). The pulmonary CYP enzymes are primarily distributed in the Clara cells and the alveolar type II cells (Krishna et al., 1994). Compared to the liver and intestine, the lung is thought to play a minor role in the metabolism of drug compounds (Yost, 1999). However, the lung is the only organ through which the entire cardiac output passes; due to this high pulmonary blood flow, the metabolic capacity of the lung should not be ignored (Ma et al., 1996). For instance, with a cardiac output of 5 l/min and 30% removal of a compound, the pulmonary clearance is 1.5 l/min. This could be compared to the maximal clearance of a compound completely metabolized in the liver which corresponds to a hepatic blood flow of 1.6 l/min (at rest) (de Wet et al., 1998).

The proteolytic activity in the epithelial lining fluid and interstitial fluid is of major interest when aiming at pulmonary delivery of therapeutic peptides since these compounds are considered to be absorbed primarily by the paracellular route (Evans et al., 1998; Wall, 1995). Generally, the lung is thought to have a lower proteolytic activity than many other organs (Hoover et al., 1992; Wall, 1995; Yang et al., 2000). Endopeptidases such as trypsin, chymotrypsin, and endopeptidase 24.11 are reported to have low activity in the rat and dog lung (Forbes B. et al., 1999; Wall et al., 1993), whereas a high activity of chymotrypsin has been found in human bronchoalveolar lavage fluid (Hayem et al., 1980). Relatively high activity of exopeptidases (e.g. aminopeptidases) have been found in rat bronchoalveolar lavage fluid, on the surfaces of the cells lining the respiratory tract, and in the pulmonary circulation (Forbes B. et al., 1999; Forbes B.J. et al., 1995; Funkhouser et al., 1991; Wall et al., 1993). Most of these enzymes are membrane bound (Wall et al., 1993). Cellular release of proteases

into the epithelial lining fluid is a component of the pulmonary host defense and occurs via phagocytosis, but may also be due to leaching from cell damage or death (Ma et al., 1996). In order not to damage the delicate lung tissue, the activity of the proteases is balanced by the release of antiproteases (e.g.  $\alpha_1$ -antitrypsin,  $\alpha_1$ -antichymotrypsin (Ma et al., 1996). However, this balance may be disturbed in the diseased lung.

### *3.4.2. Pulmonary distribution of drugs*

The lung appears to play a minimal role in drug metabolism, however, it plays a significant role in the distribution and accumulation of a variety of endogenous and exogenous compounds (de Wet et al., 1998). Lipophilic basic amines, such as imipramine, propranolol, lidocaine, fentanyl, and verapamil, have been reported to have an extensive first-pass pulmonary uptake and to partition into pulmonary tissue (Anderson et al., 1974; Dollery et al., 1976; Jorfeldt et al., 1979; Roerig et al., 1989; Suhara et al., 1998). The accumulated drug creates a slowly effluxable and displaceable pool and may have implications for drug therapy (Suhara et al., 1998). For instance, imipramine, chlorpromazine, and fentanyl have been demonstrated to displace propranolol from the lung (Kornhauser et al., 1980). The mechanism determining the distribution into the lung tissue is suggested to be simple diffusion followed by association with tissue components, such as partitioning into membranes and subcellular organelles (Ishizaki et al., 1998; Yoshida et al., 1987; Yoshida et al., 1990). Involvement of alveolar macrophages has also been suggested (Kornhauser et al., 1980). The rate and extent of lung uptake depend on drug physicochemical properties such as degree of ionization (pKa) and lipophilicity, and the affinity of the drug for plasma proteins and tissue macromolecules (Anderson et al., 1974; Audi et al., 1998; Audi et al., 1999; Junod, 1976; Roerig et al., 1989; Roerig et al., 1987). Experiments with cultured bovine pulmonary endothelial cells in vitro suggest that the extensive first-pass pulmonary uptake of fentanyl is due largely to vascular endothelial drug uptake by both a passive and a saturable active uptake process (Waters et al., 1999). Evidence of transporter facilitated uptake of fentanyl into the cells was shown in experiments in human lung microvascular endothelial cells (Waters et al., 2000). The uptake was found to be blocked by verapamil but not by an antibody blocking P-glycoprotein, which suggests that a mechanism other than P-glycoprotein transport is involved in the facilitated uptake of fentanyl (Waters et al., 2000). Hence, the identification and characterization of transporters in the lung tissue may lead to a better understanding of the factors that influence pulmonary first-pass uptake.

## **3.5 Mechanisms of drug transport across the lung barrier**

Relatively few detailed investigations have been conducted to elucidate the absorption mechanisms of inhaled pharmaceuticals. Generally, lung physiological investigations show that the airway and alveolar epithelia, not the interstitium and the endothelium, constitute the main barrier that restricts the movement of drugs and solutes from the

airway lumen into the blood circulation (Schneeberger, 1978; Schneeberger et al., 1984).

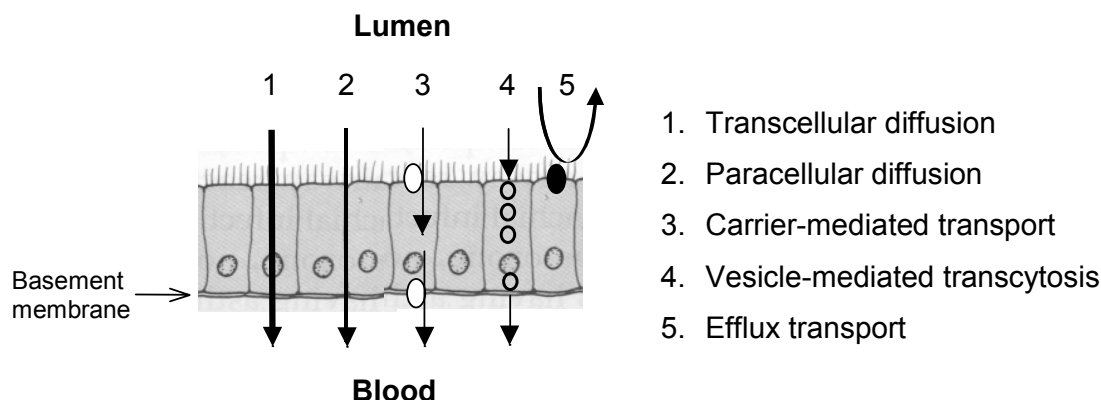


**Figure 4.** Epithelial drug transport mechanisms.

### 3.5.1. Passive diffusion

In the 70's and 80's, Schanker and coworkers conducted a series of studies on the disappearance rate of miscellaneous compounds from the lungs after intratracheal instillation and aerosol inhalation. Their studies showed that most compounds were absorbed by passive diffusion and that the rate of absorption was increased with an increase in lipophilicity for compounds with partition coefficients (chloroform/buffer pH 7.4) ranging from -3 to 2 (Brown et al., 1983; Schanker et al., 1983). The absorption of lipophilic compounds is generally considered to occur by membrane diffusion (Effros et al., 1983), whereas hydrophilic solutes appear to be absorbed by passive diffusion through the intercellular junction pores (Schneeberger, 1991). Passive diffusion is also identified as the main transport mechanism of peptides in cultured rat alveolar epithelial cell monolayers in vitro (Dodoo A.N.O. et al., 2000b; Yu et al., 1997). Likewise, most exogenous macromolecules with a molecular weight less than 40 kDa are thought to be absorbed from the air space through tight junctions by passive diffusion (Hastings et al., 1992; Matsukawa et al., 1997; Patton, 1996). The absorption rate of hydrophilic compounds is inversely related to the molecular weight (range 60- 75000 Da) (Schanker et al., 1976). However, for compounds less than 1000 Da, the effect of molecular weight on the absorption rate appears to be negligible (Niven, 1992).

The aqueous pathways for hydrophilic drug absorption are usually described in terms of intercellular pores, and the rate of diffusion has been demonstrated to be inversely proportional to the molecular radius (Berg et al., 1989; Effros et al., 1983; Taylor G., 1990). Distensions of the lung by increase of the lung volume has been reported to increase the permeability of hydrophilic solutes in human and rabbit lungs (Taylor G., 1990). The underlying mechanism is suggested to be stretching of the epithelium and a subsequent increase of the pore size (Mason G.R. et al., 2001). Species comparisons of

drug absorption from the lungs showed that the rate of absorption of hydrophilic compounds varied between species (mouse, rat, and rabbit), whereas the rate of absorption of lipophilic compounds was about the same (Schanker et al., 1986). Two investigations performed in fluid-filled rat lungs indicate the presence of several different rat alveolar pore populations, i.e. pore radius 0.5 nm and 3.4 nm (Berg et al., 1989), and 5.0 nm and 17.0 nm (Conhaim et al., 2001), among which the 0.5-nm pore is thought to comprise about 99% of all pores (Berg et al., 1989). Experiments in dog lungs have suggested the existence of three populations of pores (pore radius 1.3 nm, 40 nm, and 400 nm, respectively) in the lung epithelial barrier (Conhaim et al., 1988).

### *3.5.2 Transporter-mediated absorption and efflux*

Evidence of carrier-mediated transport through the pulmonary epithelial barrier is relatively limited. The presence of carrier systems for organic anions and amino acids have been suggested from in vivo experiments in rodents (Enna et al., 1973; Gardiner et al., 1974; Lin et al., 1981). Furthermore, carrier-mediated uptake of dipeptides into rat alveolar epithelial cell monolayers (Morimoto et al., 1993) and rabbit tracheal epithelial cell layers (Yamashita et al., 1998) have been reported. Recently, the expression of the high-affinity peptide transporter PEPT2 was demonstrated in tracheal, bronchial, smaller airway epithelial cells, and type II epithelial cells, as well as in endothelial cells of the human and rat lung (Groneberg et al., 2002; Groneberg et al., 2001). The expression of PEPT2 was found to be especially strong in the apical membrane of the epithelial cells (Groneberg et al., 2002). A higher apical to basolateral transport of albumin, immunoglobulin G, and transferrin was reported from experiments in rat alveolar monolayers in vitro, suggesting the involvement of receptor-mediated, or adsorptive endocytotic processes, or both (Matsukawa et al., 2000).

Efflux transporter proteins, first known to mediate multidrug resistance (MDR) in tumor cells, are thought to be involved in the protection of the lungs against inhaled toxic pollutants. Recent publications demonstrate the expression of MDR1-P-glycoprotein (P-gp), multidrug resistance associated protein 1 (MRP1), and major vault protein (MVP or LRP) in normal lungs from human, rat, mouse, and guinea-pig (Scheffer et al., 2002; Sugawara et al., 1997). The expression of breast cancer resistance protein (BCRP), MDR3, MRP2, and MRP3 was either undetectable or very low in the lung tissue (Scheffer et al., 2002).

### *3.5.3 Vesicle-mediated endocytosis and transcytosis*

The existence of a high numerical density of membrane vesicles within the alveolar endothelial cells and epithelial type I cells has long been recognized (Gumbleton, 2001; Newman G.R. et al., 1999). Most of the vesicles are non-coated or smooth-coated vesicle populations, morphologically recognized as caveolae (Gumbleton, 2001). The number of caveolae-like structures in the alveolar type I epithelium is less numerous than in the endothelium. The function of caveolae and the potential capacity are not clear. They may be involved in the transcytosis or vesicular movement of

macromolecules across endothelial cells (Crandall et al., 2001). For instance, albumin has been shown to be transported across the rat pulmonary endothelium by caveolae-mediated transport (Schnitzer, 2001). Direct evidence for the role of alveolar type I cell vesicle populations in transport across the alveolar epithelium is at present limited (Gumbleton, 2001). The general view is that alveolar vesicle-mediated trafficking across the air-blood barrier functions as a minor pathway in protein absorption (Gumbleton, 2001; Patton, 1996).

#### *3.5.4 Particle transport*

Ultrafine particles (diameter  $\leq 100$  nm) have been demonstrated to pass rapidly (within 5 min) from the lungs into the systemic circulation after intratracheal instillation into hamsters and aerosol inhalation in humans (Nemmar et al., 2002; Nemmar et al., 2001). Transport through large pore populations (40-nm and 400-nm pore radius) (Conhaim et al., 1988) was suggested to contribute to the rapid translocation into blood, but the exact mechanism of the particle transport remains to be established (Nemmar et al., 2002). After administration of aerosolized ultrafine particles into rats, the particles were found in the alveolar walls and in pulmonary lymph nodes (Takenaka et al., 2001), which suggests that drainage into the lymph may contribute to the air-to-blood transport of the inhaled particles.

### **3.6 Drug delivery to the lung**

#### *3.6.1 Particle deposition*

The respiratory tract can be considered as a filter that removes particles from the inspired air (Heyder et al., 2002). The effectiveness of the filter depends on particle properties (e.g. size, shape, density, and charge), respiratory tract morphology, and the breathing pattern (e.g. airflow rate and tidal volume) (Heyder et al., 2002). These parameters determine not only the quantity of particles that are deposited but also in what region of the respiratory tract the particles are deposited. As the cross-sectional area of the airways increases, the airflow rate rapidly decreases, and consequently the residence time of the particles in the lung increases from the large conducting airways towards the lung periphery (Schulz et al., 2000). The most important mechanisms of particle deposition in the respiratory tract are inertial impaction, sedimentation, and diffusion (Figure 5). Inertial impaction occurs predominantly in the extrathoracic airways and in the tracheobronchial tree, where the airflow velocity is high and rapid changes in airflow direction occurs (Schulz et al., 2000). Generally, particles with a diameter larger than  $10\ \mu\text{m}$  are most likely deposited in the extrathoracic region, whereas 2- to  $10\text{-}\mu\text{m}$  particles are deposited in the tracheobronchial tree by inertial impaction (Schulz et al., 2000). A long residence time of the inspired air favors particle deposition by sedimentation and diffusion (Heyder et al., 2002). Sedimentation is of greatest importance in the small airways and alveoli and is most pronounced for particles with a diameter of  $0.5\text{-}2\ \mu\text{m}$  (Schulz et al., 2000). Ultrafine particles ( $<0.5\ \mu\text{m}$

in diameter) are deposited mainly by diffusional transport in the small airways and lung parenchyma where there is a maximal residence time of the inspired air (Heyder et al., 2002). The relationship between particle size and total respiratory tract deposition has been demonstrated to be similar among species (Schlesinger, 1985).

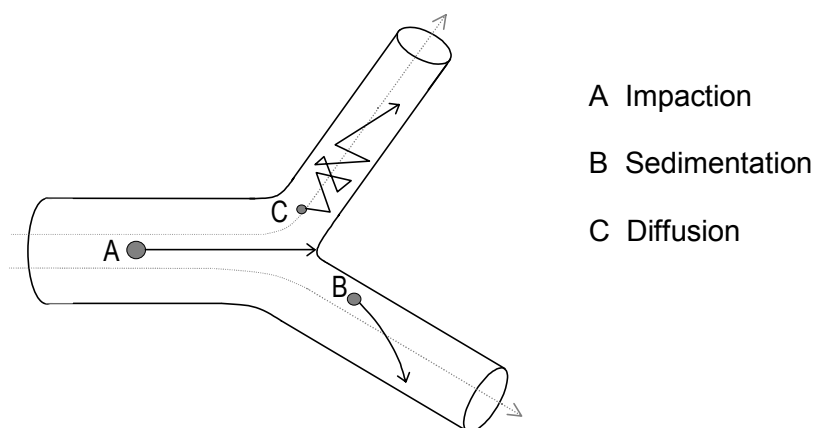


**Figure 5.** Mechanisms of particle deposition in the airways.

### 3.6.2 Techniques for pulmonary drug delivery

Optimal drug delivery to the lungs depends on an interaction between the inhaler device, the drug formulation properties, and the inhalation maneuver (Newman S.P., 1998). The devices currently available for pulmonary drug administration of pharmaceutical aerosols in clinical therapy include nebulizers, pressurized metered dose inhalers (pMDIs), and dry powder inhalers (DPIs). However, much effort is put into the development of new inhaler devices and formulations to optimize the pulmonary delivery system for local or systemic drug targeting (Edwards et al., 1997; Patton, 1997; Sakagami et al., 2002c; Schuster et al., 1997; Steiner et al., 2002; Suarez et al., 1998). For instance, regional drug deposition, delivery efficacy, and prolonged retention of the drug in the lungs are being investigated.

The use of pMDIs and DPIs for preclinical studies in small animals is limited by the need for formulation development, which often cannot be performed in early drug discovery due to short supply of test materials. Instead, liquid instillation and nebulized aerosols are the predominating delivery methods for pulmonary drug administration to experimental animals (Dahlbäck et al., 1996; Hickey et al., 2001; Raeburn et al., 1992; Sweeney et al., 1991). A number of other techniques for intratracheal administration of coarse sprays and powder formulations have also been described (Ben-Jebria et al., 2000; Byron et al., 1988; Concessio et al., 1999; Leong et al., 1998; MacIntyre, 2001; Okamoto et al., 2000).

In animal studies, the site of lung deposition is strongly related to the method of delivery.

Intratracheal instillation of liquid formulations offers rapid delivery of defined doses to small animals, but mainly results in central, patchy, and inhomogeneous lung distribution (Brain et al., 1976; Folkesson et al., 1992). To obtain reliable dosing, the liquid must be carefully instilled in order not to cause airway obstruction, disturb the normal breathing pattern of the animal, or induce cough, which would lead to rapid clearance of part of the dose from the airways into the mouth and stomach. Although there are differences in the distribution, clearance, and retention of test material when administered by instillation compared to inhalation (Driscoll et al., 2000), the instillation procedure is the most commonly used method and has been applied in many pharmacokinetic and pharmacodynamic investigations (Folkesson et al., 1998; Schanker et al., 1986; Taljanski et al., 1997). When the method is applied to rats, the typical instillation volume is about 0.1-0.5 ml (1-2 ml/kg body weight). This volume corresponds to 6-31% of the average tidal volume of the rat (1.6 ml) (Green, 1979). If these liquid instillation volumes are scaled to adult humans with an average tidal volume of 500 ml at rest (Hlastala et al., 1996), they would comprise administration of 31 to 156 ml of liquid to the airways. In contrast, only 2-4 ml of liquid, corresponding to 0.4 to 0.8% of the tidal volume, is administered as nebulized aerosols to patients in clinical therapy. Hence, the liquid instillation procedure has been pointed out as being nonphysiologic (Driscoll et al., 2000). Another concern regarding instillation is the influence of the instilled vehicle in which the drug is suspended or dissolved. If it alters the physicochemical nature of the drug, it may alter the effect of the drug in the lungs and affect the physiological barriers of the lung (Driscoll et al., 2000).

Aerosol inhalation is also used for pulmonary drug administration in animal studies. This delivery method results in a more uniform lung distribution, compared to liquid instillation, and has more pronounced distribution into the alveolar region (Brain et al., 1976; Folkesson et al., 1992). One disadvantage of the aerosol inhalation is, however, that a substantial portion of the aerosolized drug is not delivered to the lungs (i.e. delivered to the nose, mouth, skin, exhaled) during the exposure; therefore, dosimetric calculations are needed to determine the lung burden (Dahlbäck et al., 1996). An aerosol delivery systems leading the aerosol directly to the lungs of anesthetized animals via endotracheal tubes have been described (Eirefelt et al., 1992). Only a small fraction of the delivered aerosol was deposited in the lungs; hence, dosimetric calculations were still needed. The difficulty in determining the exact dose deposited in the lungs can compromise the accurate calculation of e.g. pharmacokinetic parameters. Recently, another aerosol delivery system, which allows exact calculation of both the amount of drug delivered to the lungs of the animals and the amount exhaled was reported (Lizio et al., 2001). However, in general the aerosol exposure techniques have a low dosing effectiveness, which often requires longer exposure times to administer the target dose and renders investigations of rapid kinetic events difficult. In addition, aerosol exposure requires an advanced equipment for exposure and ml-quantities of test formulation to fill up the device (Dahlbäck et al., 1996; Raeburn et al., 1992).

In experiments comparing the pulmonary drug absorption characteristics, it is important to secure a reproducible lung distribution profile of the administered drug via the

administration procedures. Regional physiological differences in the respiratory barrier may influence the rate and extent of absorption of drugs delivered to the respiratory tract (Patton, 1996). A higher pulmonary absorption rate, or bioavailability, or both have been demonstrated for various small compounds (Schanker et al., 1986) and for peptides and proteins after aerosol inhalation compared to liquid instillation (Colthorpe et al., 1995; Colthorpe et al., 1992; Folkesson et al., 1992; Niven et al., 1995). The use of a pulmonary delivery method that mimics the methods used in clinical therapy may, therefore, be important for preclinical investigations of pulmonary drug absorption.

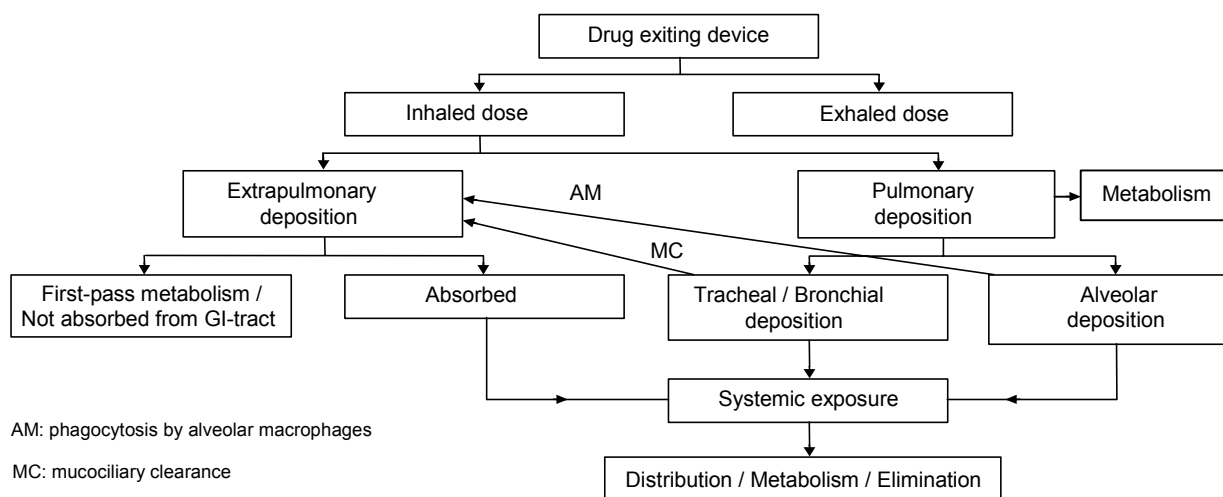


**Figure 6.** Schematic illustration of the fate of an inhaled drug.

### 3.7 Biological models for assessment of pulmonary drug absorption

Several models are available for preclinical investigations of pulmonary drug absorption and deposition. The complexity of the models range from permeability screening experiments in cell culture models to in vivo pharmacokinetic analyses in animals. The design of the experiments comprises both selection of the most relevant biological model for the specific issue, and the selection of a drug delivery system that is appropriate for the amount of test material available and that can selectively deposit a defined dose of the drug to the intended lung region (see section 3.6). A combination of in vitro and in vivo models are needed to elucidate the mechanisms, rate, and extent of absorption, as well as the distribution, metabolism and elimination of a drug after pulmonary administration.

#### 3.7.1 In vivo animal models

In vivo pharmacokinetic experiments in animals provide data on the fate of a drug and its metabolites in the body by assessment of the drug concentration in plasma or tissues.

In the absence of a significant amount of human absorption data, accurate *in vivo* pharmacokinetic investigations in animals are important to establish *in vitro-in vivo* relationships. For determination of the pulmonary absorption rate and bioavailability, plasma is sampled at predetermined time points after pulmonary drug administration and analyzed for drug content (Adjei et al., 1992; Krondahl et al., 2002; Taljanski et al., 1997). An intravenous dose may be administered as reference. For investigations of the retention of the drug in the lung tissue, or first-pass pulmonary uptake, or both, drug concentrations in lung tissue are assessed (Brown et al., 1983; Drew et al., 1981; Jendbro et al., 2001). The applied pulmonary administration procedure should be carefully selected to deliver the dose with high precision regarding both dose quantity and deposition pattern. A disadvantage of the *in vivo* models is that the animals often need to be anesthetized during drug administration to the lungs and at blood sampling. The effect of anesthesia on physiological functions should thus be considered in the design of the experiments. For instance, the use of volatile anesthetics has been demonstrated to increase the alveolar epithelial permeability (ChangLai et al., 1999; Wollmer et al., 1990) and to destabilize surfactant (Evander et al., 1987; Wollmer et al., 1990). Anesthesia may also impair the mucociliary clearance (Patrick et al., 1977).

### *3.7.2 Isolated and perfused lungs*

By the use of isolated and perfused lung models, lung-specific pharmacokinetic events can be investigated without the contribution of systemic distribution, metabolism, and elimination. In these models, the structural and cellular integrity of the lung tissue, the permeability barriers, interaction between different cell types, and biochemical activity are maintained (Mehendale et al., 1981). Procedures for lung perfusion have been described for rats, guinea pigs (Ryrfeldt et al., 1978), and rabbits (Anderson et al., 1974). Compared to *in vivo* models, the isolated and perfused lung models provides certain advantages, such as careful control of the ventilation and perfusion of the lung, facilitated administration of drugs to the airway lumen or vascular circulation, easy sampling of perfusate and lavage fluid, as well as easy determination of mass-balance. Hence, the design of the experiments can be adapted to specifically address issues regarding absorption, tissue sequestration, and metabolism. The main drawback of the lung models is that the limited viability of the preparation (about 5 hours) (Bassett et al., 1992; Fisher et al., 1980) prevents investigations of slow pharmacokinetic processes. Isolated and perfused lung models have successfully been applied to investigate drug dissolution and absorption (Niven et al., 1988; Tronde et al., 2002), mechanisms of absorption (Sakagami et al., 2002a), disposition (Audi et al., 1998; Ryrfeldt et al., 1989), and metabolism (Dollery et al., 1976; Gillespie et al., 1985; Longmore, 1982; Tronde et al., 2002).

### *3.7.3 Cell culture models*

The inaccessibility and heterogeneous composition of the airway epithelium makes it difficult to mechanistically evaluate pulmonary cellular integrity and physiological functions. For investigations of drug transport mechanisms, precise dosing and

sampling, as well as defined local drug concentration and surface area of exposure, are important parameters that need to be controllable and reproducible. Therefore, a variety of airway and alveolar epithelial cell culture models of animal and human origin have been established as in vitro absorption models (Elbert et al., 1999; Foster et al., 2000; Morimoto et al., 1993; Winton et al., 1998; Yamashita et al., 1996). The models include both cell lines (airway) and primary cell cultures (airway and alveolar). The primary cell cultures more closely resemble the native epithelia, but are less reproducible and more time-consuming to work with compared to the cell lines, which make them less suitable for permeability screening purposes. Two immortalized human bronchial epithelial cell lines, the Calu-3 and 16HBE14o-, have been suggested as suitable models to investigate the airway epithelial barrier function (i.e., tight junction properties) (Wan et al., 2000; Winton et al., 1998). The Calu-3, adenocarcinoma epithelial cells of serous origin from the bronchial airways, comprise a mixed phenotype of ciliated and secretory cells (Mathias et al., 2002) and form tight, polarized and well differentiated cell monolayers with apical microvilli in air-liquid interface culture (Foster et al., 2000; Mathias et al., 2002). The cell line has recently been applied in some experiments investigating airway drug transport mechanisms (Borchard et al., 2002; Florea et al., 2001; Hamilton et al., 2001a; Hamilton et al., 2001b; Mathias et al., 2002; Pezron et al., 2002). At present there is, to our knowledge, no characterized epithelial cell line available for investigations of the alveolar barrier functions. Instead, alveolar type II cells, isolated from normal human lungs, rats and rabbits, in primary cultures have been demonstrated to differentiate into type-I-like cells and to form tight epithelial barriers morphologically similar to the in vivo alveolar epithelium (Elbert et al., 1999; Matsukawa et al., 1997; Shen et al., 1997). These models have been used for several investigations of alveolar transport (Dodoo A.N. et al., 2000a; Elbert et al., 1999; Matsukawa et al., 1996; Morimoto et al., 1993; Saha et al., 1994; Shen et al., 1997).

**Table 2:** Factors that may affect the pulmonary absorption rate and bioavailability

Device and formulation	Drug	Physiology
particle properties (size, density, shape, charge)	dissolution rate	breathing pattern
deposition pattern	solubility	blood flow
excipients	lipophilicity	airway morphology
concentration	molecular weight	surface area
osmolarity	charge	mucociliary clearance
viscosity	hydrogen bonding potential	lung surfactant
pH	aggregation/complex binding	alveolar macrophages
dose size/volume	conformation	epithelial permeability
	chemical stability	endothelial permeability
	enzymatic stability	transporter proteins
		enzymatic/metabolic activity
		disease
		tissue composition (drug sequestration)

## 4. AIMS OF THE THESIS

The overall aim of the thesis was to investigate drug absorption characteristics of the lung, using both in vitro and in vivo biological models.

The specific aims were to:

- Adapt and evaluate the nebulization catheter device as a new approach for delivery of defined breath synchronized aerosol doses to the rat lung (*Paper I*).
- Investigate the feasibility of pulmonary delivery of the hydrophilic  $\mu$ -selective opioid tetrapeptide agonist (TArPP). The oral bioavailability of the peptide is 0.5% due to a low oral permeability and enzymatic degradation in the gastrointestinal tract (*Paper II and III*).
- Investigate the pulmonary first-pass metabolism of TArPP (*Paper II and III*).
- Investigate regional differences in bioavailability, absorption rate, and first-pass metabolism of TArPP after delivery to different regions of the respiratory tract in vivo in rats (*Paper III*).
- Compile a physicochemical profile of the inhaled drugs on the market during 2001 (*Paper V*).
- Investigate the relationships between drug physicochemical properties and the pulmonary absorption rate and bioavailability using both in vitro and in vivo absorption models (*Paper IV and V*).
- Study the air-to-blood absorption of efflux transporter substrates (*Paper IV and V*).
- Evaluate the in vitro-in vivo relationship between the drug absorption in the isolated and perfused rat lung and in rats in vivo.
- Evaluate the usefulness of the epithelial permeability screening model, Caco-2, to predict the pulmonary absorption rate and bioavailability for passively transported drugs (*Paper IV and V*).
- Compare the permeability of the pulmonary and the intestinal mucosal barriers.

## 5. MATERIALS AND METHODS

### 5.1 Drugs and marker compounds

TArPP (Tyr-D-Arg-Phe-Phe-NH<sub>2</sub> x 2HCl; MW 704 Da) was synthesized at BioChem Therapeutics (Montreal, Canada) and kindly provided by AstraZeneca R&D Södertälje (Södertälje, Sweden). Atenolol, metoprolol, and talinolol were kindly provided from AstraZeneca R&D Mölndal (Mölndal, Sweden), and terbutaline, formoterol, and budesonide from AstraZeneca R&D Lund (Lund, Sweden). Losartan was obtained from Merck (West Point, USA). Propranolol, enalapril maleate, enalaprilate, and cromolyn were purchased from Promochem (Ulricehamn, Sweden), and cyanocobalamin, FITC-dextran 10 000, Nile Blue, and Evans Blue were purchased from Sigma-Aldrich Sweden AB (Stockholm, Sweden).

TArPP is a peripherally acting  $\mu$ -selective opioid tetrapeptide agonist designed to be excluded from the central nervous system (Alari et al., 1996). The resistance of TArPP to enzymatic degradation was increased by incorporation of a D-amino acid in the second position and amidation of the C-terminus (Pert et al., 1976; Taylor M.D et al., 1995). However, despite this chemical stabilization, the peptide is extensively metabolized by pancreatic enzymes in rat jejunal fluid and in intestinal homogenates in vitro (Kron Dahl et al., 1997; Kron Dahl et al., 2000). In addition, the hydrophilic properties of the molecule,  $\log D_{\text{octanol/water pH 7.4}}$ : -3.0, positive charge at pH 7.4, hydrogen bonding potential: 17, and its relatively high molecular weight (631 Da) do not favor oral permeability. Consequently, the bioavailability of TArPP after oral delivery in rats is only about 0.5% (G. Ekström, unpublished results).

### 5.2 Animals

Male Sprague Dawley rats (Møllegaard, Ejby, and M&B A/S, Ry, Denmark) were used in the studies. After arrival, the rats were acclimatized for at least one week under standardized temperature (21-22°C), humidity (50-60%), and light (12:12 light-dark) conditions at the Veterinary Science Department at AstraZeneca R&D Lund, Sweden or at Safety Assessment AstraZeneca R&D Södertälje, Sweden. Five animals were kept in each cage (Macrolon type IV) with litter (B&K Universal, Sollentuna, Sweden) and had free access to pelleted food (lactamin R70, Lactamin, Vadstena, Sweden) and tap water. The studies in this thesis were carried out in compliance with approval number M25/98 and M5/99 issued by the Animal Ethics Committee in Lund, Sweden, and approval number S/50 issued by the Animal Ethics Committee Stockholm's Södra, Huddinge Tingsrätt, Sweden.

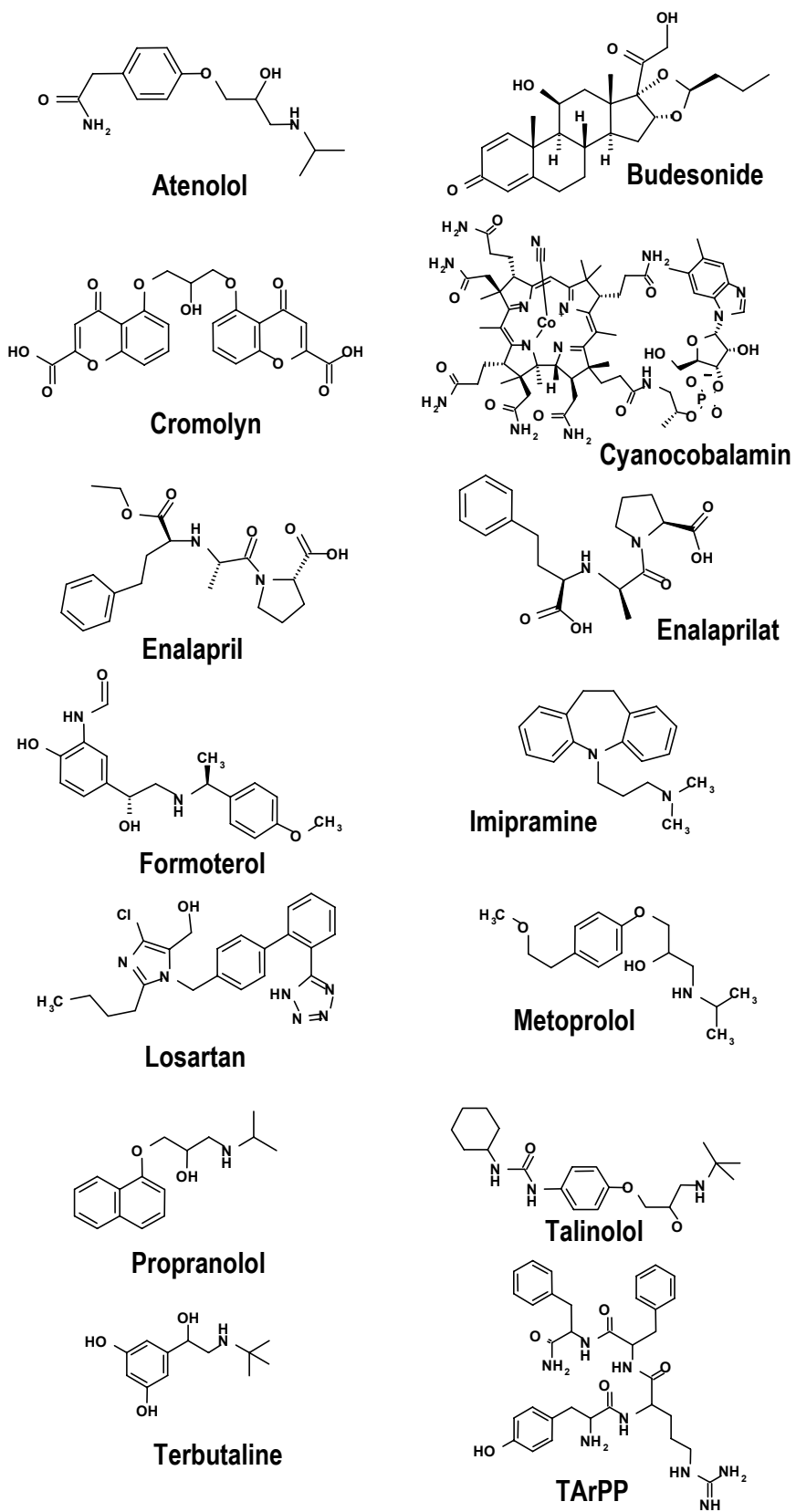


*Figure 7. Chemical structures of the investigated drugs.*

## 5.3 Nebulization catheters and breath synchronized aerosol delivery

### 5.3.1 Nebulization catheters

Nebulization catheter prototypes (AeroProbe™, [www.trudellmedical.com](http://www.trudellmedical.com)) were provided by Trudell Medical International (London, Ontario, Canada) for evaluation of the device (*Paper I*) and for lung absorption experiments (*Paper II-V*). The device was driven by compressed air. The close proximity of the air and liquid orifices at the distal tip of the catheter results in efficient aerosolization of the liquid formulation (Figure 8).

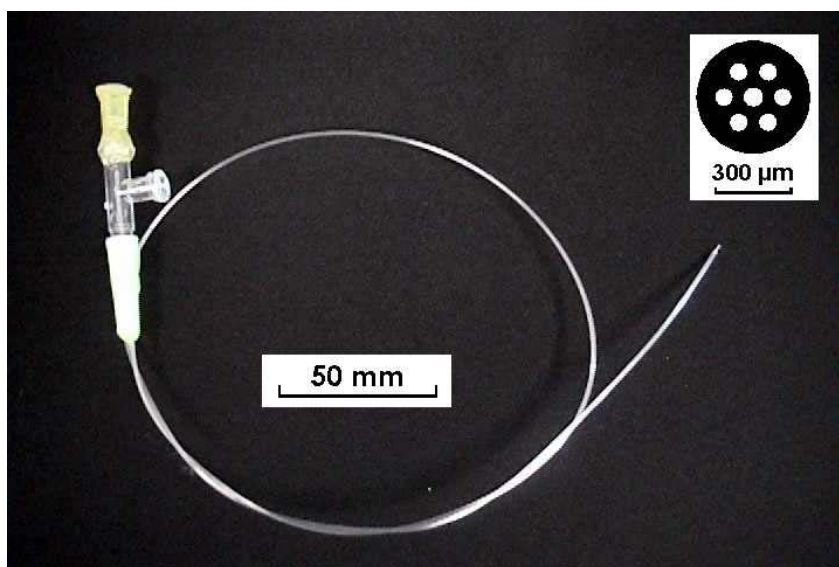


**Figure 8.** Prototype nebulization catheter consisting of a single extrusion (50 cm long) with six integral gas capillaries (diameter 57  $\mu\text{m}$ ) and a central liquid capillary (diameter 57  $\mu\text{m}$ ). The capillaries converge and terminate as tiny orifices at the distal tip of the catheter. The insert shows the cross-section of the tip.

Dosing was performed as a pulsed delivery of aerosol. A precision syringe (Trudell Medical International, London, Canada) was used as reservoir for the liquid formulation and was connected to the liquid capillary at the proximal part of the catheter. The output of liquid formulation was controlled by adjustment of a pulse time on the compressed air-driven fluid-dispensing unit (Trudell Medical International) (Figure 11). An air valve control (AVC) unit (AstraZeneca R&D Lund, Sweden) was used to set the pulse time for the atomizing air. Pressurized air, 5 bar, was used for the dose actuation and at the settings used, the volume of air ejected from the tip of the catheter was about 1-1.5 ml per puff. In the aerosol characterization experiments (*Paper I*) dose actuation was manually triggered by pressing a foot-switch.

### *5.3.2 Breath synchronized aerosol delivery in the isolated and perfused rat lung*

In the lung distribution and absorption experiments performed in the isolated and perfused rat lung model (*Paper I, II, and IV*) the dose actuation was automatically triggered and synchronized with the inspiration of the lung by connection of the AVC-unit to the ventilator (Figure 11). The synchronization was adjusted to provide reproducible aerosol delivery in each inspiration cycle when 20% of the tidal volume had been inhaled.

### *5.3.3 Breath synchronized aerosol delivery to the rat lung in vivo*

A breath-controlled dosing unit (BCDU) was developed to permit automatic triggering of aerosol doses from the nebulization catheter device, and to synchronize the dosing with the inspiration of the anesthetized and intubated rats (*Paper III and V*). The animals were intubated using an airway cannula (PE-240) with a side tube connected to a pressure transducer for continuous measurement of the tracheal pressure. A negative pressure indicated the inspiration phase of the respiratory cycle and a positive pressure indicated the expiration phase. A trigger point was set at the time point during the inspiratory phase when about 20% of the tidal volume had been inhaled.

## **5.4 Aerosol characterization and dosing uniformity (*Paper I*)**

### *5.4.1 Delivered dose weight*

The delivered liquid dose weights were determined by gravimetric analysis (*Paper I-V*).

### *5.4.2 Aerosol cloud formation*

High-speed video analysis was used to visualize the aerosol cloud formation at the catheter tip. The recorded information was used to optimize the dose actuation procedures (Figure 9) and to estimate dosing duration (*Paper I*).

### *5.4.3 Droplet-size distribution*

Laser diffraction (Malvern Mastersizer X) was used to estimate the droplet-size distribution of the generated aerosols (*Paper I-V*). The analysis function was based on the Mie theory model of light scattering using the optical properties for water in air, and the range of measurement was 0.5–180  $\mu\text{m}$ . The tip of the catheter was placed at a right angle and close to the laser beam (Figure 10). The setup minimized the risk of evaporation of droplets before the measurement, and thus alteration in droplet-size

distribution compared to the actual droplet-size distribution that enters the respiratory tract (Clark, 1995). The setup corresponded to a previously described methodology for droplet-size determination from nebulizers using laser diffraction instruments (Nerbrink, 1997).

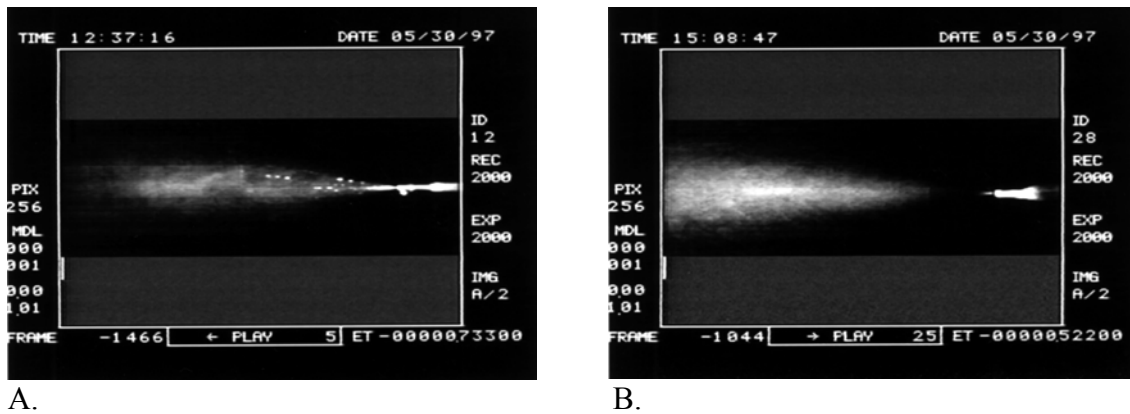


**Figure 9.** Snapshots from high-speed video analysis showing the aerosol cloud formation at the tip of the nebulization catheter at dose actuation. The pulse times for air ejection and liquid ejection were 100 ms and 50 ms, respectively. (A) No time delay between the start of air ejection and liquid ejection. (B) A 20-ms time delay between the air and liquid ejections improved the quality of the generated aerosol.

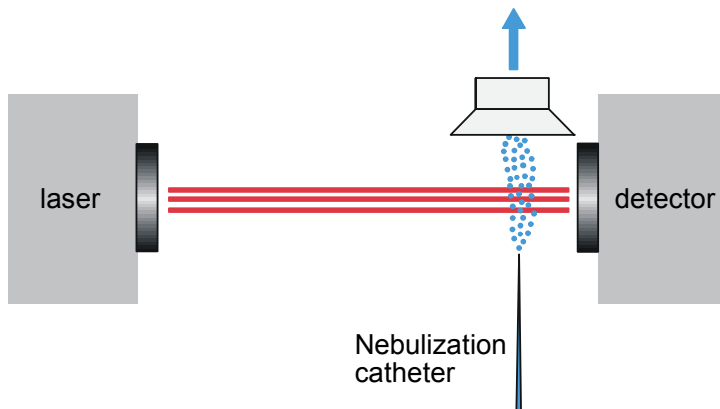


**Figure 10.** Schematic illustration of the setup used to estimate the aerosol droplet-size distribution using laser diffraction.

#### 5.4.4 Lung distribution experiments

The lung distribution profiles of the generated aerosols were investigated in the isolated and perfused rat lung, and in rat lungs in vivo, using Evans blue and Nile blue, respectively, as distribution markers (*Paper I*). The dosing procedures were adapted to suit the physiological and technical prerequisites of the respective model to achieve high delivery efficacy and distal distribution of the aerosol dose in the lung.

In the IPL-experiments, 20 µl Evans Blue solution was administered in 10 aerosol puffs synchronized with the inspiration of the lung. The breath frequency was 30 breaths/min, during the administration phase, to enhance peripheral distribution of the aerosol in the lungs. The nebulization catheter was inserted into the trachea, placing the tip of the catheter 3-5 mm above the bifurcation of trachea into main bronchi. Immediately after dosing, the perfusion was stopped and the ventilator pump switched off. The lung was removed from the chamber and dissected into parenchyma, bronchi, and upper- and lower trachea, according to previously described procedures (Dahlbäck et al., 1996).

In the in vivo experiments, in tracheal-intubated anesthetized rats, 20 µl Nile Blue solution was administered in 20 aerosol puffs synchronized with the inspiration of the animal. The breath frequency was about 80-100 breaths/min. The nebulization catheter was inserted halfway down the trachea, placing the tip of the catheter 2-3 mm past the end of the tracheal cannula. Immediately after dosing, the nebulization catheter was removed and after one minute, the tracheal cannula was also removed. The trachea and lungs were isolated and dissected into parenchyma, bronchi, and upper- and lower trachea as described above.

Evans Blue and Nile Blue were extracted from the tissue samples, by shaking in formamide or ethanol, respectively. The concentration of Evans blue and Nile blue in the samples was determined using a spectrophotometer, and the total recovery of the delivered dose in each lung was calculated. The fractional distribution in each lung region (upper- and lower trachea, bronchi, and parenchyma) was calculated by dividing the amount of marker compound extracted from each region by the total amount of marker compound recovered from the whole lung.

### 5.5 The isolated and perfused rat lung (*Paper I, II, IV*)

#### 5.5.1 Experimental setup

An isolated and perfused rat lung model (IPL) with negative pressure ventilation (Figure 11) was used for the lung deposition (*Paper I*) and lung absorption experiments (*Paper II and IV*). Briefly, after tracheotomy, the pulmonary artery and vein were cannulated, and the lungs were carefully dissected free together with the heart and suspended by the trachea in a humidified jacketed glass chamber maintained at 37°C. Ventilation was carried out by creating an alternating negative pressure inside the chamber, relative to the ambient atmosphere, using a rodent ventilator. A modified Krebs-Ringer buffer was

used to perfuse the pulmonary circulation at a constant flow rate of about 12 ml/min. After isolation, the lung preparation was allowed to stabilize during single-pass perfusion for 10 to 15 min. Perfusion was then switched to recirculation of 50 ml of buffer (except for the lung distribution experiments, *Paper I*). The perfusion flow rate, tracheal airflow, alternating negative pressure in the chamber, and the tracheal pressure were measured. Data on lung mechanics (tidal volume, dynamic compliance, airway conductance) and perfusion flow were collected and assessed during the experiments at consecutive time points to check that the preparation remained viable. Gas exchange was checked by measurement of pCO<sub>2</sub> and pO<sub>2</sub> in the perfusion medium. Visual inspection for signs of edema formation was also undertaken. The pH of the circulating buffer was maintained at 7.35-7.45 by adding CO<sub>2</sub>. An increase in the inhaled air volume was induced at regular intervals to prevent atelectasis of the peripheral airways.

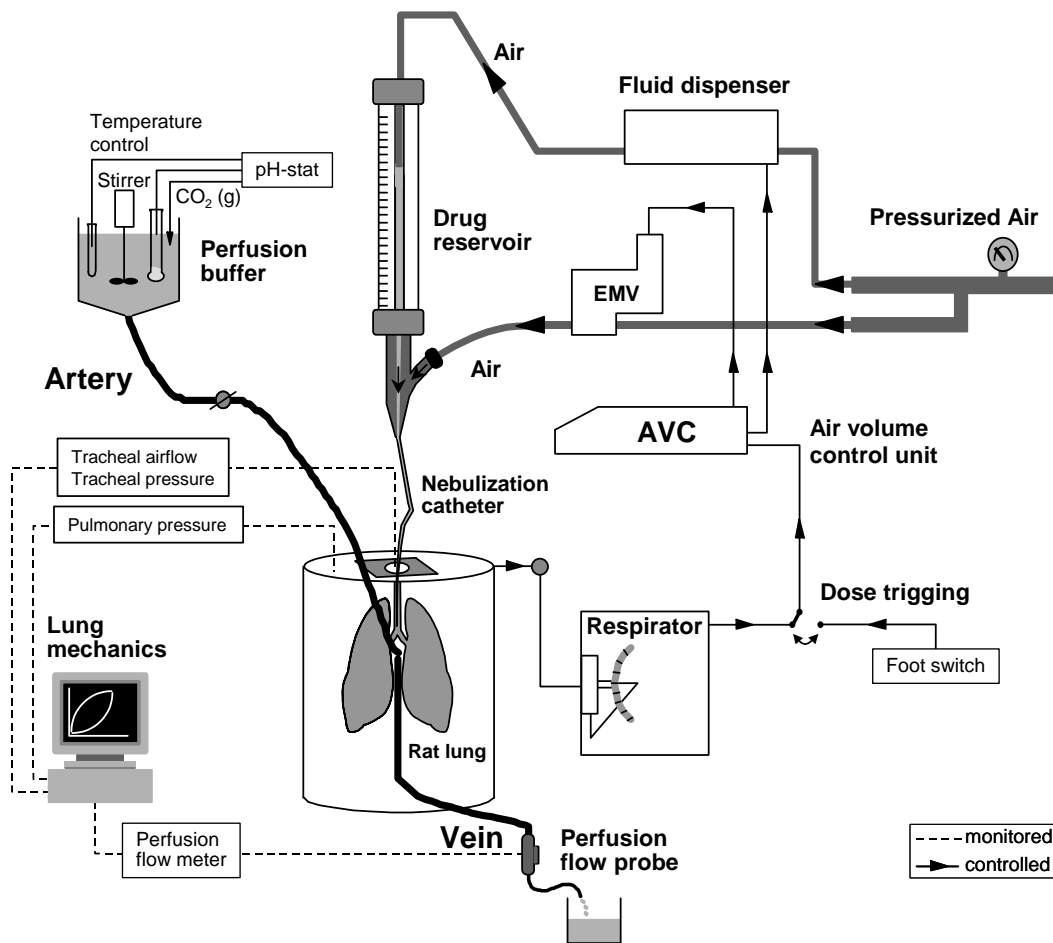


**Figure 11.** Schematic illustration of the experimental setup for the isolated and perfused rat lung, and the nebulization catheter device with dosing equipment mounted for intratracheal aerosol generation to the lung. The lung model includes real-time monitoring of calculated parameters of lung mechanics and of perfusion flow. Fluid dispenser: used to set liquid pulse time and air pressure; EMV: electromagnetic valve; AVC: air valve control unit, used to set the pulse time of atomizing air, set the number of doses to be actuated, and to synchronize dosing with respirator pump.

### 5.5.2 Lung absorption and metabolism experiments

Drug administration to the airways of the lung preparation was performed by the use of nebulization catheters. The drugs (*Paper II*, TArPP; *Paper IV*, atenolol, budesonide, enalapril, enalaprilate, formoterol, losartan, metoprolol, propranolol, and terbutaline) were dissolved in saline, filtered, and transferred to the liquid formulation reservoir (Figure 11). The intratracheal aerosol doses were delivered just above the bifurcation of trachea into the main bronchi. Before and after dosing, aerosol doses were sampled in test tubes to determine the delivered dose weight. During dosing to the lung, the breath frequency was decreased from 80 to 30 breaths/min to enhance peripheral distribution of the dose in the lungs. Immediately after dosing, the breath frequency was restored and inhalation of an enlarged volume of air was induced.

In *Paper II*, vascular administration of TArPP to the lung preparation was performed by addition of a bolus dose to the circulating perfusate.

The perfusion buffer (50 ml) was recirculated and samples were withdrawn before dosing (time 0) and then at predetermined time points during the 2-h experiments to assess the air-to-blood absorption profile of the administered drugs. Withdrawn sample volumes were replaced with fresh perfusion buffer.

In *Paper II*, bronchoalveolar lavage (BAL) was performed to determine the recovery of TArPP and metabolites (M1-M5) in the airway lumen after 2 h. In *Paper IV*, the tracheas and lung tissues dosed with budesonide were collected to analyze the content of budesonide and budesonide ester conjugates after termination of the experiments (Jendbro et al., 2001).

The drug mass-transport (% transferred) from the airway to perfusate was calculated as the mass-fraction of the given dose recovered in the perfusate, compensated for the amount in withdrawn samples. The time needed for transfer of 50% of the amount of drug recovered in the perfusate after 120 min was defined as the absorption half-life ( $t_{1/2}$ , min), modified from Byron et al. (Byron et al., 1986). The apparent first-order absorption rate constant ( $k_{a, \text{lung}}$ ) was calculated according to the equation:

$$k_{a, \text{lung}} = \frac{\ln 2}{t_{1/2}} \quad (\text{Eq. 1})$$

## 5.6 In vivo pharmacokinetic models in anesthetized rats (*Paper III, V*)

### 5.6.1 Anesthesia and treatment protocols

In vivo pharmacokinetic experiments were performed in anesthetized rats to determine the bioavailability and absorption rate of the drugs after delivery to the respiratory tract. Depending on differences in experimental design, animals of different age, different anesthesia, and different sampling procedures were applied.

In *Paper III*, male Sprague -Dawley rats (240–320g) were anesthetised with an intraperitoneal (i.p.) injection of Inactin<sup>®</sup> (thiobutabarbital sodium, Research Biochemicals International, MA, USA) and put on heating pads to maintain normal body temperature. The rats were tracheotomized with a polyethylene tube to facilitate breathing and dosing to the airways. The right femoral artery and the left jugular vein (i.v. bolus and i.v. infusion groups only) were cannulated for blood sampling and i.v. administration, respectively. The peptide, TArPP, was dissolved in saline and administered to different regions of the respiratory tract using different administration techniques (Table 3).

**Table 3.** Experimental design in *Paper III*.

Animal group	Deposition site	Administration technique	Nominal dose of TArPP ( $\mu\text{mol/kg}$ )
1	Intravenous	i.v. bolus dose	1
2	Intravenous	i.v. constant rate infusion	7
3	Nasal cavity	i.n. microinfusion	10
4	Trachea	i.t. microinfusion	10
5	Trachea and bronchi	i.t. nebulization	1
6	Trachea and bronchi	i.t. nebulization	10
7	Whole lung	aerosol inhalation	1

i.v. intravenous; i.n. intranasal; i.t. intratracheal

In the aerosol inhalation experiments, the inhaled dose (ID) was calculated using the equation (Eirefelt et al., 1992):

$$\text{ID} = \text{CC} \times \text{RMV} \times \text{ET} \quad (\text{Eq. 2})$$

where CC is the chamber concentration, estimated from filter sampling during each experiment, RMV is the respiratory minute volume calculated according to (McMahon et al., 1977), and ET is the exposure time. The dose deposited in the lungs was estimated to be 8.5% of the inhaled dose (ID) (Eirefelt et al., 1992).

In *Paper V*, male Sprague -Dawley rats (270-500g) were anesthetised by an s.c. injection of Rompun<sup>®</sup> vet. (Bayer AB, Göteborg, Sweden) followed by an i.p. injection of Ketalar<sup>®</sup> (Pfizer AB, Täby, Sweden) 10 min later, and put on heating pads to maintain normal body temperature. A Neoflon<sup>®</sup> catheter was inserted in the caudal vein for i.v. bolus administrations and for dosing of additional Ketalar when necessary to maintain anesthesia. The investigated drugs (cromolyn, cyanocobalmin, formoterol, imipramine, losartan, metoprolol, talinolol, and terbutaline) were dissolved in saline and administered as an i.v. bolus dose and intratracheal nebulization, respectively. The rats in the groups that received their dose by intratracheal nebulization were placed on a

board inclined at an angle 45° from the horizontal, and a tracheal cannula, connected to the BCDU pressure transducer, was inserted halfway down the trachea. The nebulization catheter was inserted into the tracheal cannula and inspiration synchronized dosing of the aerosol was performed. Immediately after dosing, the nebulization catheter was removed and one minute later the tracheal cannula. Venous blood samples were collected from the orbital vein, into heparinized tubes, at predetermined time points during the 360-min experiments.

### 5.6.2 Pharmacokinetic calculations

Pharmacokinetic parameters were calculated by non-compartmental analysis using WinNonlin<sup>TM</sup>, version 2.0 (*Paper III*) and version 3.2 (*Paper V*) (Pharsight Corporation, Palo Alto, CA, USA). The area under the plasma concentration-time curve (AUC) was calculated using the linear/logarithmic trapezoidal rule, with extrapolation to infinite time. The bioavailability (F) of the dose delivered to the respiratory tract was calculated according to the equation:

$$F = \frac{(AUC_{\text{resp}}/\text{Dose}_{\text{resp}})}{(AUC_{\text{iv}}/\text{Dose}_{\text{iv}})} \quad (\text{Eq. 3})$$

In *Paper III*, first-pass metabolism in the respiratory tract was evaluated by comparing the ratios of the AUC for the metabolite (M1) ( $AUC_{\text{met}}$ ) to the AUC of the parent peptide (TArPP) ( $AUC_{\text{parent}}$ ) after nasal and pulmonary delivery to the corresponding ratio obtained after i.v. administration.

A multiexponential equation was fitted to the mean concentration-time data of the respective drug after i.v. administration using nonlinear regression (WinNonlin). The disposition parameters were used to deconvolute the absorption profiles after respiratory administration in individual rats, as described by (Langenbucher, 1982) and (Verotta, 1994). The time to absorb 50% ( $T_{50\%}$ ) and 90% ( $T_{90\%}$ ) of the available dose was estimated by linear interpolation between the calculated data points (Lennernäs et al., 1993). The apparent absorption rate constant ( $k_a$ ,  $\text{min}^{-1}$ ) after pulmonary administration was calculated according to the equation:

$$k_a = \frac{\ln 2}{T_{50\%}} \quad (\text{Eq. 4})$$

where  $T_{50\%}$  corresponds to the absorption half-life (min).

## 5.7 Epithelial cell culture experiments (*Paper II, IV, V*)

### 5.7.1 Cell culture

Caco-2 cells (American Type Culture Collection, Rockwell, MD, USA), passage number 25-40, were cultured in Dulbecco's Modified Eagle Medium (DMEM, Life Technologies, UK) with 10 % fetal calf serum, 1 % nonessential amino acids, 100 U/ml penicillin and 100 µg/ml streptomycin according to standardized procedures modified from Artursson, 1990. For the transport studies, cells were seeded at a density of  $1 \times 10^5$  cells per  $\text{cm}^2$  and cultured on 12-well polyester filters with pore size  $0.4 \mu\text{m}$  ( $1.13 \text{ cm}^2$ ; Transwell<sup>®</sup> Clear, Costar, MA, USA) at  $37^\circ\text{C}$  in an atmosphere of 5 %  $\text{CO}_2$ , 95 %  $\text{O}_2$  for 14 days to form differentiated confluent monolayers. The media on both sides of the monolayers were changed on alternate days. The integrity of the monolayers was checked by measuring the transepithelial electrical resistance (TEER). For inclusion in the transport experiments each filter should have TEER values  $> 250 \Omega \times \text{cm}^2$ .

### 5.7.2 Transport experiments in Caco-2 cell monolayers

Drug transport was studied in the apical (A) to basolateral (B) (A-B) and the reversed direction (B-A) for 120 min. The transport experiments were carried out using Hank's Balanced Salt Solution (HBSS, Life Technologies, UK) with 25 mM HEPES, pH 7.4 at  $37^\circ\text{C}$ . New 12-well culture plates were saturated with culture medium, the culture medium was replaced with transport medium, and the monolayers were moved to these plates. The culture medium on the apical side was replaced with transport medium and the cells were equilibrated. TEER was measured before and after the experiments to ensure the integrity of the cell monolayers. At the start of transport experiments, the transport medium in the donor compartment was replaced with the test solution. Within 1 min, a sample was taken from the donor compartment to determine the start concentration ( $C_0$ ). After 120 min incubation, the donor and receiver compartment media were sampled for analysis by liquid chromatography with tandem mass spectrometry (LC-MS-MS). In control experiments, the permeability of the cell monolayers to  $^{14}\text{C}$ -Mannitol was monitored. The apparent permeability coefficient ( $P_{\text{app}}$ ,  $\text{cm/s}$ ) was calculated according to the equation:

$$P_{\text{app}} = \frac{dQ}{dt} \times \frac{1}{A \times C_0} \quad (\text{Eq. 5})$$

where  $dQ/dt$  is the transport rate ( $\text{mol/s}$ ),  $A$  is the surface area of the filter supporting the monolayer ( $\text{cm}^2$ ), and  $C_0$  is the initial concentration in the donor chamber ( $\text{mol/ml}$ ).

## 5.8 Sample analysis

For analysis of the test formulations, plasma samples, and samples from IPL- and Caco-2 experiments (*Paper I-V*), a number of different analytical techniques were applied. The techniques used for the respective papers are summarized in Table 4. For descriptions of the specific analytical methods and instrumentation, see the respective paper.

**Table 4.** Summary of the analytical techniques used for sample analysis in Paper *I-V*.

<i>Paper</i>	Analyte	Sample	Analytical technique
<i>I</i>	Evans Blue	test formulation trachea and lung tissue	spectrophotometer
<i>I</i>	Nile Blue	test formulation trachea and lung tissue	spectrophotometer
<i>II</i>	FITC-dextran 10 000	test formulation IPL-perfusate	fluorescence reader
<i>II, IV, V</i>	<sup>14</sup> C-Mannitol	Caco-2 transport medium	liquid scintillation counter
<i>II, III</i>	TArPP	test formulation	HPLC
<i>II</i>	TArPP and metabolites M1-M5	IPL-perfusate BAL	LC-MS
<i>II</i>	TArPP	Caco-2 transport medium	LC-MS-MS
<i>III</i>	TArPP metabolite M1	plasma test formulation	LC-MS-MS
<i>IV</i>	Atenolol, Budesonide, Enalapril, Enalaprilate, Losartan, Metoprolol, Propranolol, Terbutaline	IPL-perfusate Caco-2 transport medium test formulation	LC-MS-MS
<i>IV</i>	Formoterol	IPL-perfusate	coupled column HPLC
<i>IV</i>	Formoterol	Caco-2 transport medium	LC-MS-MS
<i>IV</i>	Budesonide Budesonide esters	trachea and lung tissue IPL-perfusate	LC-MS-MS
<i>V</i>	Cromolyn, Cyanocobalamin, Formoterol Imipramine, Losartan, Metoprolol, Talinolol, Terbutaline	plasma Caco-2 transport medium test formulation	LC-MS-MS

## 5.9 Inhaled drugs dataset (*Paper V*)

To identify the inhaled drugs, on the market worldwide in 2001, the pharmaceutical preparation catalogs “Physicians’ Desk Reference” (USA) and “FASS” (Sweden), as

well as the drug databases Adis R&D Insight (Adis International Limited, Chester, UK), Pharmaprojects, version 4.1. (PJB Publications Ltd., Richmond, Surrey, UK), Investigational Drugs Database, IDdb2 (Current Drugs Limited, London, UK), and Drugdex<sup>®</sup> System (Thomson MICROMEDEX, Greenwood Village, CO, USA) were searched.

Two databases from MDL Informations systems (San Leandro, CA, USA) the MDL Drug Data Report (MDDR) database (online version of the Drug Data Report Journal, Prous Science Publishers) and the Comprehensive Medicinal Chemistry database (CMC-3D, electronic version of Volume 6 of Comprehensive Medicinal Chemistry, Pergamon Press) were used to search for chemical structures of the compounds.

### **5.10 Calculation of drug parameters (*Paper IV, V*) and physicochemical profiling of the inhaled drugs (*Paper V*)**

cLogD (pH 7.4) and pKa were calculated using ACDlabs software (Advanced Chemistry Development Labs, version 4.5, Toronto, Canada). cLogP was calculated using the Daylight algorithm (Daylight Users Manual, Release 4.41, Copyright 1992-1995 by Daylight Chemical Information Systems Inc., Irvine, CA, USA). Geometric parameters including molecular volume, surface area (polar/non-polar), hydrogen bonding donors/acceptors, electronic parameters including charge and dipoles, and topological parameters including molecular weight, atom/bond/ring counts, and connectivities were all calculated using AstraZeneca inhouse software for descriptor calculation (Selma software, AstraZeneca R&D Mölndal, Sweden).

To summarize the most important physicochemical parameters of the inhaled drugs, principal component analysis (PCA) (Simca-P ver. 8.0, Umetrics, Umeå, Sweden) was applied (Jackson, 1991).

### **5.11 Data analysis (*Paper IV, V*)**

Relationships among drug physicochemical parameters and the pulmonary bioavailability and absorption rate in vivo, absorption characteristics in IPL, and permeation across the Caco-2 cell monolayers, respectively, were analyzed using Spotfire Decision Site 6.2 (Spotfire, Inc., Somerville, MA, USA). The multivariate regression technique Partial Least Squares (PLS) was used to find correlations between the descriptor variables (physicochemical descriptors and logP<sub>app</sub>) and the dependent variables (the determined absorption parameters), and to find predictive models (Simca-P version 8.0, Umetrics, Umeå, Sweden).

## 5.12 Statistics

All results are presented as means  $\pm$  SD. Student's unpaired t-test of equal variance was used to evaluate the differences between two mean values. A p-value < 0.05 was considered significant. When comparisons involved more than two mean values, one-way analysis of variance (ANOVA) was used. In *Paper III*, the ANOVA -analysis was coupled to Scheffé's F-test (StatView, Abacus Concepts, Inc., Berkeley, USA) for comparison of individual means. In *Paper IV*, the ANOVA -analysis was coupled to Bonferroni's F-test using Astute (Excel makro developed by AstraZeneca Mölndal, Sweden).

# 6. RESULTS AND DISCUSSION

## 6.1 Nebulization catheters as a new approach for delivery of defined aerosol doses to the rat lung (*Paper I*)

In *Paper I*, a nebulization catheter technique (Aeroprobe™) was adapted and evaluated for delivery of defined aerosol doses to the isolated and perfused rat lung and to the lungs of anesthetized rats in vivo. The device was well adapted to handle small volumes of test formulation, i.e. about 200  $\mu$ l was enough to fill up the device, compared to the ml-quantities required for the conventional nebulizers. This aspect is important for pulmonary drug delivery investigations during early drug discovery, when the new drug compounds are in short supply.

The adapted nebulization catheters delivered defined and reproducible aerosol doses to the rat lung. The recovery of the delivered dose was high,  $99 \pm 12$  and  $105 \pm 1\%$ , respectively, in the in vivo administrations and IPL-experiments, which suggested that the delivered dose was retained within the airways and was equal to the deposited dose. Thus, in contrast to established aerosol inhalation methodologies, there was no need for dosimetric calculations (Dahlbäck et al., 1996).

At the optimized settings used, 1-2  $\mu$ l of liquid was aerosolized per puff using 1-1.5 ml of air. The droplet-size distribution of the generated aerosols was broad (2-8% < 3  $\mu$ m; 10% < 4-7  $\mu$ m; 50% < 10-15  $\mu$ m and 90% < 20-40  $\mu$ m).

The droplet-size distribution of the generated aerosols could be controlled by varying the design of the catheter, air pressure, air pulse time, and liquid pulse time. However, when aiming at intratracheal drug administration to the lungs of small animals, such as the rat, there are limitations in the freedom of optimization of the air pulse. Delivery of a large volume of air, exceeding the lung volume of the animal, may damage the delicate lung tissue (Green, 1979). Therefore, the ejected volume of air per aerosol puff did not exceed the tidal volume of the animal (*Paper I-V*).

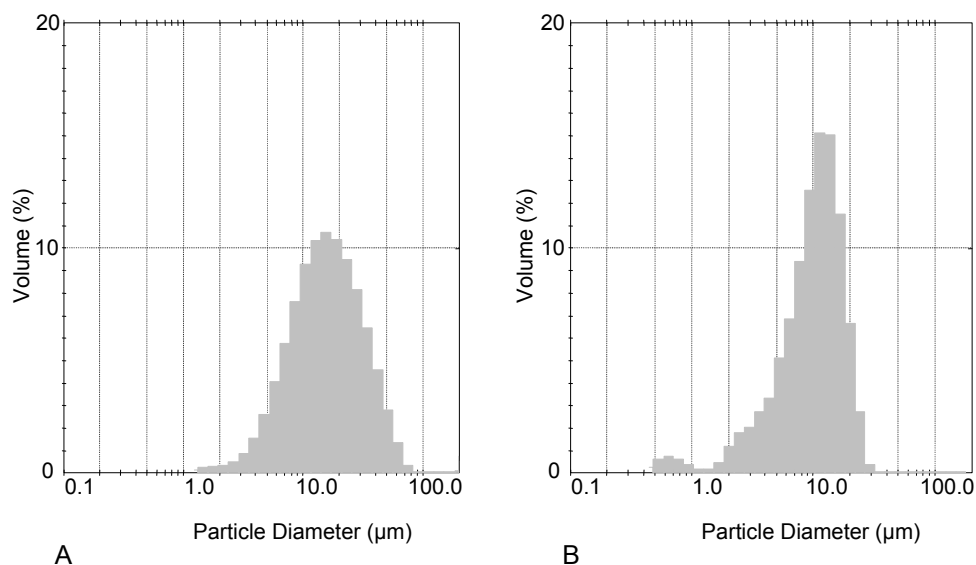


**Figure 12.** Histograms of the droplet-size distribution of aerosols generated from the nebulization catheters measured with the laser diffraction instrument Malvern Mastersizer X. The mass median diameter (MMD) for the aerosol used in the IPL-experiments (A) was  $17 \pm 1 \mu\text{m}$ , and the MMD for the aerosol used in the in vivo experiments in anesthetized and tracheal-intubated rats (B) was  $11 \pm 0.4 \mu\text{m}$ .

The intratracheal aerosol dosing was automatically synchronized with the inspiration of the lungs. The doses were triggered to be delivered when about 20% of the tidal volume had been inhaled. Besides a small double peak recorded in the inspiratory phase of the anesthetized rats, the breathing pattern was not affected by the dosing procedures (Figure 13).

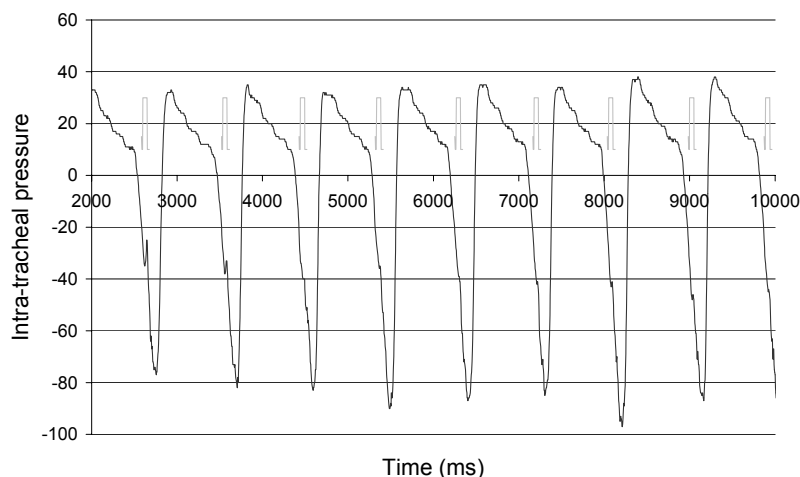
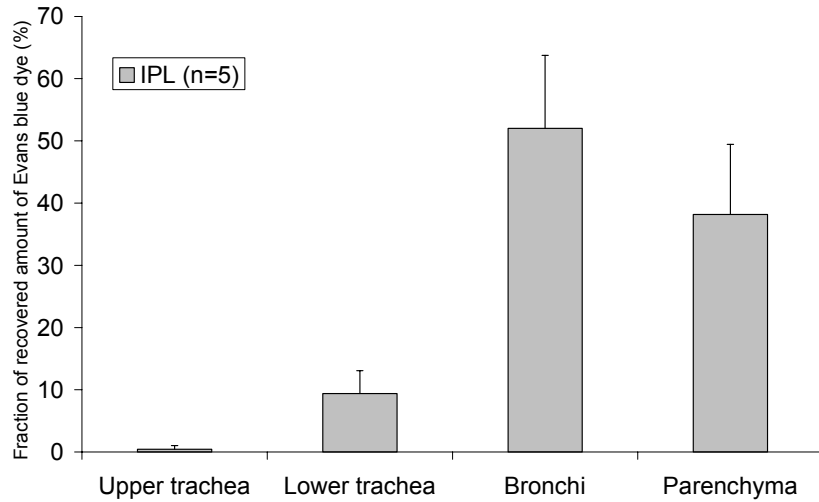
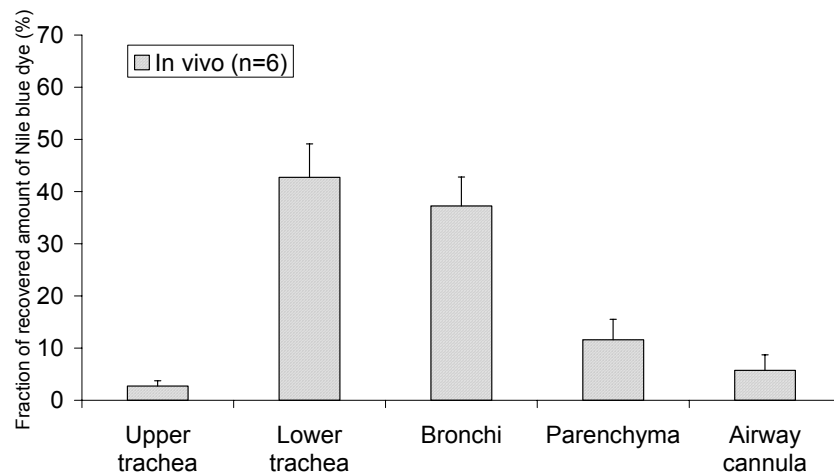


**Figure 13.** A typical breath signal recorded during dosing to an anesthetized and tracheal-intubated rat. The intra-tracheal pressure represent relative measures performed to register the breathing pattern of the rat. The breath-synchronized aerosol administrations are marked. Besides a small double peak recorded in the inspiratory phase, the breathing pattern of the animals was not affected by the dosing procedures.

After intratracheal aerosol administration to the isolated and perfused rat lungs, the dose was about equally distributed to the tracheobronchial and parenchymal regions. The fractional distribution to the lower trachea, bronchi, and parenchyma was  $9\pm 4\%$ ,  $52\pm 12\%$ , and  $38\pm 11\%$ , respectively. In the anesthetized rats, the aerosol dose was mainly distributed to the trachea ( $43\pm 6\%$ ) and bronchi ( $37\pm 6\%$ ), whereas only  $12\pm 4\%$  was distributed to the parenchymal region (Figure 14).



A



B

**Figure 14.** Lung distribution profiles of Evans blue dye in isolated and perfused rat lungs (A) and of Nile Blue dye in anesthetized tracheal-intubated rats (B) after intratracheal administration of aerosols using nebulization catheters.

The lung deposition in isolated and perfused rat lungs has been demonstrated to be inversely proportional to the respiratory frequency (Byron et al., 1986). In humans, a more uniform and peripheral lung deposition after inhalation at a slow flow rate, compared to fast rate inhalations, has been reported (Newhouse et al., 1978; Newman S.P. et al., 1982). The breath frequency in the IPL-experiments was decreased from 80 to 30 breaths/min during dosing, to facilitate a peripheral lung distribution, whereas the breath frequency in the anesthetized and spontaneously breathing rats was about 80-100 breaths/min. Even though the small particles of the generated aerosols might have followed the inhalation flow down the airways, the speed of the ejected aerosol plume was high and the main mechanism of deposition in the small airways of the rat, was therefore, assumed to be impaction. The propelling force of the ejected air together with gravity probably facilitated penetration of the aerosol into the parenchymal region of the lung. However, the particle size of the aerosols generated from the nebulization catheters has also been demonstrated to affect the lung distribution in the IPL-model (Johansson et al., 2000). Two different designs of nebulization catheters, generated aerosols with different droplet size distributions. One of the aerosols had a particle size range of 0.1-30  $\mu\text{m}$  and the other aerosol had a particle size range of 1-180  $\mu\text{m}$ . The peripheral distribution of these two aerosols was  $50\pm 15$  and  $20\pm 5\%$ , respectively.

An intratracheal nebulization technique, similar to the one evaluated in this study, has previously been reported for aerosol dosing in vivo (Leong et al., 1998). The technique was developed to increase the lung surface area in contact with the test formulation, compared to instillation delivery, and to deliver finite aerosol doses into the bronchoalveolar region of the lung (Leong et al., 1998). However, the technique did not fulfill the set requirements of dose precision. About 50% of the aerosol propelled into the lungs was exhaled, which was due to the use of a high volume (5 ml) of air to generate the aerosol (Leong et al., 1998). Another dosing method for reproducible administration of known liquid quantities to the peripheral airways has been described for use in the isolated and perfused rat lung (Byron et al., 1988). Fluorocarbon propellant was used to expel the 100- $\mu\text{l}$  liquid dose in a large vapor volume of 6.1 ml. A coarse liquid spray with a median droplet diameter of 350  $\mu\text{m}$  was generated. Still, about 65% was distributed to the peripheral lung and 95% of the administered dose was recovered (Byron et al., 1988). An aerosol delivery system leading the aerosol directly to the lungs of anesthetized rats via an endotracheal tube has also been developed (Eirefelt et al., 1992). The system efficiently delivered 80% of the lung-deposited dose to the peripheral region of the lung. However, only 7 % of the inhaled dose deposited in the lungs, and therefore filter samplings of the aerosol was required for dosimetric calculations of the inhaled dose.

## **6.2 Absorption and metabolism of the $\mu$ -selective opioid tetrapeptide agonist (TArPP) after respiratory delivery to the rat (*Paper II, III*)**

Pulmonary delivery was demonstrated to be a promising route for systemic delivery of the  $\mu$ -selective opioid tetrapeptide agonist TArPP (Tyr-D-Arg-Phe-Phe-NH<sub>2</sub>). The oral

bioavailability of the peptide is 0.5% (G. Ekström, unpublished results) due to a low oral permeability and enzymatic degradation in the gastro-intestinal tract.

In *Paper II*, the lung specific transport and metabolism of the peptide after delivery to the airway lumen and to the vascular circulation, respectively, could be followed using the isolated and perfused rat lung model. Five metabolites, M1-M5 (Table 5), were identified and quantified in the perfusate and the bronchoalveolar lavage fluid.

**Table 5.** Amino acid sequences and molecular weights for TArPP and the five metabolites (M1-M5).

Peptide abbreviation	Amino acid sequence	MW (Da)
TArPP	Tyr-D-Arg-Phe-Phe-NH <sub>2</sub>	631.4
M1	Tyr-D-Arg-Phe-Phe-OH	632.4
M2	Tyr-D-Arg-Phe-OH	485.3
M3	D-Arg-Phe-Phe-NH <sub>2</sub>	468.3
M4	D-Arg-Phe-Phe-OH	469.3
M5	D-Arg-Phe-OH	322.2

After airway administration, TArPP was rapidly and well absorbed into the perfusate. The concentration of TArPP in the recirculating perfusate reached a plateau after 75 min (Figure 15). Two hours after delivery to the airway lumen, about half of the administered peptide dose was recovered in the perfusate as intact tetrapeptide and an eighth was recovered in the BAL-fluid (Table 6). The absorption half-life of TArPP was  $29 \pm 8$  min and the apparent absorption rate constant ( $k_{a, \text{lung}}$ ) was  $0.03 \pm 0.01 \text{ min}^{-1}$ .

After administration of TArPP to the vascular circulation, all of the given dose was recovered in the perfusate either as parent peptide or as metabolites, which indicates that neither TArPP nor any of the metabolites were sequestered in the pulmonary tissue (Table 6). These results are in agreement with previous investigations for Met- and Leu-enkephalin in the IPL (Gillespie et al., 1985).

The metabolism of TArPP was higher after airway administration than after vascular administration. The main metabolites formed after administration to the lung were the deamidated tetrapeptide M1 and the tripeptide M2 (Table 6 and Figure 16). These metabolites have previously been shown to be formed from TArPP in various biological media, such as rat jejunal fluid (M1 and M2) and rat tissue homogenates (primarily M1) (Kron Dahl et al., 2000; Kron Dahl et al., 2001). The low formation of metabolites with a cleaved N-terminus (M3-M5) in both perfusate and BAL-fluid suggests that the D-amino acid in position 2 protects the peptide from degradation by lung aminopeptidases.

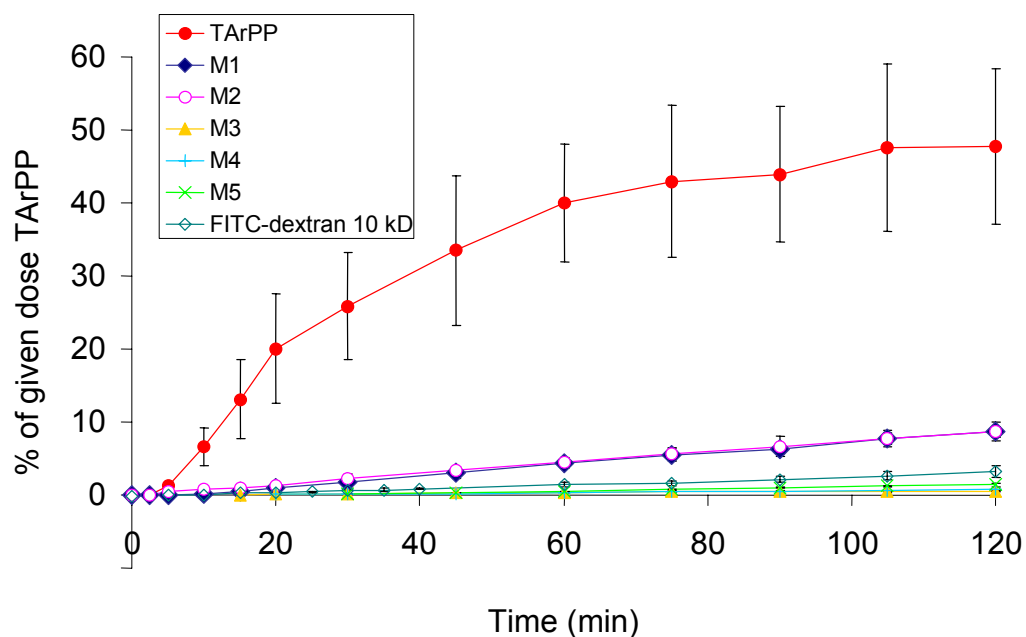


**Figure 15.** Appearance of TArPP and its metabolites (M1-M5) in the perfusate after airway delivery of TArPP to the isolated and perfused rat lung (n=4). The appearance profile of the permeability marker compound FITC-dextran MW 10 000 Da demonstrates the maintained integrity of the lung barrier of the IPL-preparation.

**Table 6.** The recovery of TArPP and its metabolites M1-M5, as a percentage of the given dose of TArPP (%), in perfusate and BAL-fluid after administration to the rat lung. Data are presented as means  $\pm$  SD, n=4.

	Airway delivery		Vascular delivery	
	Perfusate	BAL	Perfusate	BAL
TArPP	47.8 $\pm$ 10.7	12.5 $\pm$ 4.9	89.3 $\pm$ 5.3	n.d.
M1	8.7 $\pm$ 0.7	6.6 $\pm$ 2.1	4.5 $\pm$ 0.5	n.d.
M2	8.8 $\pm$ 1.3	2.5 $\pm$ 0.7	3.5 $\pm$ 0.5	n.d.
M3	0.5 $\pm$ 0.1	n.d.	0.7 $\pm$ 0.1	n.d.
M4	0.8 $\pm$ 0.2	n.d.	n.d.	n.d.
M5	1.4 $\pm$ 0.2	n.d.	0.8 $\pm$ 0.3	n.d.
Sum of metabolism	29.2 $\pm$ 1.4		9.4 $\pm$ 0.4	
Total recovery	89.5 $\pm$ 5.2		98.7 $\pm$ 5.4	

n.d.: not determined because of concentrations < LOQ

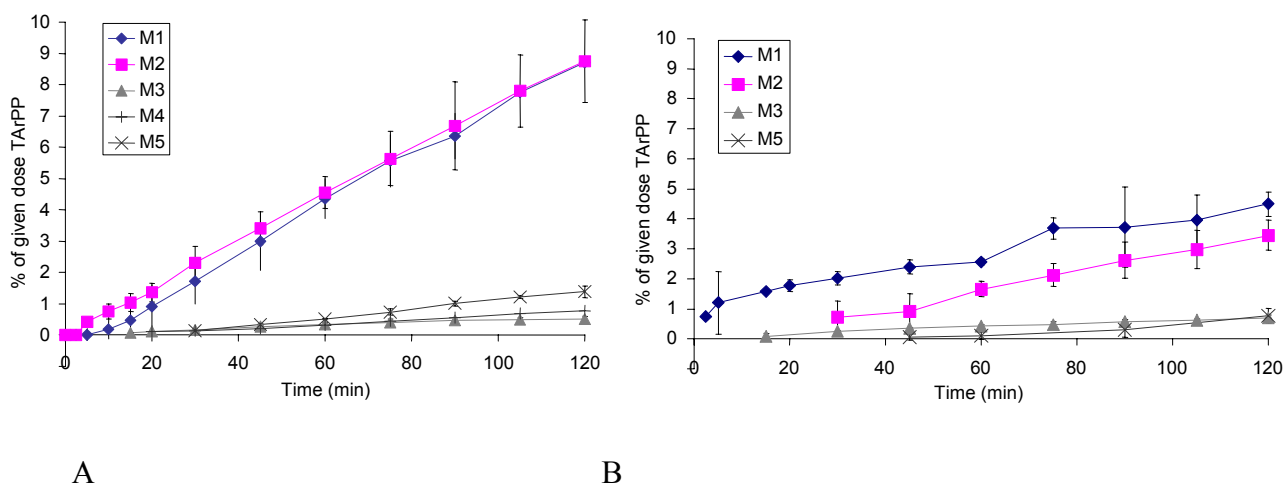


**Figure 16.** Appearance of metabolites in the perfusate after airway delivery (A) and vascular delivery (B) of TArPP to the isolated and perfused rat lung (n=4).

The lung is generally thought to have lower proteolytic activity than many other organs (Hoover et al., 1992; Wall, 1995; Yang et al., 2000). However, relatively high activity of exopeptidases (e.g. aminopeptidases) has been found in BAL-fluid, on the surfaces of cells lining the respiratory tract, and in the pulmonary circulation in rats (Forbes B. et al., 1999; Forbes B.J. et al., 1995; Funkhouser et al., 1991; Wall et al., 1993). Consequently, even hydrophilic molecules with low membrane permeation such as TArPP, which are not expected to reach intracellular enzymes to a large extent, are exposed to significant enzymatic activity in the respiratory tract. In comparison to other opioid peptides, e.g. Met- and Leu-enkephalin, TArPP was much more resistant to enzymatic degradation in the lung (Crooks et al., 1985; Gillespie et al., 1985).

The mucociliary clearance is impaired in the isolated and perfused rat lung because of cannulation and ligation of trachea. Consequently, the residence time of the peptide in the IPL-preparation was probably somewhat longer than would be expected in vivo. Hence, the exposure of the peptide to peptidases in the airways might have been prolonged compared to in vivo, leading to higher enzymatic degradation in vitro.

In *Paper III*, regional differences in the bioavailability, absorption rate, and first-pass metabolism of TArPP were investigated in vivo in the respiratory tract of anesthetized rats. Targeting to different regions of the respiratory tract were successfully performed using various administration techniques (Table 3 and 7). Intravenous administrations were performed as reference for pharmacokinetic calculations.

After i.v. administration of TArPP to rats the elimination half-life was short, about 20-25 min. This short half-life was explained by the low volume of distribution ( $374 \pm 81$  ml/kg) and the relatively high clearance ( $31 \pm 5$  ml/min/kg). The half-life of TArPP was

longer for all respiratory administrations compared to i.v. administration (Table 7), indicating absorption rate-limited pharmacokinetics.

**Table 7.** Pharmacokinetic parameters of TArPP (means  $\pm$  SD) after various routes of administration to anesthetized rats.

	IV	IN	IT	SL	SH	AERO
Dose ( $\mu\text{mol/kg}$ )	0.97 $\pm$ 0.03	9.6 $\pm$ 1.2	7.9 $\pm$ 0.5	1.3 $\pm$ 0.1	9.2 $\pm$ 2.0	1.8 $\pm$ 0.2
Number of rats	6	6	6	6	7	7
AUC/ Dose	33 $\pm$ 6 <sup>o</sup>	17 $\pm$ 3 <sup>* a b</sup>	26 $\pm$ 3 <sup>a b</sup>	37 $\pm$ 2	36 $\pm$ 6	24 $\pm$ 17 <sup>c</sup>
C <sub>max</sub> ( $\mu\text{M}$ )	5.9 $\pm$ 1.5	2.8 $\pm$ 1.0	4.7 $\pm$ 1.1	1.6 $\pm$ 0.2	9.3 $\pm$ 2.6	1.0 $\pm$ 0.5
t <sub>max</sub> (min)	0	20 $\pm$ 8	12 $\pm$ 2	9 $\pm$ 2	10 $\pm$ 0	15 $\pm$ 0
t <sub>1/2</sub> (min)	21 $\pm$ 3 <sup>a</sup>	37 $\pm$ 7 <sup>* a</sup>	32 $\pm$ 7 <sup>a</sup>	49 $\pm$ 7 <sup>* b</sup>	29 $\pm$ 3 <sup>a</sup>	40 $\pm$ 4 <sup>*</sup>
AUC <sub>met</sub> /AUC <sub>parent</sub>	0.04 $\pm$ 0.01 <sup>o</sup>	0.34 $\pm$ 0.10 <sup>*</sup>	0.15 $\pm$ 0.02 <sup>o*</sup>	0.15 $\pm$ 0.01 <sup>o*</sup>	0.16 $\pm$ 0.02 <sup>o*</sup>	0.17 $\pm$ 0.02 <sup>o*</sup>
T <sub>50%</sub> (min)	-	24 $\pm$ 3 <sup>a</sup>	17 $\pm$ 7	10 $\pm$ 1 <sup>o</sup>	13 $\pm$ 3 <sup>o</sup>	16 $\pm$ 4 <sup>o</sup>
T <sub>90%</sub> (min)	-	80 $\pm$ 7 <sup>a</sup>	61 $\pm$ 16 <sup>a</sup>	38 $\pm$ 10 <sup>o</sup>	58 $\pm$ 9 <sup>o</sup>	67 $\pm$ 12 <sup>a</sup>
F (%)	-	52 $\pm$ 9	78 $\pm$ 10	114 $\pm$ 7	111 $\pm$ 18	72 $\pm$ 52

IV= intravenous administration; IN= intranasal microinfusion; IT= intratracheal microinfusion; SL= intratracheal nebulization, low dose; SH= intratracheal nebulization, high dose; AERO= aerosol inhalation; <sup>o</sup> Different from IN; <sup>\*</sup> Different from IV; <sup>a</sup> Different from SL; <sup>b</sup> Different from SH; <sup>c</sup> Not included in the statistical analysis due to uncertain dose determination.

The rapid absorption of TArPP after both pulmonary and nasal administration (t<sub>max</sub>  $\approx$  10-20 min) (Figure 17 and 18) is supported by previous findings for small peptides and nonpeptides after nasal and pulmonary administration in animals (McMartin et al., 1987; Qui et al., 1997; Schanker et al., 1983). TArPP tended to be faster absorbed from the more peripheral regions of the lung than from the nasal cavity as shown by the T<sub>50%</sub> and T<sub>90%</sub> values (Table 7). The absorption rate after nasal and intratracheal microinfusion was not significantly different, which agrees with the morphologically and functionally similar epithelium in the nasal cavity and in the trachea (Johnson et al., 1993).

The bioavailability of TArPP after respiratory administration ranged from about 50% (after nasal microinfusion) to complete (111-114%, after intratracheal nebulization). The higher bioavailability of TArPP after intratracheal nebulization compared to intratracheal microinfusion (Table 7) is in agreement with published studies showing a higher bioavailability of peptides and proteins when absorbed from the more peripheral regions of the lung compared to the more central regions (Colthorpe et al., 1992; Folkesson et al., 1992; Niven et al., 1995). After aerosol inhalation, the bioavailability was lower than expected and the interanimal variability was high. The results were most likely explained by overestimation of the inhaled dose, due to a low and variable breathing frequency in the rats induced by the anesthesia.

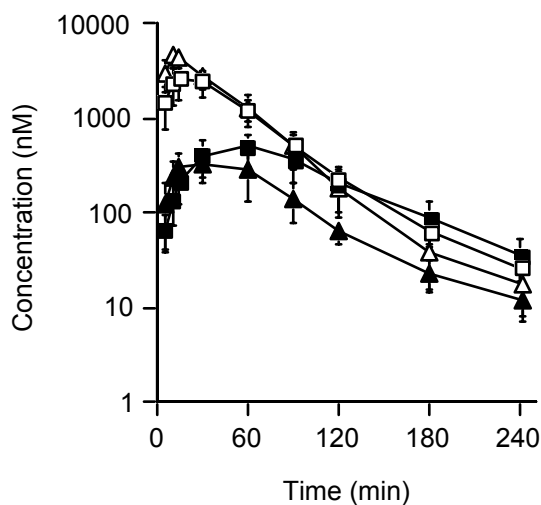
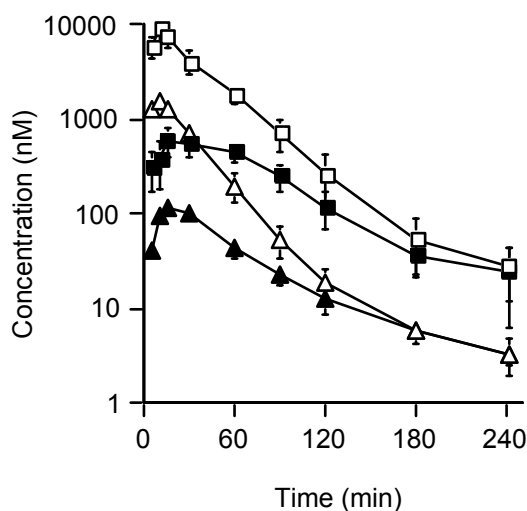
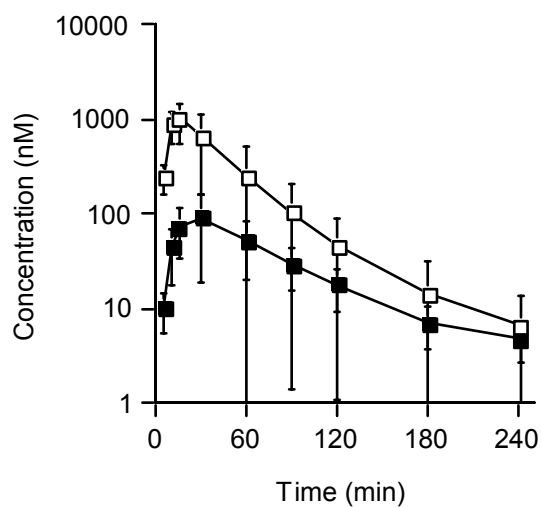


**Figure 17.** Plasma concentration-time profiles (means  $\pm$  SD) of TArPP (open symbols) and its deamidated metabolite (filled symbols) in rats after nasal (squares) and intratracheal (triangles) microinfusion of TArPP (9.6 and 7.9  $\mu$ mol/kg, respectively).



A.



B.

**Figure 18.** Plasma concentration-time profiles (means  $\pm$  SD) of TArPP (open symbols) and its deamidated metabolite (filled symbols) in rats after (A) intratracheal nebulization of TArPP at two different dose levels, 9.2  $\mu$ mol/kg (squares) and 1.3  $\mu$ mol/kg (triangles), and (B) aerosol inhalation of TArPP for 10 min.

High nasal bioavailability in rats has previously been reported for small peptides with low oral bioavailability (<1000 Da), including the pentapeptide metkephamide (65-102%) and the octapeptide SS-6 (~75%) (Langguth et al., 1994; McMartin et al., 1987;

Su et al., 1985). The lower bioavailability of TArPP after nasal than pulmonary administration was most likely due to a higher nasal first-pass metabolism (deamidation), which is supported by the higher ratio of  $AUC_{met}/AUC_{parent}$  for intranasal compared to pulmonary administration. The first-pass metabolism did not differ among the pulmonary groups (Table 7).

The experiments performed in the isolated and perfused rat lung and in anesthetized rats in vivo consistently demonstrated a higher formation of metabolites after airway administration than after vascular administration. The metabolic ratio in the in vivo study ( $AUC_{met}/AUC_{parent}$ ) was found to be 0.04 and 0.16 for intravenous and pulmonary administration respectively. In the IPL-study, the metabolic ratio (M1/TArPP, recovered in the perfusate (%)) was 0.05 and 0.18 after vascular and respiratory administration respectively. The results support the validity of the IPL-model to investigate first-pass metabolism in the lung from a qualitative as well as a quantitative point of view.

The transport mechanisms for peptides across the airway and alveolar epithelia are not fully understood; however, the main transport pathway is suggested to be paracellular diffusion (Crandall et al., 2001; Evans et al., 1998; Patton, 1996). Recently, the presence of the peptide transporter PepT2 was demonstrated in the bronchial and alveolar epithelium, and in lung endothelium of humans and rats (Groneberg et al., 2002; Groneberg et al., 2001). However, in a functional study performed on rabbit tracheal epithelial cells, the dipeptide carnosine was taken up into the cells via a dipeptide transporter, whereas transport across the epithelial monolayer seemed to occur mainly via the paracellular pathway (Yamashita et al., 1998). Likewise, the pentapeptide Met-enkephaline and the tripeptide thyrotropin releasing hormone have been suggested to be transported via the paracellular pathway across rat alveolar epithelial cells (Morimoto et al., 1994; Wang et al., 1993).

Our data in rats show that respiratory delivery is a feasible route of administration for the hydrophilic and enzymatically susceptible tetrapeptide TArPP. However, it remains to be evaluated how predictive the data from rats are for the pulmonary absorption of TArPP in humans. The use of anesthetic agents is known to increase the absorption of drugs from the nasal cavity and trachea in animals as a consequence of impaired mucociliary clearance (Mayor et al., 1997; Patrick et al., 1977). In addition, compared to the rat lung, the human lung has smaller gas-exchange surface per unit lung volume, smaller capillary volume per unit lung volume, and thicker air-blood barrier (Gehr P., 1984).

### **6.3 Physicochemical profile of inhaled drugs (*Paper V*)**

In *Paper V*, the physicochemical profiling of the inhaled drugs was based on the calculated molecular properties of the 34 low-molecular-weight drugs (Table 8), including 5 volatile anesthetics, which were found for oral inhalation on the market worldwide during 2001.

**Table 8.** List of marketed inhaled drugs during 2001 (1-34) and the oral drugs included in the in vivo pharmacokinetic study (35-39) (*Paper V*). The names in **bold** indicate the drugs selected for the pharmacokinetic study. All compounds, except cyanocobalamin, were included in the principal component analysis presented in Figure 19.

Delivery route	No. in Fig.	Name	Drug class	Structure/property class
<b>Inhaled</b>	1	Budesonide	corticosteroid	steroid
	2	Flunisolide	corticosteroid	steroid
	3	Fluocortin butyl	corticosteroid	steroid
	4	Beclometasone dipropionate	corticosteroid	steroid
	5	Fluticasone propionate	corticosteroid	steroid
	6	Triamcinolone acetonide	corticosteroid	steroid
	7	Clenbuterol	$\beta$ -2-adrenoceptor agonist	aryl, hydroxy-ethylamine
	8	Metaproterenol	$\beta$ -2-adrenoceptor agonist	aryl, hydroxy-ethylamine
	9	<b>Terbutaline</b>	<b><math>\beta</math>-2-adrenoceptor agonist</b>	<b>aryl, hydroxy-ethylamine</b>
	10	Salmeterol	$\beta$ -2-adrenoceptor agonist	aryl, hydroxy-ethylamine
	11	<b>Formoterol</b>	<b><math>\beta</math>-2-adrenoceptor agonist</b>	<b>aryl, hydroxy-ethylamine</b>
	12	Salbutamol	$\beta$ -2-adrenoceptor agonist	aryl, hydroxy-ethylamine
	13	Pirbuterol	$\beta$ -2-adrenoceptor agonist	aryl, hydroxy-ethylamine
	14	Procaterol	$\beta$ -2-adrenoceptor agonist	aryl, hydroxy-ethylamine
	15	Reproterol	$\beta$ -2-adrenoceptor agonist	aryl, hydroxy-ethylamine
	16	Bitolterol	$\beta$ -2-adrenoceptor agonist	aryl, hydroxy-ethylamine
	17	Fenoterol	$\beta$ -2-adrenoceptor agonist	aryl, hydroxy-ethylamine
	18	Tulobuterol	$\beta$ -2-adrenoceptor agonist	aryl, hydroxy-ethylamine
	19	Ribavirin	antiviral	polar
	20	Tobramycin	antibiotic	polar
	21	N-Acetylcysteine	mucolytic	acid
	22	Pranlukast	leukotriene antagonist	acid
	23	Nedocromil	histamine release inhibitor	di-acid
	24	<b>Cromolyn</b>	<b>histamine release inhibitor</b>	<b>di-acid</b>
	25	Amlexanox	histamine and leukotriene inhibitor	acid
	26	Pentamidine	antiprotozoal	di-base
	27	Nicotine	smoking cessation	base
	28	Ipratropium bromide	anticholinergic	ammonium salt
	29	Zanamivir	antiviral	zwitterion
	30	Sevoflurane	anesthetic	small lipophilic
	31	Desflurane	anesthetic	small lipophilic
	32	Enflurane	anesthetic	small lipophilic
	33	Halothane	anesthetic	small lipophilic
	34	Isoflurane	anesthetic	small lipophilic
<b>Oral</b>	35	<b>Imipramine</b>	<b>tricyclic antidepressant</b>	<b>amine</b>
	36	<b>Losartan</b>	<b>angiotensin II receptor antagonist</b>	<b>acid</b>
	37	<b>Metoprolol</b>	<b><math>\beta</math>-1-adrenoceptor blocker</b>	<b>aryloxymethyl, hydroxy-ethylamine</b>
	38	<b>Talinolol</b>	<b><math>\beta</math>-1-adrenoceptor blocker</b>	<b>aryloxymethyl, hydroxy-ethylamine</b>
	39	<b>Cyanocobalamin</b>	<b>vitamin B<sub>12</sub></b>	<b>cobalamin</b>

**Table 9.** Summary of selected calculated physicochemical properties of the inhaled drugs (No. 1-29, in Table 8) excluding the volatile anesthetics. Data are presented as median values with 10<sup>th</sup> and 90<sup>th</sup> percentile variation.

Physicochemical property	10 <sup>th</sup> percentile	Median	90 <sup>th</sup> percentile
cLogD(7.4) <sup>a</sup>	-6.3	-0.6	3.8
MW (Da) <sup>b</sup>	225	340	482
PSA (Å <sup>2</sup> ) <sup>c</sup>	65	99	178
cLogP <sup>d</sup>	-1.0	1.3	4.1
HBD <sup>e</sup>	2	3	6
HBA <sup>f</sup>	4	5	11

<sup>a</sup>) cLogD(7.4): logarithm of the calculated octanol/ water distribution coefficient at pH 7.4

<sup>b</sup>) MW: molecular weight (Da); <sup>c</sup>) PSA: molecular polar surface area (Å<sup>2</sup>); <sup>d</sup>) cLogP: logarithm of the calculated octanol/ water partitioning coefficient; <sup>e</sup>) HBD: number of hydrogen bond donors

<sup>f</sup>) HBA: number of hydrogen bond acceptors

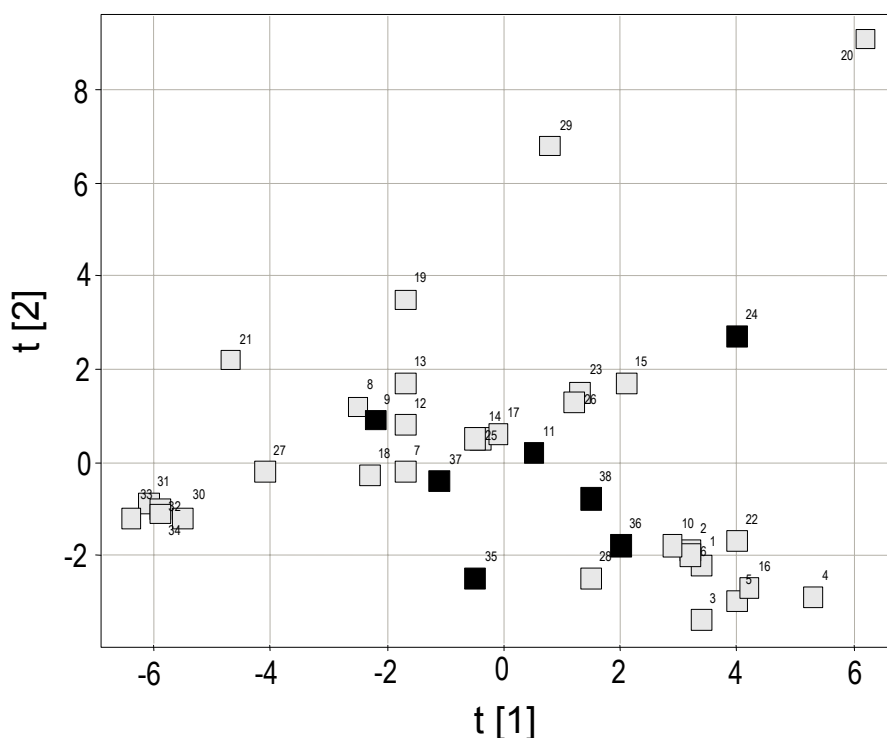


**Figure 19.** Score plot showing the diversity of the physicochemical properties of the inhaled drugs (No. 1-29) including the anesthetics (No. 30-34) and four oral drugs (No. 35-38). The black squares refer to drugs selected for the in vivo pharmacokinetic investigation (Paper V). The identity of the drugs can be found in Table 8. The plot shows the most significant variation in all 38 drugs (calculated using principal component analysis, PCA). The first dimension,  $t[1]$ , is related to size (e.g. surface area, molecular volume), and the second dimension,  $t[2]$ , is related to lipophilicity (e.g. LogD, LogP). Together these dimensions show ~74% of the total variation of the dataset.

The inhaled drugs were dominated by two compound classes, i.e. the corticosteroids (6 compounds) and the  $\beta$ -agonists (12 compounds), which generated a broad, skew distribution profile of physicochemical properties dependent on the structure class. Generally, the inhaled drugs tended to be more polar than oral drugs, corresponding to the less lipophilic character of some of these drugs (Table 9). Besides the rather low cLogD(7.4) and slightly high PSA, the calculated physicochemical properties for the inhaled dataset represented no extremes. The physicochemical diversity of the inhaled drug dataset, the volatile anesthetics, and the drugs included in the in vivo pharmacokinetic investigation (*Paper V*) are illustrated in Figure 19.

#### 6.4 Drug absorption from the rat lung (*Paper IV, V*)

To investigate the pulmonary drug absorption characteristics, drugs with different physicochemical properties were administered by intratracheal nebulization to isolated and perfused rat lungs (IPL) and to the lungs of anesthetized rats, *Paper IV and V*, respectively.

In *Paper IV*, the pulmonary absorption of nine low-molecular-weight (225-430 Da) drugs with diverse physicochemical properties (atenolol, budesonide, enalaprilate, enalapril, formoterol, losartan, metoprolol, propranolol, and terbutaline), and one high-molecular-weight compound (FITC-dextran 10,000 Da) was investigated after aerosol delivery to the IPL.

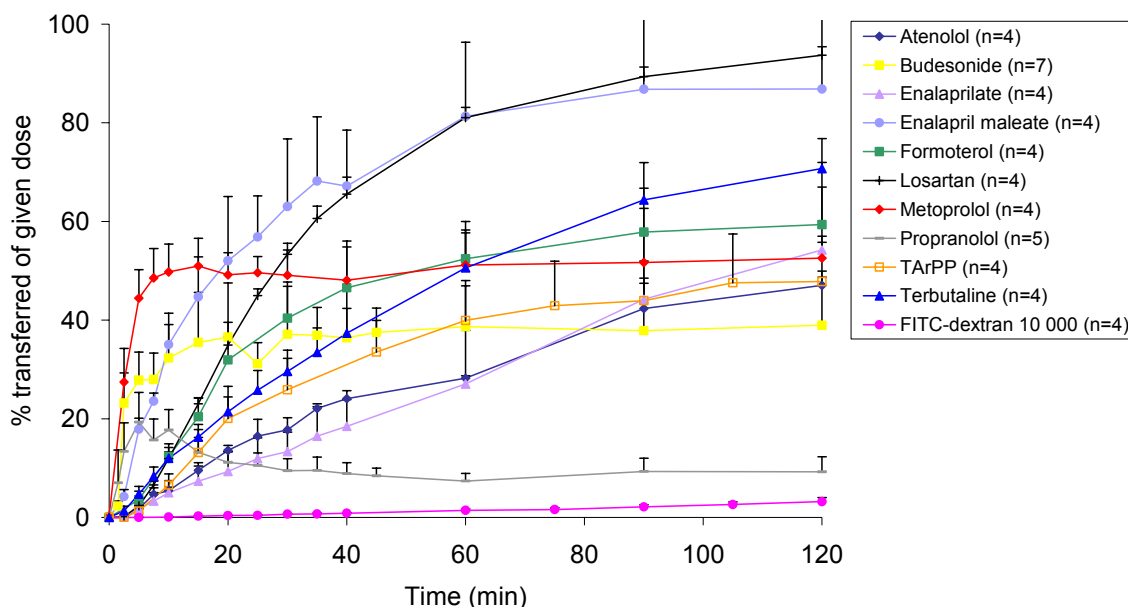


**Figure 20.** The air-to-blood absorption profiles of the investigated drugs, measured as the percent of the given dose transferred into the circulating perfusate with time after aerosol delivery to the isolated and perfused rat lung. The data for TARPP is included for comparison and is taken from *Paper II*.

The extent of air-to-blood absorption of the drugs was about 21 to 94% (Table 10). The absorption of the membrane permeability marker FITC-dextran 10,000 was 3% in 2 h, which corresponds to the reported absorption of this compound from rat lungs in vivo, and demonstrates the maintained integrity of the lung barrier of the IPL (Morita et al., 1993). The air-to-blood absorption profiles of atenolol, enalaprilate, and terbutaline were almost linear during the experiments and did not reach a plateau level. Budesonide, enalapril, metoprolol, and propranolol were, on the other hand, rapidly absorbed across the lung barrier, and the fraction absorbed reached a plateau in the perfusate (Figure 20). Small differences in the pulmonary absorption rate and extent of absorption, between the investigated drugs, were significantly separated using the IPL-model. No correlation was found between the absorption rate and the extent of absorption of the drugs.

**Table 10.** Rate and extent of absorption of drug compounds across the lung barrier of the isolated and perfused rat lung. Data are presented as the mean  $\pm$  SD.

Compound	$n^a$	$ka_{lung} \text{ (min}^{-1}\text{)}^b$	$t_{1/2} \text{ abs (min)}^c$	% transferred in 2 h <sup>d</sup>
Atenolol	4	0.018 $\pm$ 0.003	39 $\pm$ 6	47 $\pm$ 2
Budesonide	7	0.325 $\pm$ 0.121	2.4 $\pm$ 0.1	39 $\pm$ 11
Enalaprilate	4	0.012 $\pm$ 0.003	59 $\pm$ 12	54 $\pm$ 18
Enalapril	4	0.051 $\pm$ 0.019	15 $\pm$ 5	87 $\pm$ 19
Formoterol	4	0.036 $\pm$ 0.003	20 $\pm$ 2	59 $\pm$ 9
Losartan	4	0.027 $\pm$ 0.001	26 $\pm$ 1	94 $\pm$ 2
Metoprolol	4	0.286 $\pm$ 0.060	2.5 $\pm$ 0.6	53 $\pm$ 3
Propranolol	5	0.388 $\pm$ 0.172	2.0 $\pm$ 0.7	21 $\pm$ 6 (peak) 9.4 $\pm$ 2.7 (2h)
TArPP <sup>e</sup>	4	0.026 $\pm$ 0.010	29 $\pm$ 8	48 $\pm$ 11
Terbutaline	4	0.019 $\pm$ 0.002	37 $\pm$ 5	71 $\pm$ 7
FITC-dextran 10 000	4	0.010 $\pm$ 0.002	69 $\pm$ 10	3.2 $\pm$ 0.8

<sup>a)</sup> number of lungs; <sup>b)</sup> apparent absorption rate constant  $ka_{lung} = \ln 2 / t_{1/2} \text{ abs}$ ; <sup>c)</sup> absorption half-life; <sup>d)</sup> % of given dose transferred from the air-to-blood side in 2 h; <sup>e)</sup> data collected from *Paper II*

The air-to-blood transport process in the isolated and perfused rat lung model is composed of the permeability process and the disposition of the drugs in the lung tissue. The high absorption rate of budesonide, metoprolol, and propranolol in combination with a relatively low extent of air-to-blood absorption suggested that the drugs were bound to the lung tissue.

Propranolol and metoprolol are lipophilic basic drugs, which have been demonstrated to be highly distributed to tissues (Bodin et al., 1975; Dollery et al., 1976; Kornhauser et al., 1980). The absorption profile of propranolol differed significantly from the absorption profile of the other drugs. After reaching a peak level, the amount in the perfusate decreased to a plateau level. After vascular administration of propranolol to isolated and perfused rat lungs, little or no metabolism was found (Dollery et al., 1976).

Therefore, the decrease in perfusate concentration was most likely due to distribution of the drug in the tissue, not metabolism. In the present study, the extent of air-to-blood absorption was higher for metoprolol than propranolol. The results are consistent with reported *in vivo* data and were due to the more lipophilic properties of propranolol (Bodin et al., 1975).

Budesonide was rapidly absorbed into the perfusate. However, the extent of absorption of budesonide was only  $37.6 \pm 15.3\%$ . After the experiments, the perfusate, trachea, and lung tissue were analyzed for the content of budesonide and budesonide esters (Jendbro et al., 2001). The total recovery of budesonide, budesonide oleate, and budesonide palmitate in the perfusate, trachea and lung tissue was  $94 \pm 13\%$  of the given dose (Figure 21). No budesonide esters were found in the perfusate. The uptake of budesonide in the trachea and lung as well as the formation of lipophilic fatty acid esters is in accordance with the results reported by previous investigators (Jendbro et al., 2001; Miller-Larsson et al., 1998; Ryrfeldt et al., 1989).

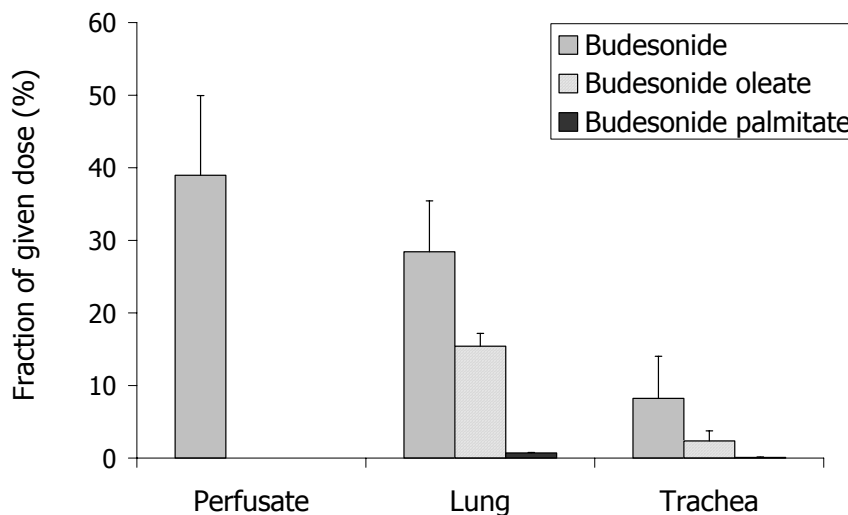


**Figure 21.** The recovery of budesonide and budesonide esters in tissue and perfusate samples 2 h after administration to the isolated and perfused rat lung.

The rate and extent of absorption were higher for the prodrug enalapril than for the pharmacologically active enalaprilate. After delivery of enalapril,  $7.7 \pm 1.6\%$  of the given dose was recovered as enalaprilate in the perfusate. Hence, in total about 95% of the delivered dose of enalapril was transferred into the perfusate. The observed differences in the absorption characteristics may be due to the more lipophilic properties of enalapril compared to enalaprilate. However, the intestinal uptake of enalapril is mediated by the oligopeptide carrier; hence, the results in the present study may suggest the presence of a high capacity oligopeptide carrier, which facilitates the transport of enalapril across the pulmonary epithelium (Schoenmakers et al., 1999). This hypothesis is supported by recent evidence for the localization of the peptide transporter PepT2 in

the alveolar type II cells and bronchial epithelium of the rat lung, but requires further investigation (Groneberg et al., 2001).

The presence of transporter proteins such as P-glycoprotein, multidrug resistance associated protein (MRP), and lung resistance protein (LRP) in lung endothelium and bronchial- and lung epithelial cells have been reported (Bagrij et al., 1998; Beaulieu et al., 1999; Scheffer et al., 2002; Sugawara et al., 1997; Wright et al., 1998). However, the efflux transporter substrate losartan was highly transported across the air-blood barrier of the isolated and perfused rat lung, which indicates an insignificant role for efflux transporters, such as P-gp, in limiting the absorption of losartan from the rat lung (Soldner et al., 2000).

It is often assumed that only the pulmonary circulation is engaged in the isolated and perfused lung model, and that air-to-blood drug absorption experiments performed in the model only reflects the absorption from the pulmonary region (Byron et al., 1986; Sakagami et al., 2002b). In contrast to this hypothesis, we found that two of the investigated drugs, losartan and enalapril, were absorbed to an extent of about 95% of the given dose, which indicates that the deposited dose was delivered to a tissue compartment well perfused by the circulating buffer. Consequently, also the fraction of the dose delivered to the tracheobronchial region was available for absorption. Our data are supported by results obtained by Kröll et al., who demonstrated that the tracheobronchial microcirculation is well perfused in the isolated lung preparation, because of the existence of extensive broncho-pulmonary anastomoses between abundant capillary-venular plexuses along the airway tree (Kröll, 1989). We, therefore, conclude that the applied IPL-model can be used to investigate drug absorption from both the tracheobronchial and pulmonary regions of the lung.

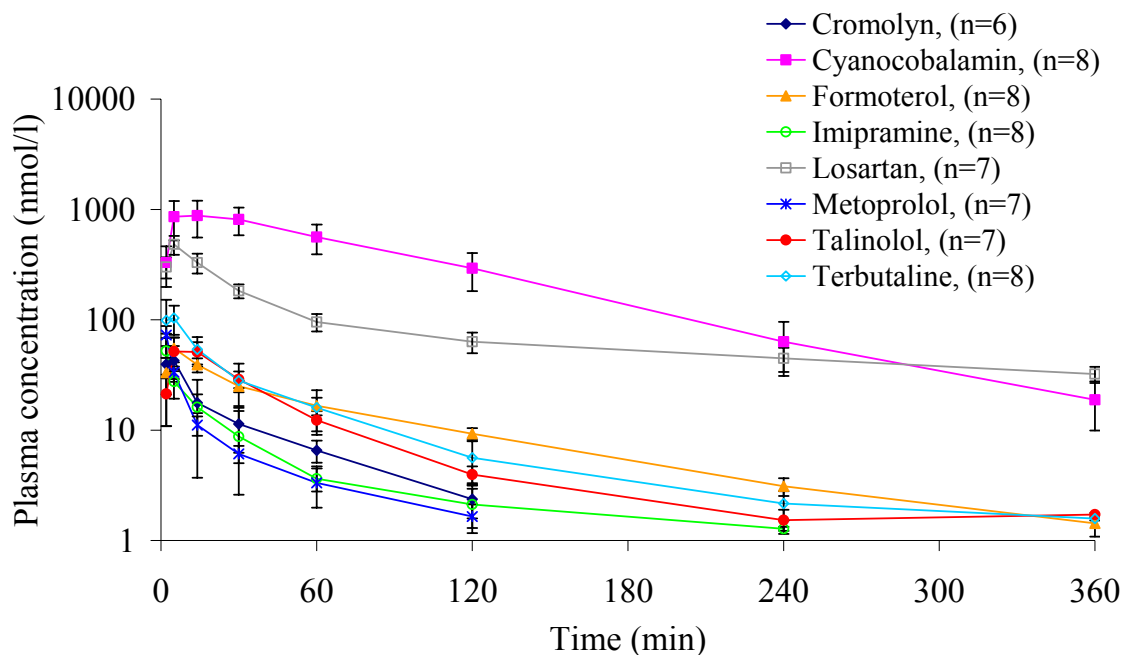


**Figure 22.** Plasma concentration-time profile (mean  $\pm$  SD) of the selected drugs in anesthetized rats after intratracheal nebulization.

In *Paper V*, an in vivo pharmacokinetic investigation of the pulmonary bioavailability and absorption rate of eight selected drugs (cromolyn, cyanocobalamin, formoterol, imipramine, losartan, metoprolol, talinolol and terbutaline) representing diverse physicochemical properties was performed in anesthetized rats.

The pulmonary bioavailability (F) of the drugs was generally found to be high. F for the efflux transporter substrates talinolol and losartan was 81% and 92%, respectively (Table 11). Thus, this study provides functional evidence for an insignificant role of efflux transporters, such as P-glycoprotein, in limiting the systemic availability of these drugs from the rat lung.

**Table 11.** Non-compartmental pharmacokinetic parameters of investigated drugs (means  $\pm$  SD) after intravenous (IV) and pulmonary (intratracheal nebulization, ITN) administration to anesthetized rats.

Drug	Delivery route	<i>n</i>	Dose ( $\mu\text{mol/kg}$ )	AUC/Dose ( $\text{min/L*kg}$ )	$C_{\text{max}}$ ( $\mu\text{M}$ )	$t_{\text{max}}$ (min)	F (%)
Cromolyn	IV	7	$1.7 \pm 0.2$	$17.1 \pm 3.2$	$6.8 \pm 2.8$	0	-
	ITN	6	$0.21 \pm 0.01$	$6.2 \pm 1.1$	$0.05 \pm 0.02$	$3.5 \pm 1.6$	$36 \pm 6$
Cyanocobalamin	IV	9	$2.1 \pm 0.1$	$156.6 \pm 39.5$	$15.8 \pm 3.8$	0	-
	ITN	8	$0.71 \pm 0.03$	$131.1 \pm 42.7$	$0.99 \pm 0.31$	$13.3 \pm 8.5$	$84 \pm 27$
Formoterol	IV	6	$0.25 \pm 0.04$	$10.1 \pm 2.1$	$0.07 \pm 0.01$	0	-
	ITN	8	$0.35 \pm 0.04$	$10.2 \pm 1.0$	$0.06 \pm 0.01$	$5.3 \pm 0.7$	$101 \pm 10$
Imipramine	IV	8	$2.2 \pm 0.1$	$4.4 \pm 0.6$	$0.49 \pm 0.13$	0	-
	ITN	8	$0.24 \pm 0.04$	$4.3 \pm 0.8$	$0.05 \pm 0.02$	$2.4 \pm 1.1$	$98 \pm 19$
Losartan	IV	8	$1.8 \pm 0.0$	$202.9 \pm 42.6$	$11.1 \pm 2.9$	0	-
	ITN	7	$0.22 \pm 0.00$	$186.7 \pm 30.8$	$0.48 \pm 0.09$	$4.6 \pm 1.1$	$92 \pm 15$
Metoprolol	IV	7	$0.95 \pm 0.06$	$6.5 \pm 0.9$	$0.43 \pm 0.17$	0	-
	ITN	7	$0.11 \pm 0.01$	$9.0 \pm 1.5$	$0.07 \pm 0.02$	$2.3 \pm 0.5$	$138 \pm 23$
Talinolol	IV	6	$1.4 \pm 0.1$	$19.0 \pm 1.1$	$5.3 \pm 0.9$	0	-
	ITN	7	$0.17 \pm 0.01$	$15.4 \pm 2.4$	$0.05 \pm 0.02$	$10.9 \pm 5.5$	$81 \pm 13$
Terbutaline	IV	8	$2.2 \pm 0.1$	$17.2 \pm 3.5$	$4.9 \pm 1.1$	0	-
	ITN	8	$0.29 \pm 0.01$	$12.7 \pm 2.7$	$0.11 \pm 0.04$	$3.6 \pm 1.5$	$74 \pm 15$

The absorption of the drugs across the lung barrier into the systemic circulation was rapid, as shown by the short  $t_{\text{max}}$  (2-13 min) and the deconvolution results (Table 11 and 12). The absorption half-life ( $T_{50\%}$ ) was 1-17 min for all drugs and the time required to absorb 90% of the available dose ( $T_{90\%}$ ) was 2-94 min.

Imipramine and metoprolol are lipophilic basic amines, which have been demonstrated to be highly distributed to the lung and other tissues (Bodin et al., 1975; Suhara et al., 1998). High affinity of metoprolol to lung tissue was also demonstrated in *Paper IV*. In *Paper V*, the deconvolution of the pharmacokinetic data demonstrated very short absorption times ( $T_{50\%}$  and  $T_{90\%}$ ) for these drugs (Table 12). The high rate of distribution is consistent with the high apparent permeabilities of these compounds in Caco-2 cell monolayers (Table 13).

**Table 12.** Deconvolution parameters (means  $\pm$  SD) of the investigated drugs after pulmonary administration to anesthetized rats.

	Cro	Cyan	For	Imi	Los	Met	Tal	Ter
$T_{50\%}$ (min)	14 $\pm$ 6	15 $\pm$ 5	4 $\pm$ 0	1 $\pm$ 1	5 $\pm$ 1	1 $\pm$ 0	17 $\pm$ 5	11 $\pm$ 5
$T_{90\%}$ (min)	74 $\pm$ 16	77 $\pm$ 29	13 $\pm$ 4	4 $\pm$ 2	17 $\pm$ 3	2 $\pm$ 0	72 $\pm$ 56	94 $\pm$ 25

Drug abbreviations: Cro = Cromolyn; Cyan = Cyanocobalamin; For = Formoterol; Imi = Imipramine; Los = Losartan; Met = Metoprolol; Tal = Talinolol; Ter = Terbutaline.

$T_{50\%}$  and  $T_{90\%}$  denote the time to absorb 50% and 90%, respectively, of the available dose.

## 6.5 Permeability characteristics of investigated drugs in the epithelial permeability screening model, Caco-2 (*Paper II, IV-V*)

In *Paper II, IV and V*, the bi-directional permeability of the investigated drugs was studied using the frequently applied permeability screening model Caco-2. There was no directional difference in the permeation of the drugs, except for losartan and talinolol (*Paper IV and V*). The permeability of these compounds was found to be about four times higher in the B-A direction compared to the A-B direction ( $p < 0.05$ ), indicating possible interaction with efflux transporters present in the Caco-2 cell monolayers. Talinolol is generally known as a substrate for the P-glycoprotein efflux transporter, which confirms the obtained results (Spahn Langguth et al., 1998). Regarding losartan, the results are also supported by published evidence for the involvement of P-glycoprotein and other yet unidentified intestinal efflux transporters in the transport of losartan across Caco-2 cell monolayers (Soldner et al., 2000). In *Paper II*, the permeability of the Caco-2 monolayers to TArPP was found to be slightly higher in the A-B direction compared to the B-A direction. However, the permeability in both directions was lower than that for  $^{14}\text{C}$ -mannitol; hence, the results were not considered as any facilitated transport.

**Table 13.** Bi-directional permeability of Caco-2 cell monolayers to the investigated drugs (*Paper II, IV, and V*) and the reference permeability marker <sup>14</sup>C-Mannitol. The drug concentration in the donor compartment was 10 μM and the incubation time 120 min. The data are presented as means ± SD.

Compound	Paper	n <sup>a</sup>	P <sub>app</sub> × 10 <sup>-6</sup> (cm/s)		Ratio B-A / A-B
			A-B <sup>b</sup>	B-A <sup>c</sup>	
Atenolol	IV	4	0.7 ± 0.4	0.63 ± 0.16	0.9
Budesonide	IV	3	10.7 ± 2.6	8.7 ± 3.9	0.8
Cromolyn	V	2	0.1 ± 0.0	0.1 ± 0.0	1.0
Cyanocobalamin	V	2	0.1 ± 0.1	0.1 ± 0.0	1.0
Enalapril	IV	4	0.2 ± 0.2	0.2 ± 0.1	0.7
Enalaprilate	IV	4	0.2 ± 0.1	0.1 ± 0.1	0.7
Formoterol	IV, V	4	1.9 ± 1.0	2.1 ± 1.0	1.1
Imipramine	V	1	10.8	12.1	1.1
Losartan <sup>d</sup>	IV, V	4	1.0 ± 0.5	3.7 ± 0.5*	3.7
Metoprolol	IV, V	4	10.9 ± 3.7	7.3 ± 3.2	0.7
Propranolol	IV	5	7.4 ± 2.5	5.5 ± 1.6	0.7
Talinolol <sup>d</sup>	V	2	0.3 ± 0.01	1.2 ± 0.1*	4.0
TArPP <sup>e</sup>	II	3	0.6 ± 0.10	0.2 ± 0.01	0.3
Terbutaline	IV, V	5	0.8 ± 0.5	1.1 ± 0.5	1.4
<sup>14</sup> C-Mannitol	II, IV, V	27	0.5 ± 0.2	<i>n.a.</i>	<i>n.a.</i>

<sup>a</sup>) In each experiment two filters were run A-B and one filter B-A; <sup>b</sup>) A-B: apical to basolateral direction;

<sup>c</sup>) B-A: basolateral to apical direction; <sup>d</sup>) Established efflux transporter substrates (Soldner et al., 2000; Spahn Langguth et al., 1998); <sup>e</sup>) Concentration in donor compartment 5 μM; \* Different from P<sub>app</sub> (A-B) (p < 0.05); *n.a.* not assessed

## 6.6 Influence of drug physicochemical properties and epithelial permeability on the absorption rate and bioavailability after pulmonary drug administration (*Paper IV, V*)

### *Lipophilicity*

The pulmonary apparent first-order absorption rate constant of the investigated drugs in vivo and in the IPL-model, as well as the apparent permeability across the Caco-2 cell monolayers (P<sub>app</sub>), respectively, were found to correlate to the drug lipophilicity. The results are in agreement with previous investigations showing that the permeability of epithelial barriers to drugs correlates to the lipophilicity of the compound (Brown et al., 1983; Saha et al., 1994; Winiwarter et al., 1998). cLogD(7.4) correlated more strongly than cLogP, indicating the influence of drug charge, which is generally recognized for epithelial barriers, such as the intestine.

The pulmonary bioavailability was also correlated to the drug lipophilicity. The drugs investigated in *Paper V* showed an almost complete bioavailability (<80%) when the cLogD(7.4) was higher than zero (0).

### *Hydrogen bonding*

Negative correlations were obtained between the apparent absorption rate across the lung barrier of rats and the number of hydrogen bonds both in vivo and in the IPL-model.

### *Polar molecular surface area*

The pulmonary apparent first-order absorption rate constant of the investigated drugs in vivo and in the IPL-model, the pulmonary bioavailability, as well as the apparent permeability across the Caco-2 cell monolayers ( $P_{app}$ ), respectively, were found to correlate to the polar molecular surface area (static) of the drugs.

The dynamic polar surface area has previously been suggested to be a better theoretical descriptor of intestinal drug absorption than calculated lipophilicity (cLogD(7.4)) or hydrogen bonding potential (Palm et al., 1998). Orally administered drugs with large polar molecular surface areas (PSA) ( $\geq 120-140 \text{ \AA}^2$ ) have been demonstrated to be hardly absorbed (< 10%) by passive diffusion, whereas drugs with a small molecular surface area (<  $60 \text{ \AA}^2$ ) were almost completely absorbed (Kelder et al., 1999; Palm et al., 1997). A small molecular polar surface area (<  $60-70 \text{ \AA}^2$ ) was also required for brain penetration of the orally administered drugs (Kelder et al., 1999). In our in vivo pharmacokinetic study (*Paper V*), cyanocobalamin had the highest polar molecular surface area (PSA  $479 \text{ \AA}^2$ ) among the investigated compounds. Yet, the pulmonary bioavailability after aerosol administration was found to be 84%. Similarly, the hydrophilic tetrapeptide TArPP, which has a polar molecular surface area of  $234 \text{ \AA}^2$  and an oral bioavailability of 0.5% (G. Ekström, unpublished results), was completely absorbed after pulmonary administration to rats (*Paper III*). Thus, in contrast to the intestinal mucosa and the blood-brain barrier, the pulmonary epithelium is highly permeable to compounds with a high molecular polar surface area. In *Paper IV and V*, we found stronger correlations between the bioavailability and absorption rate, and the %PSA compared to PSA, which suggests that %PSA may be a better determinant for pulmonary absorption. Particularly, %PSA should be more appropriate when comparing a much wider range of molecular properties, e.g. low- and high-molecular-weight compounds. The drug with the highest %PSA in our dataset was cromolyn, which after pulmonary administration had a bioavailability of 36%. Even though this bioavailability is lower than reported previously in rats (> 75%), it is still much higher than 1-4%, which is the reported oral bioavailability of the compound (Cox et al., 1970).

### *Molecular flexibility*

The molecular flexibility, measured by the number of rotatable bonds, has, in addition to PSA and hydrogen bond count (HB), been found to be an important predictor of good oral bioavailability (Veber et al., 2002). However, we were not able to find any corresponding correlations between the pulmonary bioavailability or absorption rate and the molecular flexibility for the drugs in *Paper IV and V*.

### *PLS-model for prediction of the pulmonary absorption rate (Paper IV)*

Using these most significant descriptor variables,  $\log P_{app}$ , %PSA, and  $c\text{LogD}(7.4)$  (in order of significance) a PLS-model for prediction of the first-order absorption rate constant in IPL,  $k_{a\text{lung}}$ , was obtained. The correlation of the observed and predicted  $k_{a\text{lung}}$ - values is presented in Figure 23. The PLS-model was described by the equation:

$$\log k_{a\text{lung}} = 1.43 + 0.32\log P_{app} - 0.030\%PSA + 0.087c\text{LogD}(7.4) \quad (\text{Eq. 6})$$

( $Q^2=0.74$ ,  $R^2=0.78$ , and the standard error of prediction = 0.27).

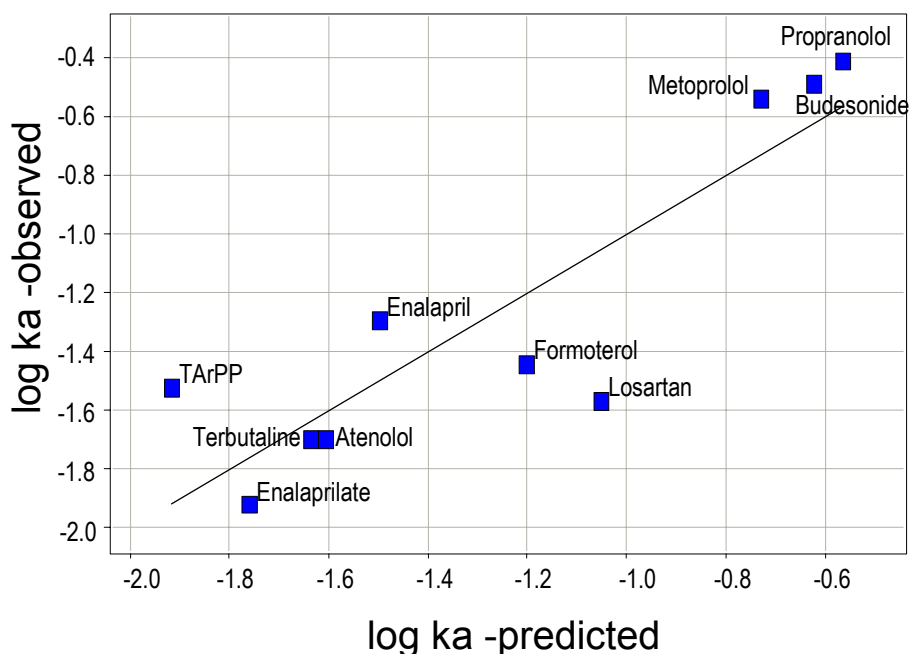


**Figure 23.** PLS-correlation of the observed versus the predicted apparent absorption rate constant in the isolated and perfused rat lung. The PLS-model is based on the most significant descriptor variables ( $\log P_{app}$ , %PSA, and  $c\text{LogD}(7.4)$ , in order of significance).

## 6.7 Applicability of the biological models used to investigate the pulmonary drug absorption and distribution (*Paper II-V*).

The experiments performed in the isolated and perfused rat lung and in anesthetized rats *in vivo* consistently demonstrated a higher formation of metabolites after airway administration than after vascular administration of TArPP (*Paper II and III*). In addition, the metabolic ratio ( $AUC_{met}/AUC_{parent}$ ) obtained in the IPL-model was quantitatively consistent with that observed *in vivo*. Thus, the results demonstrate the validity of the IPL-model to investigate first-pass metabolism in the lung from a qualitative as well as a quantitative point of view.

Data from *Paper IV and V* was used to evaluate the *in vitro-in vivo* correlation between the pulmonary absorption half-life in IPL and the absorption half-life *in vivo*. A strong log linear relationship ( $r=0.96$ ), presented in Figure 24, was obtained, which supports the use of the IPL-model for investigations of the pulmonary absorption rate of inhaled drugs. The obtained correlation was described by the equation:

$$\log T_{50\%} = 0.0294 t_{1/2 \text{ abs}} + 0.011 \quad (\text{Eq.7})$$

Accordingly, the strong *in vitro-in vivo* correlation may suggest that the PLS-model, described in section 6.6, could be used to predict the absorption half-life *in vivo*, combining the equations 1, 6, and 7.

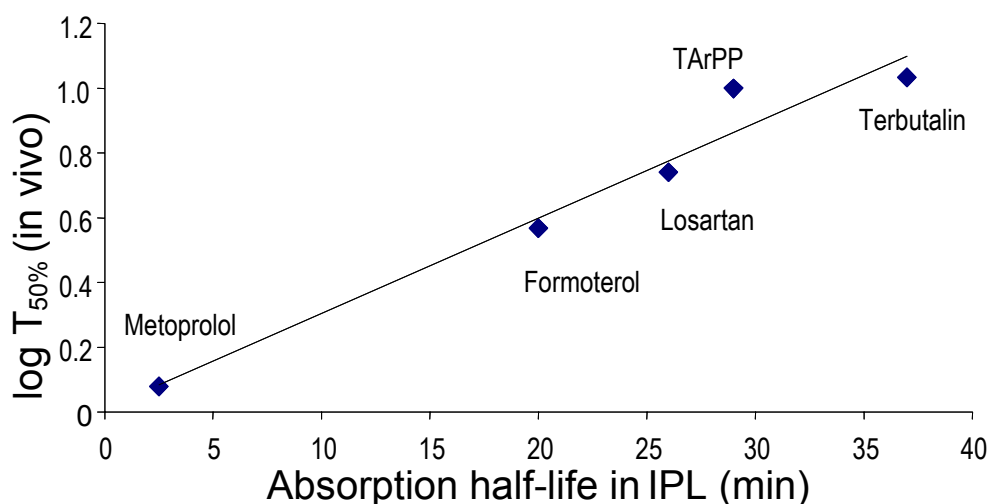
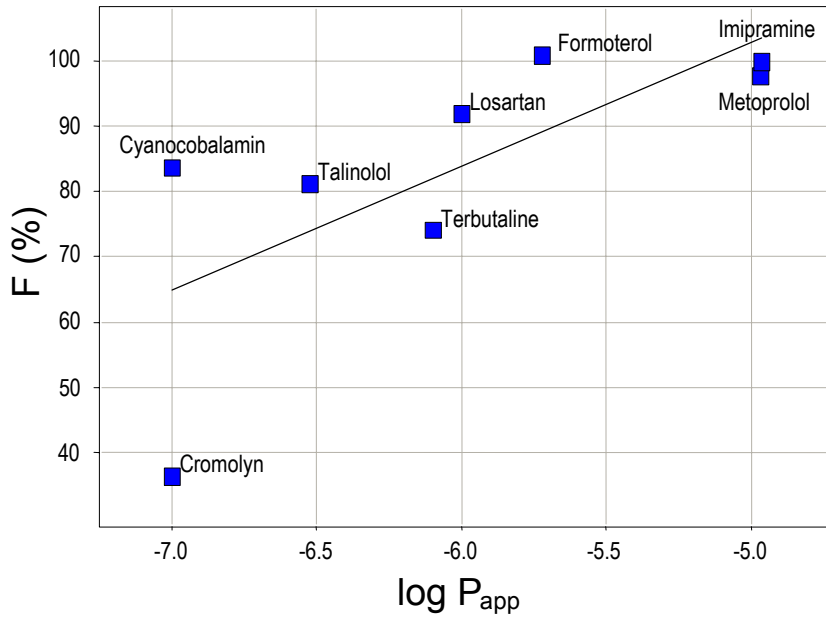
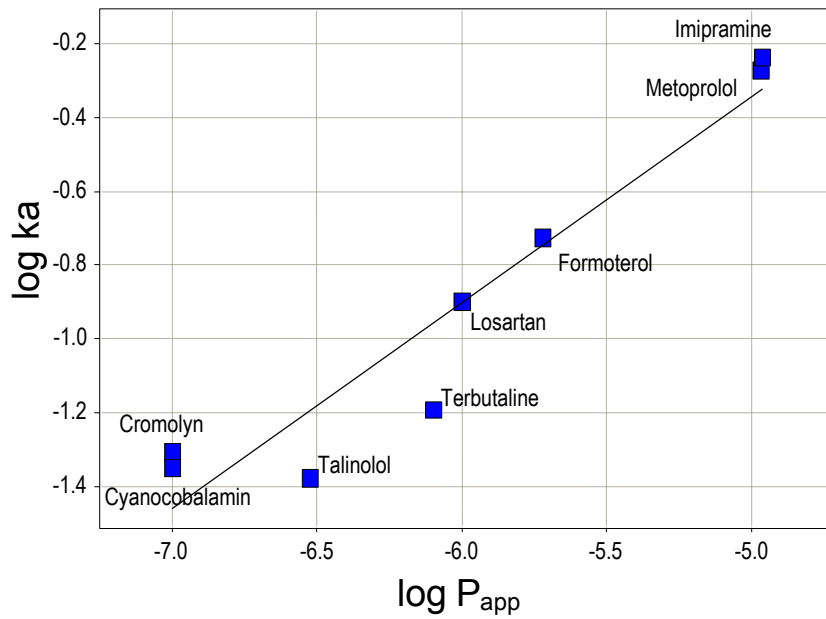


**Figure 24.** *In vitro-in vivo* correlation plot illustrating the relationship between the logarithm of the *in vivo* lung absorption half-life ( $T_{50\%}$ , min) and the absorption half-life in IPL ( $t_{1/2 \text{ abs}}$ , min). The correlation is described by the equation:  $\log T_{50\%} = 0.0294 t_{1/2 \text{ abs}} + 0.011$ ; ( $r=0.96$ ).



A



B

**Figure 25.** Scatter plots illustrating the relationships between the pulmonary bioavailability (A) and absorption rate (B) and the apparent permeability of Caco-2 cells ( $P_{app}$ ). The relationships are described by the equations: (A)  $F = 198 + 19.1 \log P_{app}$  ( $r = 0.72$ ), and (B)  $\log k_a = 2.45 + 0.56 \log P_{app}$  ( $r = 0.96$ ), (Paper V).

A good agreement in rank order was found when comparing the pulmonary absorption rate ( $k_a$ ) and bioavailability ( $F$ ) to the apparent permeability in Caco-2 cell monolayers ( $P_{app}$ ) (Figure 25).

In *Paper IV and V*, strong correlations were found when plotting the logarithm of the pulmonary absorption rate in the IPL-model ( $r=0.96$ ) and in vivo ( $r=0.96$ ), respectively, against the logarithm of  $P_{app}$ . However, drugs classified as low-permeability compounds in the Caco-2 cell model, such as TArPP, terbutaline, cromolyn, and cyanocobalamin, were still highly transported in the lung. For instance, in *Paper II* we found that the permeability of TArPP was so low that the compound could have been excluded from further development. However, the pulmonary bioavailability of TArPP was high (72-114%), which demonstrates the potential of the lung to effectively absorb hydrophilic, low-permeability peptides. Thus, permeability screens of compounds intended for pulmonary administration should be carefully designed to avoid exclusion of promising compounds from further development.

In *Paper IV*, the high air-to-blood absorption rate of budesonide, metoprolol, and propranolol were consistent with the high permeability values of the compounds in the Caco-2 cell monolayers. However, the lung tissue affinity of these drugs was clearly demonstrated and measurable using the isolated and perfused rat lung model, but could not be foreseen from the Caco-2  $P_{app}$ -values.

## **6.8 Comparison of the transport of drugs across the pulmonary and intestinal barriers (*Paper V*)**

The absorption characteristics of the selected drugs across the pulmonary and intestinal mucosal barriers (literature data) are presented in Table 14. The data show an apparent trend for generally higher bioavailability after pulmonary compared to oral administration. For instance, polar drugs were better absorbed from the lung than from the intestine. These data are consistent with results reported by previous investigators (Enna et al., 1972). They showed that the intestinal absorption of mannitol and inulin in rats was less than 2% in 1 hr, compared to 50% and 17%, respectively, after administration to rat lungs.

**Table 14.** Summary of bioavailability and absorption characteristics of the selected drugs across the rat lung and the human intestine\*.

Drug	Lung		Intestine			
	F (%)	ka (min <sup>-1</sup> ) <sup>a</sup>	F (%) <sup>b</sup>	fa (%)	P <sub>eff</sub> × 10 <sup>-4</sup> (cm/s) <sup>c</sup>	Caco-2 P <sub>app</sub> × 10 <sup>-6</sup> (cm/s)
Cromolyn	36	0.05	1-4 <sup>d</sup>	1 <sup>b</sup>	0.04	0.1
Cyanocobalamin	84	0.04	<i>n.a.</i>	<i>n.a.</i>	5.5 × 10 <sup>-9</sup>	0.1
Formoterol	101	0.19	<i>n.a.</i>	<i>n.a.</i>	0.2	1.9
Imipramine	98	0.53	39 ± 7	100 <sup>e</sup>	22	10.8
Losartan	92	0.13	33	100 <sup>f</sup>	0.8	1.0
Metoprolol	138	0.58	38 ± 14	100 <sup>f</sup>	1.7	10.9
Talinolol	81	0.04	55	55 <sup>f, g</sup>	0.2	0.3
Terbutaline	74	0.06	14 ± 2	40-50 <sup>f</sup>	0.3	0.8

\* Convincing evidence for the similarity of human and rat oral absorption data (fa) has been presented by several investigators (Amidon et al., 1988; Chiou et al., 1998; Fagerholm et al., 1996)

<sup>a</sup>) Apparent first-order rate constant ( $\ln 2 / T_{50\%}$ ); <sup>b</sup>) Data collected from Goodman & Gilman's *The Pharmacological Basis of Therapeutics*, 9<sup>th</sup> ed. (Goodman et al., 1996); <sup>c</sup>) Predicted according to the equation:  $\log P_{eff} = -2.546 - 0.011 PSA - 0.278 HBD$ , according to (Winiwarter et al., 1998); <sup>d</sup>) Data from (Cox et al., 1970); <sup>e</sup>) Data from (Chiou et al., 1998); <sup>f</sup>) Data from (Lennernäs, 2002); <sup>g</sup>) 99% of the orally administered dose is excreted unchanged in the urine, which indicates that the fraction absorbed is equal to the bioavailability; *n.a.*: not available

## 7. CONCLUSIONS

- The adapted nebulization catheter technique provides a complement to existing methodologies for pulmonary drug delivery in small animals, especially in investigations that require high dose precision such as pulmonary pharmacokinetics. With this new technique, defined aerosol doses can be reproducibly delivered into the rat lung with no need for aerosol dosimetry. The dosing procedure is synchronized with the inspiration of the lung and does not interrupt the normal breathing pattern of the animal. Small volumes of air (1-1.5 ml), adjusted to the tidal volume of the animal, efficiently aerosolise the test formulation (1-2  $\mu$ l/puff). The nebulization catheter device is well adapted to handle small amounts of test formulation (i.e. about 200  $\mu$ l), which makes it suitable for early preclinical investigations.
- Pulmonary delivery is a promising route for systemic administration of the hydrophilic  $\mu$ -selective opioid tetrapeptide agonist TArPP. The peptide is well absorbed across the lung barrier of the isolated and perfused rat lung and shows a complete bioavailability in rats *in vivo* after pulmonary delivery.
- TArPP is susceptible to some first-pass metabolism after airway delivery, although much less than after oral administration. The metabolism of the peptide is higher after delivery to the airway lumen of the isolated and perfused rat lung, than after delivery to the vascular circulation. Likewise, the metabolism of the peptide is higher after airway delivery compared to intravenous delivery in rats *in vivo*.
- There are regional differences in bioavailability, absorption rate, and first-pass metabolism of TArPP after delivery to different regions of the respiratory tract in rats. The bioavailability increases from the upper to the lower respiratory regions, i.e. nose < trachea < lung. A significantly higher nasal first-pass metabolism of the peptide may explain the lower bioavailability after nasal compared to pulmonary administration.
- The inhaled drugs on the market during 2001 (34 drugs) are dominated by the  $\beta_2$ -agonists and corticosteroids, which generated a broad, skew distribution profile of physicochemical properties dependent on the structure class. Compared to oral drugs, the cLogD(7.4) tended to be lower and the molecular polar surface area (PSA) slightly higher.
- The lipophilicity, PSA, and hydrogen bonding potential are the most influential physicochemical properties for the pulmonary absorption of structurally diverse drugs. There is a stronger correlation between the pulmonary absorption rate and the cLogD(7.4) compared to cLogP. Furthermore, the results suggest that %PSA may better determine pulmonary absorption than PSA. In contrast to the intestinal mucosa and blood-brain barrier, the pulmonary epithelium is highly permeable to drugs with high molecular polar surface area.

- The high pulmonary bioavailability of the efflux transporter substrates losartan and talinolol suggests an insignificant role of efflux transporters in limiting the absorption of these drugs in the rat lung.
- The isolated and perfused rat lung (IPL) is a good model for investigations of the absorption rate across the lung barrier. The drug absorption half-life in the IPL strongly correlates with the absorption half-life in vivo after aerosol delivery. In addition, lung tissue affinity of the drugs is clearly demonstrated and measurable in the IPL-model.
- There is a good agreement in rank order when comparing the pulmonary absorption rate ( $k_a$ ) and bioavailability to the apparent permeability in Caco-2 cell monolayers ( $P_{app}$ ). However, drugs that are classified as low-permeability compounds in the Caco-2 cell model are still highly transported in the lung. The transport experiments should thus be carefully evaluated to avoid exclusion of promising compounds from further development. Lung tissue affinity is not foreseen from the permeability screens using Caco-2 cell monolayers.
- Based on the high bioavailability of the efflux transporter substrates, and the relationships between the pulmonary absorption rate and the  $\log P_{app}$  and the physicochemical descriptors, passive diffusion is suggested to be the predominating mechanism of absorption of the investigated drugs in the rat lung.
- Generally, the bioavailability of the investigated drugs was higher after pulmonary than after oral delivery.
- The results of this thesis provide further evidence of the potential of the lung to absorb drugs with a wide range of lipophilicity and polarity, which makes the pulmonary route an interesting alternative for the delivery of drugs that are inadequately absorbed after oral administration.

## 8. PERSPECTIVES

In the absence of a significant amount of human lung absorption data, there is an obvious need for accurate pharmacokinetic *in vivo* investigations in animals to establish *in vitro-in vivo* relationships and to assess preliminary structure-absorption relationships to guide drug discovery programs. The results in this thesis provide new systematic *in vitro* and *in vivo* pharmacokinetic data on absorption of drugs from the lungs. In addition, the refined analysis of the absorption characteristics of the lung barrier in the relation to drug physicochemical properties provides some guidance of important drug properties. The results may, thus, contribute to the establishment of prediction models of pulmonary drug absorption useful in the development of new inhaled drugs for local and systemic action. Furthermore, the results give some guidance on the applicability of some available *in vitro* and *in vivo* pulmonary pharmacokinetic models.

Pulmonary drug delivery offers the possibility not only for extending and rationalizing local drug therapy for lung diseases, but also for using the pulmonary route for systemic administration of drugs with low oral bioavailability. At present, such drugs are most likely excluded from drug development or bound to parenteral delivery. Drug inhalation also presents an opportunity to attain a more rapid onset of drug action than can be attained by the oral route.

Even though the pulmonary route provides opportunities for absorption of drugs with a wide range of physicochemical properties, there are certain limitations in the use of the pulmonary route that need to be considered. The presently available inhalation devices cannot conveniently deliver more than about 5-10 mg of drug to the lung. Thus, the ideal inhaled drug should be highly potent to allow the administration of the dose by one or two inhalations. Moreover, the risk of inducing immunologic reactions due to particulate insolubility or the nature of the drug (e.g. peptides and proteins) should also be carefully considered.

## 9. ACKNOWLEDGMENTS

The studies in this thesis were performed at AstraZeneca R&D Lund, AstraZeneca R&D Södertälje, AstraZeneca Safety Assessment Södertälje, Sweden, Trudell Medical International, London, Ontario, Canada, and at the Department of Pharmacy, Faculty of Pharmacy, Uppsala University, Sweden. I am grateful to the generous support and kind help provided to me by people at these research centers.

*I would especially like to express my sincere gratitude to:*

*Ursula Hultkvist Bengtsson, min handledare på AstraZeneca R&D Lund, för vetenskaplig handledning, ditt stora engagemang kring lungfysiologi och inhalation, stöd, uppmuntran, vänskap och omtanke i alla lägen, samt för trevligt resesällskap och delat intresse för italiensk glass, shopping och historia.*

*Hans Lennernäs, min handledare på Uppsala Universitet, för stimulerande vetenskapliga diskussioner, din entusiasm, uppmuntran och vänskap, samt för många trevliga luncher och fikapausar under manusdiskussioner och seminarier i ABS-gruppen.*

*Anders Tunek, Lena Gustavsson och mina kollegor på "Kinetik & Metabolism", AstraZeneca R&D Lund, för trevlig gemenskap och utmärkt arbetsmiljö under min doktorandtid.*

*Elisabeth Nilsson, Ann-Britt Jeppsson, Elisabeth Hjertberg, Manaf Sababi, Jan-Eric Annerfeldt, Anna-Karin Asztély, Helena Mattsson och Anders Hall i f.d. "Absorptionsgruppen" för vänskap, trevligt samarbete och många ovetenskapliga och vetenskapliga diskussioner. Speciellt tack till Elisabeth Nilsson för att du lärde upp mig till att bli en "riktig perfunderare", för många roliga stunder på IPL-labbet och för eminent handledning i konsten att ha "många bollar i elden" och "järn i luften".*

*Mina medförfattare Eva Krondahl, Bo Nordén, Ann-Britt Jeppsson, Stefan Eirefelt, Per Brunmark, Elisabeth Nilsson, Gunilla Ekström, Hans Marchner, Anna-Karin Wendel, Heidi Forsmo-Bruce och Hans von Euler-Chelpin för stimulerande, lärorikt och gott samarbete. Speciellt tack till Eva för alla roliga och intensiva dagar på labbet, kinetikdiskussioner och hjälp med korrekturläsning av mina manuskript.*

*Stefan Eirefelt och Magnus Dahlbäck för er vänskap, gott samarbete genom åren och för att ni generöst delat med er av eran stora kunskap kring inhalation.*

*George Baran and Bryan Finlay at Trudell Medical International, Canada, for excellent co-operation, commitment, support, and friendship during my research work. I hope to get a chance to finally meet with you somewhere, sometime...*

*Pontus Holm, Lennart Berggren och Thomas Wendel för allt utvecklingsarbete och teknisk support för "LISA", "Incontinentia" och "TENA", för era smittande skratt och aldrig sinande hjälpsamhet, samt för att ni frikostigt förmedlat era hemligheter kring elektronikens trolltrummor och voodookonster.*

*Carin Sandberg, Carina Hörnsten och Janne Persson för all hjälp med ITS-studien.*

*Sten Sturefelt, Ola Nerbrink och Bengt Malmberg för råd och hjälp med att mäta och visualisera aerosoldoser.*

*Caroline Ritswall, Karin Sjödin, Britt-Marie Kennedy, Elizabeth Karlsson, Ann Svensson, Mats Gustavsson, Margaretha Maxe, Anna Olsson och Anders Blomgren för ovärderlig hjälp med analyser.*

*Information Science & Library, AstraZeneca R&D Lund, för er fantastiska hjälpsamhet. Speciellt tack till Inga Elding, Anna-Carin Larsen och Göran Hollenby.*

*Veterinary Science, AstraZeneca R&D Lund, för utmärkt service.*

*Lars Borgström, Johan Rosenborg och Eva Bondesson för stimulerande diskussioner kring inhalation.*

*Cosme Idris för alla fina postrar till konferenser och hjälp med bildhantering för manuskript.*

*Före detta och nuvarande doktorandkollegor i absorptionsgruppen i Uppsala: Eva Krondahl, Urban Fagerholm, Rikard Sandström, Anders Lindahl, Eve-Irene Lepist, Helena Engman, Sofia Berggren, Christer Tannergren och Niclas Petri för förmedlad "gruppkänsla" ända ner till Lund.*

*Karin Dahl, Eva Nises-Ahlgren och Ulla Wästberg-Galik för all tänkbar praktisk hjälp.*

*Steve Scott-Robson for excellent and rapid linguistic revisions of manuscripts and this thesis, and for your exciting reports of everyday life in Colombia.*

*Anna Malmgren för stöd under färdigställandet av min avhandling.*

*Alla mina underbara vänner för att ni finns!*

*Havet, stranden och solen, min källa till energi, för skön avkoppling och perspektiv på livet.*

*Min familj för alla trevliga stunder, er uppmuntran och ert stöd. En stor kram till mamma Bibbi för all omtanke, alla godsaker och utsökta middagar som du skämt bort mig med. Kie och Olle för ivrigt påhejande och för att ni med stort intresse läser mina "alster".*

*Min älskade bästis Ulf för obegränsad kärlek, vänskap, hjälp med korrekturläsning och bilder till denna avhandling samt för superb "markservice" och alla gourmetmiddagar! ♥ Du är mitt allt!!!*



The financial support from AstraZeneca R&D Lund is gratefully acknowledged.

## 10. REFERENCES

- Adjei, A., Sundberg, D., Miller, J., and Chun, A. (1992). Bioavailability of leuprolide acetate following nasal and inhalation delivery to rats and healthy humans, *Pharm Res* 9, 244-249.
- Alari, L., and Martel, R. (1996). Antinociceptive effects of LEF553, a peripherally acting opioid peptide in mice. In: (8th) World Congress on Pain (IASP Press), pp.455.
- Amidon, G. L., Sinko, P., and Fleisher, D. (1988). Estimating human oral fraction dose absorbed: a correlation using rat intestinal membrane permeability for passive and carrier-mediated compounds, *Pharm Res* 5, 651-654.
- Anderson, M. W., Orton, T. C., Pickett, R. D., and Eling, T. E. (1974). Accumulation of amines in the isolated perfused rabbit lung, *J Pharmacol Exp Ther* 189, 456-466.
- Anonymous (1946). Inhaler for penicillin: notes and news, *Lancet* 1, 986.
- Anttila, S., Hukkanen, J., Hakkola, J., Stjernvall, T., Beaune, P., Edwards, R. J., Boobis, A. R., Pelkonen, O., and Raunio, H. (1997). Expression and localization of CYP3A4 and CYP3A5 in human lung, *Am J Respir Cell Mol Biol* 16, 242-249.
- Artursson, P. (1990). Epithelial transport of drugs in cell culture: I: A model for studying the passive diffusion of drugs over intestinal absorptive (Caco-2) cells, *J Pharm Sci* 79, 476-482.
- Audi, S. H., Dawson, C. A., Linehan, J. H., Krenz, G. S., Ahlf, S. B., and Roerig, D. L. (1998). Pulmonary disposition of lipophilic amine compounds in the isolated perfused rabbit lung, *J Appl Physiol* 84, 516-530.
- Audi, S. H., Roerig, D. L., Ahlf, S. B., Lin, W., and Dawson, C. A. (1999). Pulmonary inflammation alters the lung disposition of lipophilic amine indicators, *J Appl Physiol* 87, 1831-1842.
- Bagrij, T., Hladky, S. B., Stewart, S., Scheper, R. J., and Barrand, M. A. (1998). Studies of multidrug transport proteins in cells derived from human lung samples, *Int J Clin Pharmacol Ther* 36, 80-81.
- Bassett, D. J. P., and Roth, R. A. (1992). The isolated perfused lung preparation. In: In vitro methods of toxicology, Watson, R. R., ed. (Boca Raton, Florida, CRC Press), pp. 143-155.
- Beaulieu, E., Demeule, M., Jetté, L., and Béliveau, R. (1999). Comparative assessment of P-glycoprotein expression in mammalian tissues by immunoblotting, *Int J Bio-Chromatogr* 4, 253-269.
- Ben-Jebria, A., Eskew, M. L., and Edwards, D. A. (2000). Inhalation systems for pulmonary aerosol drug delivery systems in rodents using large porous particles, *Aerosol Sci Technol* 32, 421-433.
- Berg, M. M., Kim, K. J., Lubman, R. L., and Crandall, E. D. (1989). Hydrophilic solute transport across rat alveolar epithelium, *J Appl Physiol* 66, 2320-7.
- Bhat, P. G., Flanagan, D. R., and Donovan, M. D. (1995). The limiting role of mucus in drug absorption: drug permeation through mucus solution, *Int J Pharm* 126, 179-187.
- Bodin, N.-O., Borg, K. O., Johansson, R., Ramsay, C.-H., and Skånberg, I. (1975). Tissue distribution of metoprolol-(<sup>3</sup>H) in the mouse and the rat, *Acta Pharmacol Toxicol* 36, 116-124.

- Borchard, G., Cassará, M. L., Roemelé, P. E. H., Florea, B. I., and Junginger, H. E. (2002). Transport and local metabolism of budesonide and fluticasone propionate in human bronchial epithelial cell line (Calu-3), *J Pharm Sci* 91, 1561-1567.
- Brain, J. D., Bloom, S. D., Valberg, P. A., and Gehr, P. (1984). Correlation between the behavior of magnetic iron oxide particles in the lungs of rabbits and phagocytosis, *Exp Lung Res* 6, 115-131.
- Brain, J. D., Knudson, D. E., Sorokin, S. P., and Davis, M. A. (1976). Pulmonary distribution of particles given by intratracheal instillation or by aerosol inhalation, *Environ Res* 11, 13-33.
- Brewis, R. A. L., Corrin, B., Geddes, D. M., and Gibson, G. J., eds. (1995). *Respiratory Medicine*, second edition, (London, W.B. Saunders Company Ltd).
- Brown, R. A., and Schanker, L. S. (1983). Absorption of aerosolized drugs from the rat lung, *Drug Metab Dispos* 11, 355-360.
- Byron, P. R., and Niven, R. W. (1988). A novel dosing method for drug administration to the airways of the isolated perfused rat lung, *J Pharm Sci* 77, 693-695.
- Byron, P. R., Sian, N., Roberts, R., and Clark, A. R. (1986). An isolated perfused rat lung preparation for the study of aerosolized drug deposition and absorption, *J Pharm Sci* 75, 168-171.
- Camps, P. W. L. (1929). A note on the inhalation treatment of asthma, *Guy's Hosp Rep* 79, 496-498.
- ChangLai, S. P., Hung, W. T., and Liao, K. K. (1999). Detecting alveolar epithelial injury following volatile anesthetics by <sup>99m</sup>Tc DTPA radioaerosol inhalation lung scan, *Respiration* 66, 506-510.
- Chediak, A. D., and Wanner, A. (1990). The circulation of the airways: anatomy, physiology and potential role in drug delivery to the respiratory tract, *Adv Drug Deliv Rev* 5, 11-18.
- Chiou, W. L., and Barve, A. (1998). Linear correlation of the fraction of oral dose absorbed of 64 drugs between humans and rats, *Pharm Res* 15, 1792-1795.
- Clark, A. R. (1995). The use of laser diffraction for the evaluation of the aerosol clouds generated by medical nebulizers, *Int J Pharm* 115, 69-78.
- Colthorpe, P., Farr, S. J., Smith, I. J., Wyatt, D., and Taylor, G. (1995). The influence of regional deposition on the pharmacokinetics of pulmonary-delivered human growth hormone in rabbits, *Pharm Res* 12, 356-359.
- Colthorpe, P., Farr, S. J., Taylor, G., Smith, I. J., and Wyatt, D. (1992). The pharmacokinetics of pulmonary-delivered insulin: a comparison of intratracheal and aerosol administration to the rabbit, *Pharm Res* 9, 764-768.
- Concessio, N. M., Oort, M. M. V., Knowles, M., and Hickey, A. J. (1999). Pharmaceutical dry powder aerosols: correlation of powder properties with dose delivery and implications for pharmacodynamic effect, *Pharm Res* 16, 833-839.
- Conhaim, R. L., Eaton, A., Staub, N. C., and Heath, T. D. (1988). Equivalent pore estimate for the alveolar-airway barrier in isolated dog lung, *J Appl Physiol* 64, 1134-1142.
- Conhaim, R. L., Watson, K. E., Lai-Fook, S. J., and Harms, B. A. (2001). Transport properties of alveolar epithelium measured by molecular hetastarch absorption in isolated rat lungs, *J Appl Physiol* 91, 1730-1740.
- Cox, J. S. G., Beach, J. E., Blair, A. M. J. N., Clarke, A. J., King, J., Lee, T. B., Loveday, D. E. E., Moss, G. F., Orr, T. S. C., Ritchie, J. T., and Sheard, P. (1970). Disodium cromoglycate (Intal), *Adv Drug Res* 5, 115-196.

- Crandall, E. D., and Matthay, M. A. (2001). Alveolar epithelial transport, *Am J Respir Crit Care Med* 162, 1021-1029.
- Crapo, J. D., Barry, B. E., Gehr, P., Bachofen, M., and Weibel, E. R. (1982). Cell number and cell characteristics of the normal human lung, *Am Rev Respir Dis* 125, 740-745.
- Crooks, P. A., Krechniak, J. W., Olson, J. W., and Gillespie, M. N. (1985). High-performance liquid chromatographic analysis of pulmonary metabolites of Leu- and Met-enkephalins in isolated perfused rat lung, *J Pharm Sci* 74, 1010-1012.
- Dahlbäck, M., Eirefelt, S., and Nerbrink, O. (1996). Aerosol delivery to the respiratory tract in experimental animals. In: *Aerosol Inhalation: Recent Research Frontiers*, Marijnissen, J. C. M., and Gradon, L., eds. (Kluwer academic publishers), pp. 235-246.
- Dale, O., and Brown, B. R. J. (1987). Clinical pharmacokinetics of the inhalation anaesthetics, *Clin Pharmacokinetics* 12, 145-167.
- de Wet, C., and Moss, J. (1998). Metabolic functions of the lung, *Anesthesiol Clin North America* 16, 181-199.
- Dershwitz, M., Walsh, J. L., Morishige, R. J., Connors, P. M., Rubsamen, R. M., Shafer, S. L., and Rosow, C. E. (2000). Pharmacokinetics and pharmacodynamics of inhaled versus intravenous morphine in healthy volunteers., *Anesthesiology* 93, 619-628.
- Dodoo, A. N., Bansal, S. S., Barlow, D. J., Bennet, F., Hider, R. C., Lansley, A. B., Lawrence, M. J., and Marriot, C. (2000a). Use of alveolar cell monolayers of varying electrical resistance to measure pulmonary peptide transport, *J Pharm Sci* 89, 223-231.
- Dodoo, A. N. O., Bansa, S., Barlow, D. J., Bennet, F. C., Hider, R. C., Lansley, A. B., Lawrence, M. J., and Marriot, C. (2000b). Systematic investigations of the influence of molecular structure in the transport of peptides across cultured alveolar cell monolayers, *Pharm Res* 17, 7-14.
- Dollery, C. T., and Junod, A. F. (1976). Concentration of ( $\pm$ )-propranolol in isolated, perfused lungs of rat, *Br J Pharmacol* 57, 67-71.
- Drew, R., Siddik, Z., Mimnaugh, E. G., and Gram, T. E. (1981). Species and dose differences in the accumulation of imipramine by mammalian lungs, *Drug Metab Dispos* 9, 322-326.
- Driscoll, K. E., Costa, D. L., Hatch, G., Henderson, R. F., Oberdörster, G., Salem, H., and Schlesinger, R. B. (2000). Intratracheal instillation as an exposure technique for the evaluation of respiratory tract toxicity: uses and limitations, *Toxicol Sci* 55, 24-35.
- Edwards, D. A., Hanes, J., Caponetti, G., Hrkach, J., Deaver, D., Lotan, N., and Langer, R. (1997). Large porous particles for pulmonary drug delivery, *Science* 276, 1868-1871.
- Effros, R. M., and Mason, G. R. (1983). Measurements of pulmonary epithelial permeability in vivo, *Am Rev Respir Dis* 127, S59-S65.
- Egan, W. J., and Lauri, G. (2002). Prediction of intestinal permeability, *Adv Drug Deliv Rev* 54, 273-289.
- Eirefelt, S., Nerbrink, O., and Dahlbäck, M. (1992). Selective aerosol delivery to intubated rats; a comparison with nose only exposure, *J Aerosol Sci* 23, S491-S494.
- Elbert, K. J., Schäfer, U. F., Schäfers, H. J., Kim, K. J., Lee, V. H. L., and Lehr, C.-M. (1999). Monolayers of human alveolar epithelial cells in primary culture for pulmonary drug delivery and transport studies, *Pharm Res* 16, 601-608.
- Enna, S. J., and Schanker, L. S. (1972). Absorption of saccharides and urea from the rat lung, *Am J Physiol* 222, 409-414.
- Enna, S. J., and Schanker, L. S. (1973). Phenol red absorption from the rat lung: evidence of carrier transport, *Life Sci* 12, 231-239.

- Evander, E., Wollmer, P., Jonson, B., and Lachmann, B. (1987). Pulmonary clearance of inhaled  $^{99m}\text{Tc}$  DTPA: Effects of surfactant depletion by lung lavage, *J Appl Physiol* 62, 1611-1614.
- Evans, J. P., Tudball, N., Dickinson, P. A., Farr, S. J., and Kellaway, I. W. (1998). Transport of a series of D-phenylalanine-glycine hexapeptides across rat alveolar epithelia in vitro, *J Drug Targeting* 6, 251-259.
- Fagerholm, U., Johansson, M., and Lennernäs, H. (1996). Comparison between permeability coefficients in rat and human jejunum, *Pharm Res* 13, 1336-1342.
- Fisher, A. B., Dodia, C., and Linask, J. (1980). Perfusate composition and edema formation in isolated rat lungs, *Exp Lung Res* 1, 13-21.
- Florea, B. I., van der Sandt, I. C. J., Schrier, S. M., Kooiman, K., Deryckere, K., de Boer, A. G., Junginger, H. E., and Borchard, G. (2001). Evidence of P-glycoprotein mediated apical to basolateral transport of flunisolide in human broncho-tracheal epithelial cells (Calu-3), *Br J Pharmacol* 134, 1555-1563.
- Folkesson, H. G., Weström, B. R., and Karlsson, B. W. (1998). Effects of systemic and local immunization on alveolar epithelial permeability to protein in the rat, *Am J Respir Crit Care Med* 157, 324-327.
- Folkesson, H. G., Weström, B. R., Dahlbäck, M., Lundin, S., and Karlsson, B. W. (1992). Passage of aerosolized BSA and the nona-peptide dDAVP via the respiratory tract in young and adult rats, *Exp Lung Res* 18, 595-614.
- Folkesson, H. G., Weström, B. R., Pierzynowski, S. G., and Karlsson, B. W. (1991). Lung to blood passage of different-sized molecules during inflammation in the rat, *J Appl Physiol* 71, 1106-1111.
- Forbes, B., Wilson, C. G., and Gumbleton, M. (1999). Temporal dependence of ectopeptidase expression in alveolar epithelial cell culture: implications for study of peptide absorption, *Int J Pharm* 180, 225-234.
- Forbes, B. J., Wilson, C. G., and Gumbleton, M. (1995). Extraction of peptidase substrates by the isolated and perfused rat lung, *Pharm Sci* 1, 569-572.
- Foster, K. A., Avery, M. L., Yazdanian, M., and Audus, K. L. (2000). Characterization of the Calu-3 cell line as a tool to screen pulmonary drug delivery, *Exp Cell Res* 243, 359-366.
- Funkhouser, J. D., Tangada, S. D., Jones, M., Seung-Jun, O., and Peterson, R. D. (1991). p146 type II alveolar epithelial cell antigen is identical to aminopeptidase N, *Am J Physiol* 260, L274-279.
- Gardiner, T. H., and Schanker, L. S. (1974). Absorption of disodium cromoglycate from the rat lung: evidence of carrier transport, *Xenobiotica* 4, 725-731.
- Gehr, P. (1984). Respiratory tract structure and function, *J Toxicol Environ Health* 13, 235-249.
- Gehr, P., Mwangi, D., K., Ammann, A., Maloij, G., M.O., Taylor, R., C., and Weibel, E., R. (1981). Design of the mammalian respiratory system. V. Scaling morphometric pulmonary diffusing capacity to body mass: wild and domestic mammals, *Respir Physiol* 44, 61-86.
- Gillespie, M. N., Krechniak, J.W., Crooks, P.A., Altieri, R.J., and Olson, J.W. (1985). Pulmonary metabolism of exogenous enkephalins in isolated perfused rat lungs, *J Pharmacol Exp Ther* 232, 675-681.
- Girod, S., Zahm, J. M., Plotkowski, C., Beck, G., and Puchelle, E. (1992). Role of the physicochemical properties of mucus in the protection of the respiratory epithelium, *Eur Respir J* 5, 477-487.
- Godfrey, R. W. (1997). Human airway epithelial tight junctions, *Microsc Res Tech* 38, 488-499.

- Goodman, A., Gilman, A. G., Hardman, J. G., Limbard, L. E., Molinoff, P. B., and Ruddon, R. W. (1996). Goodman & Gilman's The Pharmacological Basis of Therapeutics, 9/e (The McGraw-Hill Companies, Inc.).
- Graeser, J. B., and Rowe, A. H. (1935). Inhalation of epinephrine for relief of asthmatic symptoms, *J Allergy* 6, 415-420.
- Green, C. J. (1979). Animal Anesthesia (London, Laboratory Animals Ltd.).
- Greiff, L., Andersson, M., Svensson, J., Wollmer, P., Lundin, S., and Persson, C. G. A. (2002). Absorption across nasal airway mucosa in house dust mite perennial allergic rhinitis, *Clin Physiol Func Im* 22, 55-57.
- Groneberg, D. A., Eynott, P. R., Döring, F., Thai Dinh, Q., Oates, T., Barnes, P. J., Chung, K. F., Daniel, H., and Fischer, A. (2002). Distribution and function of the peptide transporter PEPT2 in normal and cystic fibrosis human lung, *Thorax* 57, 55-60.
- Groneberg, D. A., Nickolaus, M., Springer, J., Döring, F., Daniel, H., and Fischer, A. (2001). Localization of the peptide transporter PEPT2 in the lung: Implications for pulmonary oligopeptide uptake, *Am J Pathol* 158, 707-714.
- Gumbleton, M. (2001). Caveolae as potential macromolecule trafficking compartments within alveolar epithelium, *Adv Drug Deliv Rev* 49, 281-300.
- Haley, P. J., Muggenburg, B. A., Weissman, D. N., and Bice, D. E. (1991). Comparative morphology and morphometry of alveolar macrophages from six species, *Am J Anatomy* 191, 401-407.
- Hamilton, K. O., Backström, G., Yazdanian, M. A., and Audus, K. L. (2001a). P-glycoprotein efflux pump expression and activity in Calu-3 cells, *J Pharm Sci* 90, 647-658.
- Hamilton, K. O., Yazdanian, M. A., and Audus, K. L. (2001b). Modulation of P-glycoprotein activity in Calu-3 cells using steroids and  $\beta$ -ligands, *Int J Pharm* 228, 171-179.
- Hamm, H., Fabel, H., and Bartsch, W. (1992). The surfactant system of the adult lung: physiology and clinical perspectives, *Clin Investig* 70, 637-657.
- Hashmi, N., Matthews, G. P., Martin, A. B., Lansley, A. B., and Forbes, B. (1999). Effect of mucus on transepithelial drug delivery [abstract], *J Aerosol Med* 12, 139.
- Hastings, R. H., Grady, M., Sakuma, T., and Matthay, M. A. (1992). Clearance of different-sized proteins from the alveolar space in humans and rabbits, *J Appl Physiol* 73, 1310-1317.
- Hayem, A., Scharfman, A., Laine, A., Lafitte, J. J., and Sablonniere, B. (1980). Proteases and antiproteases in bronchoalveolar lavage fluid, *Bull Eur Physiopathol Respir* 16, 247-260.
- Heyder, J., and Svartengren, M. U. (2002). Basic principles of particle behavior in the human respiratory tract. In: Drug delivery to the lung, Bisgaard, H., O'Callaghan, C., and Smaldone, G. C., eds. (New York, Marcel Dekker, Inc.).
- Hickey, A. J., and Garcia-Contreras, L. (2001). Immunological and toxicological implications of short-term studies in animals of pharmaceutical aerosol delivery to the lungs: relevance to humans, *Crit Rev Ther Drug Carrier Syst* 18, 387-431.
- Hlastala, M. P., and Berger, A. J. (1996). Physiology of respiration (New York, Oxford University Press, Inc.).
- Hogg, J. C. (1981). Bronchial mucosal permeability and its relationship to airways hyperreactivity, *J Allergy Clin Immunol* 67, 421-425.
- Hoover, J. L., Rush, B. D., Wilkinson, K. F., Day, J. S., Burton, P. S., Vidmar, T. J., and Ruwart, M. J. (1992). Peptides are better absorbed from the lung than the gut in the rat, *Pharm Res* 9, 1103-1106.

- Ilowite, J. S., Bennet, W. D., Sheetz, W. S., Groth, M. L., and Nierman, D. M. (1989). Permeability of the bronchial mucosa to <sup>99m</sup>Tc-DTPA in asthma, *Am Rev Respir Dis* 139, 1139-1143.
- Ishizaki, J., Yokogawa, K., Nakashima, E., Ohkuma, S., and Ichimura, F. (1998). Uptake of basic drugs into rat lung granule fraction in vitro, *Biol Pharm Bull* 21, 858-861.
- Jackson, J. E. (1991). *A Users Guide to Principal Components* (New York, Wiley).
- Jeffery, P. K. (1995). Microscopic structure of normal lung. In *Respiratory Medicine*, Brewis, R. A. L., Corrin, B., Geddes, D. M., and Gibson, G. J., eds. (London, W.B. Saunders Company Ltd).
- Jendbro, M., Johansson, C.-J., Strandberg, P., Falk-Nilsson, H., and Edsbäcker, S. (2001). Pharmacokinetics of budesonide and its major ester metabolite after inhalation and intravenous administration of budesonide in the rat, *Drug Metab Dispos* 29, 769-776.
- Johansson, A., Lennernäs, H., Baran, G., and Hultkvist Bengtsson, U. (2000). Nebulization catheters for regional pulmonary targeting of drugs to the isolated and perfused rat lung. Paper presented at: Millennial World Congress of Pharmaceutical Sciences. (San Fransisco, International Pharmaceutical Federation USA).
- Johnson, L. G., and Boucher, C. (1993). Macromolecular transport across nasal and respiratory epithelia. In *Biological barriers to protein delivery*, Audus, K. L., and Raub, T. J., eds. (New York, Plenum Press), pp. 161-178.
- Jones, J. G., Minty, B. D., Lawler, P., Hulands, G., Crawley, J. C., and Veall, N. (1980). Increased alveolar epithelial permeability in cigarette smokers, *Lancet* 1, 66-68.
- Jorfeldt, L., Lewis, D. H., Löfström, J. B., and Post, C. (1979). Lung uptake of lidocaine in healthy volunteers, *Acta Anaesth Scand* 23, 567-574.
- Junod, A. (1976). Uptake, release and metabolism of drugs in the lungs, *Pharmac Ther, B* 2, 511-521.
- Kelder, J., Grootenhuis, P. D. J., Bayada, D. M., Delbressine, L. P. C., and Ploemen, J.-P. (1999). Polar molecular surface as a dominating determinant for oral absorption and brain penetration of drugs, *Pharm Res* 16, 1514-1519.
- Kornhauser, D. M., Vestal, R. E., and Shand, D. G. (1980). Uptake of propranolol by the lung and its displacement by other drugs: Involvement of the alveolar macrophage, *Pharmacology* 20, 275-283.
- Krishna, D. R., and Klotz, U. (1994). Extrahepatic metabolism of drugs in humans, *Clin Pharmacokinet* 26, 144-160.
- Krondahl, E., Orzechowski, A., Ekström, G., and Lennernäs, H. (1997). Rat jejunal permeability and metabolism of  $\mu$ -selective tetrapeptides in gastrointestinal fluids from humans and rats, *Pharm Res* 14, 1780-1785.
- Krondahl, E., Tronde, A., Eirefelt, S., Forsmo-Bruce, H., Ekström, G., Hultkvist Bengtsson, U., and Lennernäs, H. (2002). Regional differences in bioavailability of an opioid tetrapeptide agonist in vivo in rats after administration to the respiratory tract., *Peptides* 23, 479-488.
- Krondahl, E., von Euler-Chelpin, H., Orzechowski, A., Ekström, G., and Lennernäs, H. (2000). Investigations of the in-vitro metabolism of three opioid tetrapeptides by pancreatic and intestinal enzymes, *J Pharm Pharmacol* 52, 785-795.
- Krondahl, E., von Euler-Chelpin, H., Orzechowski, A., Ekström, G., and Lennernäs, H. (2001). In vitro metabolism of opioid tetrapeptide agonists in various tissues and subcellular fractions from rats, *Peptides* 22, 613-622.

- Kröll, F. (1989) Purines and sensory neuropeptides in the regulation of airway resistance in guinea-pig isolated perfused lungs, Thesis, University of Lund, Sweden, Lund.
- Kröll, F., Karlsson, J. A., and Persson, C. G. A. (1987). Tracheobronchial microvessels perfused via the pulmonary artery in guinea-pig isolated lungs., *Acta Physiol Scand* 129, 445-446.
- Langenbucher, F. (1982). Improved understanding of convolution algorithms correlating body response with drug input, *Pharm Ind* 44, 1275-1278.
- Langguth, P., Merkle, H. P., and Amidon, G. L. (1994). Oral absorption of peptides: The effect of absorption site and enzyme inhibition on systemic availability of metkephamid, *Pharm Res* 11, 528-535.
- Leak, L. V., and Jamuar, M. P. (1983). Ultrastructure of pulmonary lymphatic vessels, *Am Rev Respir Dis* 128, S59-65.
- Lennernäs, H. (2002). Personal communication.
- Lennernäs, H., and Regårdh, C. G. (1993). Evidence for an interaction between the  $\beta$ -blocker pafenolol and bile salts in the intestinal lumen of the rat leading to dose-dependent oral absorption and double peaks in the plasma concentration-time profile, *Pharm Res* 10, 879-883.
- Leong, B. K. J., Coombs, J. K., Sabaitis, C. P., Rop, D. A., and Aaron, C. S. (1998). Quantitative morphometric analysis of pulmonary deposition of aerosol particles inhaled via intratracheal nebulization, intratracheal instillation or nose-only inhalation in rats, *J Appl Toxicol* 18, 149-160.
- Lethem, M. I. (1993). The role of tracheobronchial mucus in drug administration to the airways, *Adv Drug Deliv Rev* 11, 271-298.
- LiCalsi, C., Christensen, T., Bennett, J. V., Phillips, E., and Witham, C. (1999). Dry powder inhalation as a potential delivery method for vaccines., *Vaccine* 17, 1796-1803.
- Lin, Y. J., and Schanker, L. S. (1981). Pulmonary absorption of amino acids in the rat: evidence of carrier transport, *Am J Physiol* 240, C215-221.
- Lipworth, B. J. (1996). Pharmacokinetics of inhaled drugs, *Br J Clin Pharmacol* 42, 697-705.
- Lizio, R., Marx, D., Nolte, T., Lehr, C.-M., Sarlikiotis, A. W., Borchard, G., Jahn, W., and Klenner, T. (2001). Development of a new aerosol delivery system for systemic pulmonary delivery in anesthetized and orotracheal intubated rats, *Laboratory Animals* 35, 261-270.
- Longmore, W. J. (1982). The isolated perfused lung as a model for studies of lung metabolism. In: *Lung Development: Biological and Clinical Perspectives*, Farrel, P. M., ed. (Academic Press Inc.), pp. 101-110.
- Ma, J., Bhat, M., and Rojanasakul, Y. (1996). Drug metabolism and enzyme kinetics in the lung. In: *Inhalation Aerosols*, Hickey, A. J., ed. (New York, Marcel Dekker, Inc).
- MacIntyre, N. R. (2001). Intratracheal catheters as drug delivery systems, *Respir Care* 46, 193-197.
- Mason, G. R., Peters, A. M., Bagdades, E., Myers, M. J., Snooks, D., and Hughes, J. M. B. (2001). Evaluation of pulmonary alveolar epithelial integrity by the detection of restriction to diffusion of hydrophilic solutes of different molecular sizes, *Clin Sci* 100, 231-236.
- Mason, R. J., and Crystal, R. G. (1998). Pulmonary cell biology, *Am J Respir Crit Care Med* 157, S72-81.
- Mathias, N. R., Timoszyk, J., Stetsko, P. I., Megill, J. R., Smith, R. L., and Wall, D. A. (2002). Permeability characteristics of Calu-3 human bronchial epithelial cells: In vitro- in vivo correlation to predict lung absorption in rats., *J Drug Targeting* 10, 31-40.

- Matsukawa, Y., Lee, V. H. L., Crandall, E. D., and Kim, K.-J. (1997). Size-dependent dextran transport across rat alveolar epithelial cell monolayers, *J Pharm Sci* 86, 305-309.
- Matsukawa, Y., Yamahara, H., Lee, V. H. L., Crandall, E. D., and Kim, K.-J. (1996). Horseradish peroxidase transport across rat alveolar epithelial cell monolayers, *Pharm Res* 13, 1331-1335.
- Matsukawa, Y., Yamahara, H., Yamashita, F., Lee, V. H., and Crandall, E. D. (2000). Rates of protein transport across rat alveolar epithelial cell monolayers, *J Drug Targeting* 7, 335-342.
- Mayor, S. H., and Illum, L. (1997). Investigation of the effect of anesthesia on nasal absorption of insulin in rats, *Int J Pharm* 149, 123-129.
- McAllister, S. M., Alpar, H. O., Teitelbaum, Z., and Bennett, D. B. (1996). Do interactions with phospholipids contribute to the prolonged retention of polypeptides within the lung?, *Adv Drug Deliv Rev* 19, 89-110.
- McMahon, T. A., Brain, J. D., and LeMott, S. (1977). Species differences in aerosol deposition. In: *Inhaled Particles IV*, Walton, W. H., ed. (Oxford, Pergamon Press), pp. 23-33.
- McMartin, C., Hutchinson, L. E., Hyde, R., and Peters, G. E. (1987). Analysis of structural requirements for the absorption of drugs and macromolecules from the nasal cavity, *J Pharm Sci* 76, 535-540.
- Mehendale, H. M., Angevine, L. S., and Ohmiya, Y. (1981). The isolated perfused lung - A critical evaluation, *Toxicology* 21, 1-36.
- Mercer, R. R., Russell, M. L., and Crapo, J. D. (1992). Mucous lining layers in human and rat airways, *Am Rev Respir Dis* 145, 355.
- Miller, F. J., Mercer, R. R., and Crapo, J. D. (1993). Lower respiratory tract structure of laboratory animals and humans: Dosimetry implications, *Aerosol Sci Technol* 18, 257-271.
- Miller-Larsson, A., Mattsson, H., Hjertberg, E., Dahlbäck, M., Tunek, A., and Brattsand, R. (1998). Reversible fatty acid conjugation of budesonide: Novel mechanism for prolonged retention of topically applied steroid in airway tissue, *Drug Metab Dispos* 26, 623-630.
- Morgenroth, K., and Bolz, J. (1985). Morphological features of the interaction between mucus and surfactant on the bronchial mucosa, *Respiration* 47, 225-231.
- Morimoto, K., Yamahara, H., Lee, V. H., and Kim, K. J. (1993). Dipeptide transport across rat alveolar epithelial cell monolayers, *Pharm Res* 10, 1668-1674.
- Morimoto, K., Yamahara, H., Lee, V. H., and Kim, K. J. (1994). Transport of thyrotropin-releasing hormone across rat alveolar epithelial cell monolayers, *Life Sci* 54, 2083-2092.
- Morita, T., Yamamoto, A., Hashida, M., and Sezaki, H. (1993). Effects of various absorption promoters on pulmonary absorption of drugs with different molecular weights, *Biol Pharm Bull* 16, 259-262.
- Mygind, N., and Dahl, R. (1998). Anatomy, physiology and function of the nasal cavities in health and disease, *Adv Drug Deliv Rev* 29, 3-12.
- Nemmar, A., Hoet, P. H. M., Vanquickenborne, B., Dinsdale, D., Thomeer, M., Hoylaerts, M. F., Vanbilloen, H., Mortelmans, L., and Nemery, B. (2002). Passage of inhaled particles into the blood circulation in humans, *Circulation* 105, 411-414.
- Nemmar, A., Vanbilloen, H., Hoylaerts, M. F., Hoet, P. H. M., Verbruggen, A., and Nemery, B. (2001). Passage of intratracheally instilled ultrafine particles from the lung into the systemic circulation in hamster, *Am J Respir Crit Care Med* 164, 1665-1668.
- Nerbrink, O. (1997) Investigation of the output characteristics of nebulisers and development of a novel inhalation system for large animals, doctoral dissertation, Lund University, Lund.

- Newhouse, M. T., and Ruffin, R. E. (1978). Deposition and fate of aerosolized drugs, *Chest* 73, 936-943.
- Newman, G. R., Campbell, L., von Ruhland, C., Jasani, B., and Gumbleton, M. (1999). Caveolin and its cellular and subcellular immunolocalisation in lung alveolar epithelium: implications for alveolar type I cell function, *Cell Tissue Res* 295, 111-120.
- Newman, S. P. (1998). Optimizing delivery of drugs to the lungs, *Clin Asthma Rev* 2, 123-128.
- Newman, S. P., Pavia, D., Garland, N., and Clarke, S. W. (1982). Effects of various inhalation modes on the deposition of radioactive pressurized aerosols., *Eur J Respir Dis* 63, 57-65.
- Nicod, L. P. (1999). Pulmonary defence mechanisms, *Respiration* 66, 2-11.
- Niven, R. W. (1992). Modulated drug therapy with inhalation aerosols. In: Pharmaceutical inhalation aerosol technology, Hickey, A. J., ed. (Chicago, Marcel Dekker, Inc), pp. 321-359.
- Niven, R. W. (1995). Delivery of biotherapeutics by inhalation aerosol. In: Crit Rev Ther Drug Carrier Syst, Bruck, S. D., ed. (New York, Begell House Inc), pp. 151-231.
- Niven, R. W., and Byron, P. R. (1988). Solute absorption from the airways of the isolated rat lung. I. The use of absorption data to quantify drug dissolution or release in the respiratory tract, *Pharm Res* 5, 574-579.
- Niven, R. W., Whitcomb, L. K., Shaner, L., Ip, A. Y., and Kinstler, O. B. (1995). The pulmonary absorption of aerosolized and intratracheally instilled rhG-CSF and monoPEGylated rhG-CSF, *Pharm Res* 12, 1343-1349.
- Norinder, U., and Haerberlein, M. (2002). Computational approaches to the prediction of the blood-brain distribution, *Adv Drug Deliv Rev* 54, 291-313.
- O'Byrne, P. M., Dolovich, M., Dirks, R., Roberts, R. S., and Newhouse, M. T. (1984). Lung epithelial permeability: relation to non-specific airway responsiveness, *J Appl Physiol* 57, 77-84.
- Okamoto, H., Aoki, M., and Danjo, K. (2000). A novel apparatus for rat in vivo evaluation of dry powder formulations for pulmonary administration, *J Pharm Sci* 89, 1028-1035.
- Palm, K., Luthman, K., Ungell, A-L., Strandlund, G., Beigi, F., Lundahl, P., and Artursson, P. (1998). Evaluation of dynamic polar molecular surface area as predictor of drug absorption: Comparison with other computational and experimental predictors, *J Med Chem* 41, 5382-5392.
- Palm, K., Stenberg, P., Luthman, K., and Artursson, P. (1997). Polar molecular surface properties predict the intestinal absorption of drugs in humans, *Pharm Res* 14, 568-571.
- Pang, J. A., Butland, R. J. A., Brooks, N., Cattell, M., and Geddes, D. M. (1982). Impaired lung uptake of propranolol in human pulmonary emphysema., *Am Rev Respir Dis* 125, 194-198.
- Patrick, G., and Stirling, C. (1977). Measurement of mucociliary clearance from the trachea of conscious and anaesthetised rats, *J Appl Physiol* 42, 451-455.
- Patton, J. S. (1996). Mechanisms of macromolecule absorption by the lungs, *Adv Drug Deliv Rev* 19, 3-36.
- Patton, J. S. (1997). Deep-lung delivery of therapeutic proteins, *Chemtech*, 34-38.
- Persson, C. G. A., and Erjefält, J. S. (1997). Airway epithelial restitution after shedding and denudation. In: The lung, Crystal, R. G., and West, J. B., eds. (Philadelphia, Lippincott-Raven Publishers), pp. 2611-2627.
- Pert, C. B., Pert, A., Chang, J. K., and Fong, B. T. W. (1976). [D-Ala<sup>2</sup>]-metenkephalinamide: a potent long-lasting synthetic pentapeptide analgesic., *Science* 194, 330-332.

- Pezron, I., Mitra, R., Pal, D., and Mitra, A. K. (2002). Insulin aggregation and asymmetric transport across human bronchial epithelial cell monolayers (Calu-3), *J Pharm Sci* 91, 1135-1146.
- Plopper, C. G. (1996). Structure and function of the lung. In: Respiratory system, Jones, T. C., Dungworth, D. L., and Mohr, U., eds. (Berlin, Springer Verlag), pp. 135-150.
- Puchelle, E., Girod de Bentzmann, S., and Higenbottam, T. (1995). Airway secretions and lung liquids. In: Respiratory Medicine, Brewis, R. A. L., Corrin, B., Geddes, D. M., and Gibson, G. J., eds. (London, W.B. Saunders Company Ltd), pp. 97-111.
- Qui, Y., Gupta, P. K., and Adjei, A. L. (1997). Absorption and bioavailability of inhaled peptides and proteins. In: Inhalation delivery of therapeutic peptides and proteins, Adjei, A. L., and Gupta, P. K., eds. (New York, Marcel Dekker), pp. 89-131.
- Raeburn, D., Underwood, S. L., and Villamil, M. E. (1992). Techniques for drug delivery to the airways, and the assessment of lung function in animal models, *J Pharmacol Toxicol Methods* 27, 143-149.
- Redington, A. E. (2001). Airway remodelling in asthma, *CME Bull Resp Med* 3, 37-40.
- Rennard, S. I., Beckmann, J. D., and Robbins, R. A. (1991). Biology of airway epithelial cells. In: The Lung: Scientific Foundations, Crystal, R. G., and West, J. B., eds. (New York, Raven Press Ltd.), pp. 157-167.
- Roerig, D. L., Kotrly, K. J., Dawson, C. A., Ahlf, S. B., J.F., G., and Kampine, J. P. (1989). First-pass uptake of verapamil, diazepam, and thiopental in the human lung, *Anesth Analg* 69, 461-466.
- Roerig, D. L., Kotrly, K. J., and Vucins, E. J. (1987). First pass uptake of fentanyl, meperidine and morphine in the human lung, *Anesthesiology* 67, 466-472.
- Rubin, B. K. (1996). Therapeutic aerosols and airway secretions, *J Aerosol Med* 9, 123-130.
- Russell, K. E., Read, M. S., Bellinger, D. A., Leitermann, K., Rup, B. J., McCarthy, K. P., Keith, J. C., Khor, S. P., Schaub, R. G., and Nichols, T. C. (2001). Intratracheal administration of recombinant human factor IX (BeneFix<sup>TM</sup>) achieves therapeutic levels in hemophilia B dogs., *Thromb Haemost* 85, 445-449.
- Ryrfeldt, Å., and Nilsson, E. (1978). Uptake and biotransformation of ibuterol and terbutaline in isolated perfused rat and guinea pig lungs, *Biochem Pharmacol* 27, 301-305.
- Ryrfeldt, Å., Persson, G., and Nilsson, E. (1989). Pulmonary disposition of the potent glucocorticoid budesonide, evaluated in an isolated and perfused rat lung model, *Biochem Pharmacol* 38, 17-22.
- Saha, P., Kim, K.-J., Yamahara, H., Crandall, E. D., and Lee, V. H. L. (1994). Influence of lipophilicity on beta-blocker permeation across rat alveolar epithelial cell monolayers, *J Control Release* 32, 191-200.
- Sakagami, M., Byron, P. R., and Rypacek, F. (2002a). Biochemical evidence for transcytotic absorption of polyaspartamide from the rat lung: Effects of temperature and metabolic inhibitors, *J Pharm Sci* 91, 1958-1968.
- Sakagami, M., Byron, P. R., Venitz, J., and Rypacek, F. (2002b). Solute disposition in the rat lung in vivo and in vitro: Determining regional absorption kinetics in the presence of mucociliary escalator, *J Pharm Sci* 91, 594-604.
- Sakagami, M., Kinoshita, W., Sakon, K., Sato, J.-I., and Makino, Y. (2002c). Mucoadhesive beclomethasone microspheres for powder inhalation: their pharmacokinetics and pharmacodynamics evaluation, *J Control Release* 2002, 207-218.

- Salathé, M., O'Riordan, T. G., and Wanner, A. (1997). Mucociliary clearance. In: *The Lung: Scientific Foundations*, Crystal, R. G., and West, J. B., eds. (Philadelphia, Lippincott-Raven Publishers), pp. 2295-2308.
- Samet, J. M., and Cheng, P.-W. (1994). The role of airway mucus in pulmonary toxicology, *Environ Health Perspect* 102, 89-103.
- Schanker, L. S., and Burton, J. A. (1976). Absorption of heparin and cyanocobalamin from the rat lung, *Proc Soc Exp Biol Med* 152, 377-380.
- Schanker, L. S., and Hemberger, J. A. (1983). Relation between molecular weight and pulmonary absorption rate of lipid-insoluble compounds in neonatal and adult rats, *Biochem Pharmacol* 32, 2599-2601.
- Schanker, L. S., Mitchell, E. W., and Brown, R. A., Jr. (1986). Species comparison of drug absorption from the lung after aerosol inhalation or intratracheal injection, *Drug Metab Dispos* 14, 79-88.
- Scheffer, G. L., Pijnenborg, A. C. L. M., Smit, E. F., Müller, M., Postma, D. S., Timens, W., van der Valk, P., de Vries, E. G. E., and Scheper, R. J. (2002). Multidrug resistance related molecules in human and murine lung, *J Clin Pathol* 55, 332-339.
- Schlesinger, R. B. (1985). Comparative deposition of inhaled aerosols in experimental animals and humans: A review, *J Toxicol Environ Health* 15, 197-214.
- Schmekel, B., Borgström, L., and Wollmer, P. (1991). Difference in pulmonary absorption of inhaled terbutaline in healthy smokers and non-smokers, *Thorax* 46, 225-228.
- Schneeberger, E. E. (1978). Structural basis for some permeability properties of the air-blood barrier, *Fed Proc* 37, 2471-2478.
- Schneeberger, E. E. (1980). Heterogeneity of tight junction morphology in extrapulmonary and intrapulmonary airways in the rat., *Anat Rec* 198, 193-208.
- Schneeberger, E. E. (1991). Airway and alveolar epithelial cell junctions. In: *The Lung: Scientific Foundations*, Crystal, R. G., and West, J. B., eds. (New York, Raven Press), pp. 205-214.
- Schneeberger, E. E., and McCormack, J. M. (1984). Intercellular junctions in upper airway submucosal glands of the rat: a tracer and freeze-fracture study., *Anat Rec* 210, 421-433.
- Schnitzer, J. E. (2001). Caveolae: from basic trafficking mechanisms to targeting transcytosis for tissue-specific drug and gene delivery in vivo, *Adv Drug Deliv Rev* 49, 265-280.
- Schoenmakers, R. G., Stehouwer, M. C., and Tukker, J. J. (1999). Structure-transport relationship for the intestinal small-peptide carrier: Is the carbonyl group of the peptide bond relevant for transport?, *Pharm Res* 16, 62-68.
- Schulz, H., Brand, P., and Heyder, J. (2000). Particle deposition in the respiratory tract. In: *Particle-lung interactions*, Gehr, P., and Heyder, J., eds. (New York, Marcel Dekker, Inc.), pp. 229-290.
- Schuster, J., Rubsamen, R., Lloyd, P., and Lloyd, J. (1997). The AERX aerosol delivery system, *Pharm Res* 14, 354-357.
- Shen, J., Elbert, K. J., Lehr, C.-M., Yamashita, F., Kim, K. J., and Lee, V. H. L. (1997). Cultured rabbit alveolar epithelial barrier for organic cation transport studies, *Pharm Res* 14, S-134.
- Simionescu, M. (1991). Lung endothelium: Structure-function correlates. In: *The Lung: Scientific foundations*, Crystal, R. G., and West, J. B., eds. (New York, Raven Press, Ltd.), pp. 301-312.

- Skyler, J. S., Cefalu, W. T., Kourides, I. A., Landschulz, W. H., Balagtas, C. C., Cheng, S.-L., and Gelfand, R. A. (2001). Efficacy of inhaled human insulin in type 1 diabetes mellitus: a randomised proof-of-concept study, *Lancet* 357, 331-335.
- Soldner, A., Benet, L. Z., Mutschler, E., and Christians, U. (2000). Active transport of the angiotensin-II antagonist losartan and its main metabolite EXP 3174 across MDCK-MDR1 and Caco-2 cell monolayers, *Br J Pharmacol* 129, 1235-1243.
- Spahn Langguth, H., Baktir, G., Radschuweit, A., Okyar, A., Terhaag, B., Ader, P., Hanafy, A., and Langguth, P. (1998). P-glycoprotein transporters and the gastrointestinal tract: evaluation of the potential in vivo relevance of in vitro data employing talinolol as model compound, *Int J Clin Pharmacol Ther* 36, 16-24.
- Staub, N. C. (1991). Basic Respiratory Physiology (New York, Churchill Livingstone Inc.).
- Steiner, S., Pfützner, A., Wilson, B. R., Harzer, O., Heinemann, L., and Rave, K. (2002). Technosphere<sup>TM</sup>/Insulin- proof of concept study with a new insulin formulation for pulmonary delivery, *Exp Clin Endocrinol Diabetes* 110, 17-21.
- Stone, K. C., Mercer, R. R., Gehr, P., Stockstill, B., and Crapo, J. D. (1992). Allometric relationships of cell numbers and size in the mammalian lung, *Am Respir Cell Mol Biol* 6, 235-243.
- Su, K. S., Campanale, K. M., Mendelsohn, L. G., Kerchner, G. A., and Gries, C. L. (1985). Nasal delivery of polypeptides I: nasal absorption of enkephalins in rats, *J Pharm Sci* 74, 394-398.
- Suarez, S., GonzalezRothi, R. J., Schreier, H., and Hochhaus, G. (1998). Effect of dose and release rate on pulmonary targeting of liposomal triamcinolone acetonide phosphate, *Pharm Res* 15, 461-465.
- Sugawara, I., Akiyama, S., Scheper, R. J., and Itoyama, S. (1997). Lung resistance protein (LRP) expression in human normal tissues in comparison with that of MDR1 and MRP, *Cancer Lett* 112, 23-31.
- Suhara, T., Sudo, Y., Yoshida, K., Okubo, Y., Fukuda, H., Obata, T., Yoshikawa, K., Suzuki, K., and Sasaki, Y. (1998). Lung as reservoir for antidepressants in pharmacokinetic drug interactions, *Lancet* 351, 332-335.
- Summers, Q. A. (1991). Inhaled drugs and the lung, *Clin Exp Allergy* 21, 259-268.
- Sweeney, T. D., and Brain, J. D. (1991). Pulmonary deposition: determinants and measurement techniques, *Toxicol Pathol* 19, 384-97.
- Takenaka, S., Karg, E., Roth, C., Schulz, H., Ziesenis, A., Heinzmann, U., Schramel, P., and Heyder, J. (2001). Pulmonary and systemic distribution of inhaled ultrafine silver particles in rats, *Environ Health Perspect* 109, 547-551.
- Taljanski, W., Pierzynowski, S. G., Lundin, P. D., Weström, B. R., Eirefelt, S., Podlesny, J., Dahlbäck, M., Siwinska Golebiowska, H., and Karlsson, B. W. (1997). Pulmonary delivery of intratracheally instilled and aerosolized cyclosporine A to young and adult rats, *Drug Metab Dispos* 25, 917-920.
- Taylor, G. (1990). The absorption and metabolism of xenobiotics in the lung, *Adv Drug Deliv Rev* 5, 37-61.
- Taylor, M. D., and Amidon, G. L. (1995). Peptide-based drug design: controlling transport and metabolism (Washington DC, American Chemical Society).
- Tronde, A., Krondahl, E., von Euler-Chelpin, H., Brunmark, P., Hultkvist Bengtsson, U., Ekström, G., and Lennernäs, H. (2002). High airway-to-blood transport of an opioid tetrapeptide in the isolated rat lung after aerosol delivery, *Peptides* 23, 469-478.
- Twigg, H. L. (1998). Pulmonary host defenses, *J Thoracic Imaging* 13, 221-233.

- Upton, R. N., and Doolette, D. J. (1999). Kinetic aspects of drug disposition in the lung, *Clin Exp Pharmacol Physiol* 26, 381-391.
- Wall, D. A. (1995). Pulmonary absorption of peptides and proteins, *Drug delivery* 2, 1-20.
- Wall, D. A., and Lanutti, A. T. (1993). High levels of exopeptidase activity are present in rat and canine bronchoalveolar lavage fluid, *Int J Pharm* 97, 171-181.
- van den Bosch, J. M. M., Westermann, C. J. J., Aumann, J., Edsbäcker, S., Tönnesson, M., and Selroos, O. (1993). Relationship between lung tissue and blood plasma concentrations of inhaled budesonide., *Biopharm Drug Dispos* 14, 455-459.
- Wan, H., Winton, H. L., Soeller, C., Stewart, G. A., Thompson, P. J., Gruenert, D. C., Cannell, M. B., Garrod, D. R., and Robinson, C. (2000). Tight junction properties of the immortalized human bronchial epithelial cell lines Calu-3 and 16HBE14o-, *Eur Respir J* 15, 1058-1068.
- Van' t Veen, A., Gommers, D., Verbrugge, S. J. C., Wollmer, P., Mouton, J. W., Kooij, P. P. M., and Lachmann, B. (1999). Lung clearance of intratracheally instilled Tc-99m-tobramycin using pulmonary surfactant as vehicle, *Br J Pharmacol* 126, 1091-1096.
- Van' t Veen, A., Mouton, J. W., Gommers, D., Kluytmans, J. A. J. W., Dekkers, P., and Lachmann, B. (1995). Influence of pulmonary surfactant on in vitro bactericidal activities of amoxicillin, ceftazidime, and tobramycin, *Antimicrob Agents Chemother* 39, 329-333.
- Wang, L. Y., Toledo-Velasquez, D., Schwegler-Berry, D., Ma, J. K. H., and Rojanasakul, Y. (1993). Transport and hydrolysis of enkephalins in cultured alveolar epithelial monolayers, *Pharm Res* 10, 1662-1667.
- Waters, C. M., Avram, M. J., Krejcie, T. C., and Henthorn, T. K. (1999). Uptake of fentanyl in pulmonary endothelium, *J Pharmacol Exp Ther* 288, 157-163.
- Waters, C. M., Krejcie, T. C., and Avram, M. J. (2000). Facilitated uptake of fentanyl, but not alfentanil, by human pulmonary endothelial cells, *Anesthesiology* 93, 825-831.
- Veber, D. F., Johnson, S. R., Cheng, H-Y., Smith, B. R., Ward, K. W., and Kopple, K. D. (2002). Molecular properties that influence the oral bioavailability of drug candidates, *J Med Chem* 45, 2615-2623.
- Weibel, E. R. (1991). Design of airways and blood vessels considered as branching trees. In: *The Lung: Scientific Foundations*, Crystal, R. G., and West, J. B., eds. (New York, Raven Press Ltd.), pp. 711-720.
- Weibel, E. R., and Crystal, R. G. (1991). Structural organization of the pulmonary interstitium. In: *The Lung: Scientific Foundations*, Crystal, R. G., and West, J. B., eds. (New York, Raven Press, Ltd), pp. 369-380.
- Verotta, D. (1994). Deconvolution, *Anaesthetic Pharmacol Rev* 2, 250-259.
- Wiedmann, T. S., Bhatia, R., and Wattenberg, L. W. (2000). Drug solubilization in lung surfactant, *J Control Release* 65, 43-47.
- Winiwarter, S., Bonham, N. M., Ax, F., Hallberg, A., Lennernäs, H., and Karlén, A. (1998). Correlation of human jejunal permeability (in vivo) of drugs with experimentally and theoretically derived parameters. A multivariate data analysis approach, *J Med Chem* 41, 4939-4949.
- Winton, H. L., Wan, H., Cannell, M. B., Gruenert, D. C., Thompson, P. J., Garrod, D. R., Stewart, G. A., and Robinson, C. (1998). Cell lines of pulmonary and non-pulmonary origin as tools to study the effects of house dust mite proteinases on the regulation of epithelial permeability, *Clin Exp Allergy* 28, 1273-1285.

- Wollmer, P., Schairer, W., Bos, J. A., Bakker, W., Krenning, E. P., and Lachmann, B. (1990). Pulmonary clearance of  $^{99m}\text{Tc}$ -DTPA during halothane anesthesia., *Acta Anaesthesiol Scand* 34, 572-575.
- Wright, S. R., Boag, A. H., Valdimarsson, G., Hipfner, D. R., Campling, B. G., Cole, S. P., and Deeley, R. G. (1998). Immunohistochemical detection of multidrug resistance protein in human lung cancer and normal lung, *Clin Cancer Res* 4, 2279-2289.
- Yamashita, F., Kim, K. J., and Lee, V. H. L. (1998). Dipeptide uptake and transport characteristics in rabbit tracheal epithelial cell layers cultured at an air interface, *Pharm Res* 15, 979-983.
- Yamashita, F., Mathias, N. R., Kim, K.-J., and Lee, V. H. L. (1996). Dipeptide transport properties of rabbit tracheal epithelial cell monolayers cultured at an air-interface, *Respir Drug Deliv* 5, 432-4.
- Yang, X., Ma, J. K. A., Malanga, C. J., and Rojanasakul, Y. (2000). Characterization of proteolytic activities of pulmonary alveolar epithelium, *Int J Pharm* 195, 93-101.
- Yoshida, H., Okumura, K., and Hori, R. (1987). Subcellular distribution of basic drugs accumulated in the isolated perfused lung, *Pharm Res* 4, 50-53.
- Yoshida, H., Okumura, K., and Hori, R. (1990). Contribution of monoamine oxidase (MAO) to the binding of tertiary basic drugs in isolated perfused rat lung, *Pharm Res* 7, 398-401.
- Yost, G. S. (1999). Sites of metabolism: lung. In: *Drug Metabolism*, Erhardt, P.W. (Oxford, Blackwell Science), pp. 263-278.
- Yu, J., and Chien, Y. W. (1997). Pulmonary drug delivery: physiologic and mechanistic aspects, *Crit Rev Ther Drug Carrier Syst* 14, 395-453.